Spectral characterisation of variable reactance devices

Ekaterini Fifa

DEDICATED

To

A.FIFAS and L.FIFA

SPECTRAL CHARACTERISATION OF VARIABLE REACTANCE DEVICES

By

Ekaterini Fifa

Graduate Society

A thesis submitted to the Faculty of Science,
University of Durham, for the degree of
Master of Science

Department of Applied Physics and Electronics,
School of Engineering and Applied Science,
University of Durham, UK.

April 1987

ABSTRACT

Low Noise Figure communication receivers require more efficient frequency converters. Frequency conversion and multiplication processes cannot take place without the existence of harmonics in the system and the inherent property of a nonlinear element is to generate a harmonic spectrum. Such nonlinearity, in general, may be provided by semiconductor diodes. This research project deals with the theoretical analysis as well as the properties of a nonlinear reactive device, i.e. Varactor Diode.

The power series solutions for the exponential diodes do not normally converge quickly enough to be of practical value for numerical evaluations. A different approach is proposed for the evaluation of harmonic amplitudes and phases. The harmonic generating properties of four diodes of the same type were examined using two different approaches and a good agreement was found between the two methods.

Many analyses published over the years have tended to introduce severe approximations which were only valid in practice over limited ranges of operation. However, it is believed that the new sampling method presented here evaluates fully the capabilities of these diodes in practice.

ACKNOWLEDGEMENTS

I would like to express my gratitude to my supervisors, Dr. B.L.J.Kulesza and Dr. J.S. Thorp for their guidance, enthusiasm and continued interest throughout the entire period of research. I am especially indebted to Dr. B.L.J. Kulesza for introducing me to the fascinating subject of nonlinear systems and his active supervision. I am also grateful to Dr. J.Welford who was very keen to help in every possible way in writing the "F.F.T" program.

My appreciation is also due to my colleagues in the High Frequency Measurements and Applications Research Group, and the technical staff of the department for their generous co-operation.

Last, but not least, I am most grateful to my parents whose love, encouragement and support throughout my work made it possible for me to produce this Thesis.

Ekaterini Fifa

Durham

April 1987

CONTENTS

CHAPTER 1

INTRODUCTION

Generation of microwave frequencies at milliwatt power levels has in the past been generally achieved employing klystrons and other electron beam devices. However, in many satellite, missile and portable equipment applications the weight, size and power consumption of these devices needing high voltage supplies have proved to be a severe handicap. To overcome these problems solid state devices are being increasingly exploited.

Many high frequency systems extensively use nonlinear semiconductor devices for various essential purposes. The design of circuits incorporating such components requires a thorough knowledge of their electrical characteristics and behaviour. The basic principles of amplification with a nonlinear reactance are not new. Just to mention one example, nonlinear inductances have been employed in magnetic amplifiers for many years. As a consequence, the nonlinearity has always been a subject of great mathematical and physical interest especially in communications and electronics fields.

Many microwave semiconductor devices derive their usefulness from the nonlinearity of the current-voltage characteristic and are called varistors (variable resistances). Nonlinearity of the charge-voltage characte-

ristic, i.e. the nonlinearity of a capacitance, is the major feature of the diodes which are called variable reactances or varactors.

The process of diffusion has also been important in the development of junction diodes. As a consequence the fragility, burn out and frequency limitation disadvantages of the point-contact diodes have been eliminated. The improved diodes have led to advances in the design of crystal mixers and detectors, especially with respect to noise figure and frequency limits.

When operated in the forward-biased directions, junction diodes behave as nonlinear resistances and hence have low Q values with relatively high RC products. However, they perform as voltage-dependent or nonlinear capacitors (varactors) when operated in the reverse-biased directions. Their nonlinear capacitance characteristics can be especially useful in low-noise parametric amplification.

The varactor diode has also been important in raising the efficiency of microwave harmonic generators, modulators and switches. The power levels of the diodes have been raised through the use of higher temperature materials such as GaAs and higher voltages can be applied when thin layer of intrinsic material are used in their construction. Conversion efficiencies have been improved simultaneously so that harmonic generators could supply milliwats of power up to X-band frequencies and microwatts in the millimeter region.

A semiconductor diode has a junction capacitance associated with it and while it may present an undesirable feature in more conventional uses of the diode, it is an important mechanism in varactors. This capacitance actually varies with the applied voltage if the diode is back-biased. Shockley showed that the "Depletion Layer Capacitance" for a planar geometry diode is given by

$$C(v) = \frac{K}{(\phi - v)^{\gamma}}$$

When the junction is biased in the reverse direction the depletion layer widens and the capacitance value falls. The conduction taking place across the junction is due to the motion of hole and electron distributions. Its exact dependence on the applied voltage varies with the nature of the junction.

The quality of the varactor operation is affected by the series resistance to a great extent and a lot of trouble is taken in the design in order to reduce its value to an absolute minimum.

Although the theoretical foundations of parametric amplification and harmonic generation using variable capacitance elements had been laid as early as November 1948 by A. Van der Ziel in "On the Mixing Properties of Non-Linear Condensers" [1] very low-loss diodes were not available and hence the initial experiments did not produce predicted high gains, high efficiencies or low-noise

figures.

A major breakthrough came in July 1957 when Bakanowski, Cranna and Uhlir reported the discovery of a technique for making low-loss silicon and germanium nonlinear capacitors [2]. The fabrication process used was solid-state diffusion. The resulting graded junctions were of planar structure. The important advantage of the "one-dimensional" or "planar" geometry is that, since the depletion layer capacitance and series resistance are respectively, directly and inversely proportional to the area, the RC product and hence the cut-off frequncy are independent of it.

A "hyper-abrupt" varactor diode fabricated by an alloy-diffusion process was reported by Shimiza and Nishizawa in September 1961 in "Alloy-Diffused Variable Capacitance Diode with Large Figure of Merit" [3]. The resulting junction in which the impurity concentration decreases with distance from the p-n boundary showed high voltage sensitivity of the capacitance.

Results of further investigations were reported by Sukegawa, Fugikawa and Nishizawa in January 1963 in "Si Alloy-Diffused Variable Capacitance Diode" [4]. An experimental varactor was obtained. Its capacitance for only a few volts of reverse bias reduced to one-hundredth of its zero bias value, a variation not realisable with ordinary abrupt or graded junctions.

Since their losses are much lower than in varistors, varactors are preferred elements for harmonic generation,

modulation or up-conversion and low-noise amplifications. It is therefore advantageous to know the full extent of their capabilities for an efficient performance. At the present time, the extent and the method of characterisation of these devices, especially at high frequencies, is inadequate for many applications. Normally, the device parameters available are for the static characteristics and these are usually obtained from low frequency measurements. If the dynamic characteristics are given, they are generally at one particular test frequency and drive level.

At the present time there is no detailed quantitative analysis available to give exact values for the harmonics generated within the junction diodes. In order therefore to assess the properties of a nonlinear device at high frequencies, there is a need to determine experimentally the generated frequency spectrum. Such a spectrum must logically be a unique representation of the device nonlinearity.

The main objective of this work is to characterise a number of devices, the varactor diodes, by means of the generated spectral components. This characterisation provides information useful in the device evaluation for particular applications.

In chapter 2, the theory of construction and properties of the practical varactors are reviewed. The practical devices and their applications are also discussed.

Chapter 3 outlines the meaning of spectral evaluation.

A review of Fourier Analysis is given and the device characterisation, or "fingerprinting" using the method of the spectral representation is presented.

The theory of the new technique developed for the spectrum measurements is described in chapter 4. The nonlinear device driven by a sinusoidal signal produces a distorted output response which contains all the necessary information for each evaluation. Via a computer this output is Fourier-analyzed and the resulting frequency spectrum of the device is calculated using an appropriate programme. The equipment and the experimental arrangements are first described followed by the outline of the intended test procedures for a practical system.

In chapter 5, measurements and experimental setup are covered. Other detailed aspects relevant to the technique such as the choice of drive level and measurement of C-V and Q-V characteristics are presented, followed by the experimental procedures.

The harmonic measurement results of the four diodes are displayed in the form of graphs in chapter 6. The properties of each diode and the resulting spectral representation are interpreted and discussed.

Finally, in chapter 7, an assessment of the sampler method dealing with the accuracy, significance and possible improvements is presented. Suggestions and recommendations for future work arising from these investigations are proposed.

CHAPTER 2

CONSTRUCTION AND PROPERTIES OF PRACTICAL VARACTORS

2.1 Introduction

A varactor diode is a semiconductor device which is principally employed in electrical circuits and networks as a nonlinear, variable-capacitance element. Such a diode consists of a semiconductor wafer on which a junction is formed normally by a diffusion process and a suitable encapsulation. The depletion capacitance of the junction provides the variable element which is a function of the applied voltage.

Because of its nonlinearity, the varactor will generate sums, differences and harmonics when two or more frequencies are applied. Manley and Rowe [5] have derived a set of equations relating the powers flowing into and out of a nonlinear capacitance. The basic idea behind the equations was to show that , if the device is lossless, the sum of the powers flowing into and out of it at all frequencies will be zero.

The nonlinear capacitance of a varactor is used in many applications. Low-noise high frequency parametric amplification is probably one of the most important. Additionally, they may be employed in the design of other frequency converters, frequency multipliers, dividers and modulators for frequency control and comparison systems. For such

circuits based on variable capacitance devices, the Manley and Rowe equations also provide the information for the gain and stability. Furthermore, the conditions, under which the production of harmonics and other frequencies is possible are given.

Semiconductor rectifiers in the past frequently exhibited a noticeable nonlinear capacitance effect under reverse bias. Before 1950's those variable capacitance diodes were manufactured mainly for voltage tuning applications. However, such diodes were relatively lossy and therefore were highly inefficient especially at microwave frequencies. Low loss variable capacitance diodes were developed in the middle 1950's under the direction of Uhlir [6] of Bell Laboratories. They were first reported in a paper by Bakanowski, Cranna, and Uhlir in 1959 and to dinstinguish these devices from the more lossy diodes then available, they were named, variable reactances or varactors.

2.2 Theory

2.2.1 Physics of Varactors

Varactors are basicaly semiconductor junction devices which exhibit a nonlinear depletion or barrier capacitance variations with applied voltage. This effect is enhanced and predominates when the diode is reverse-biased; the junction becomes a variable-capacitance element. Its behaviour depends on the so called impurity profile

achieved by introducing appropriate dopants on each side of the semiconductor junction. Ideally, the diode impurity profile can either be abrupt or graded as shown in Figs. 2.1 and 2.2 , respectively. In practice the devices will fall somewhere between the two extreme profiles.

At some high reverse voltage the junction breaks down which is caused by an avalanche multiplication process when holes and electrons are generated rapidly resulting in a large reverse current. This effect, must be taken into account and establishes the reverse voltage limit on the magnitude of the driving signal. There may also be other effects present producing excess reverse currents sometimes even at lower voltages. This may happen in diodes with very large doping densities which results in the so called Zener effect. The breakdown voltage limit encompasses all these effects and is designated as V_B in the analyses [7].

For the varactor to function properly no forward current must flow. The small potential barrier on the junction does not cause appreciable conduction and hence does not interfere with the varactor operation. Under forward conduction, the junction can be represented by a diffusion capacitance whilst for the reverse bias the most important depletion layer capacitance predominates. When in such a condition all the mobile charge carriers are withdrawn from the depletion region leaving a net fixed charge density of donors and acceptors. The depleted width decreases with the reduction in reverse bias to a finite

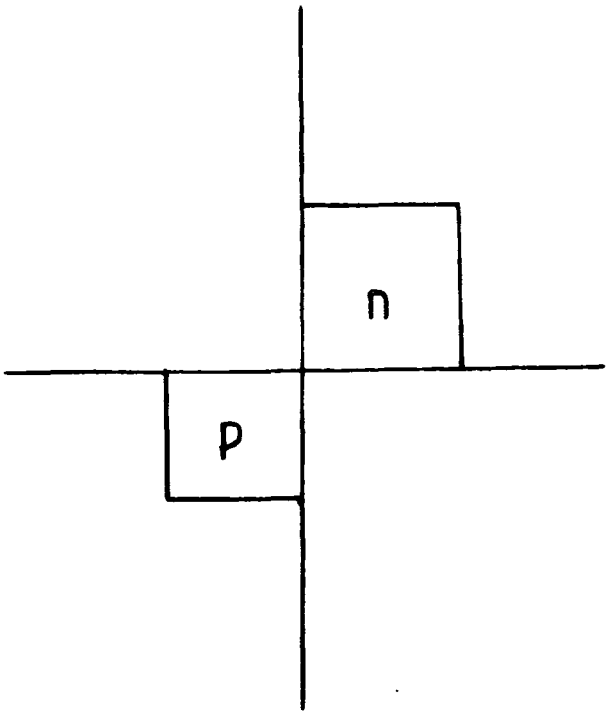

Fig. 2.1 Abrupt Junction

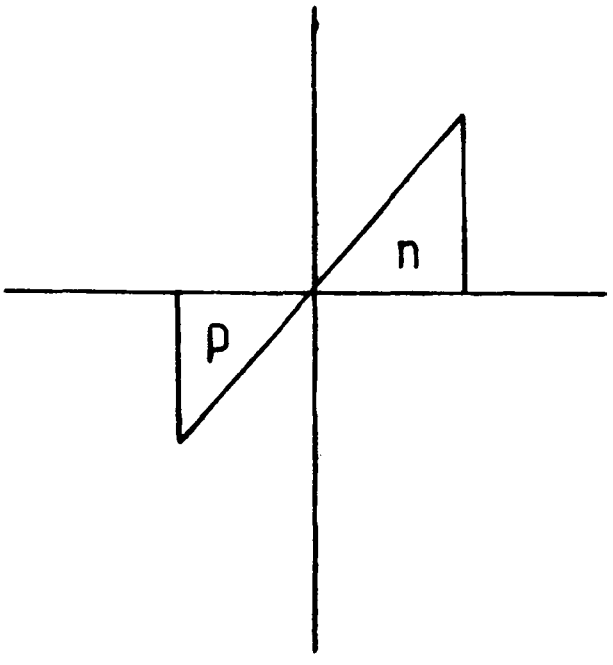

Fig. 2.2 Graded Junction

width because of the potential barrier voltage which would still exist across the junction.

The fundamental relationship between the charge, voltage and capacitance is usually expressed as

$$Q = V\ C \tag{2.1}$$

The depletion capacitance of a varactor as a function of the voltage v behaves according to the formula [6]

$$C(v) = \frac{C_o}{\left(1 - \frac{v}{\phi}\right)^{\gamma}} = \frac{dQ}{dv} \tag{2.2}$$

where

C_o = total capacitance at zero bias,

ϕ = barrier potential,

γ = elastance-voltage exponent,

and v = applied junction voltage.

Combining these two above equations it is possible to show that the relationship between the charge and the voltage is [5], (see appendix A)

$$\frac{\phi - v}{\phi - V_B} = \left(\frac{q_\phi - q}{q_\phi - Q_B}\right)^{(1/1-\gamma)} \tag{2.3}$$

where

$$v \leq \emptyset \ , \quad q \leq q_{\emptyset}$$

and

$$v = \emptyset \ , \quad q \geq q_{\emptyset}$$

The $q_{\emptyset}$ (positive) is the charge stored at $v = \emptyset$, and Q_B (negative) is the charge stored at reverse breakdown, $v = V_B$

The symbol γ represents the impurity profile of the varactor, being 1/2 for the abrupt and 1/3 for the graded junction.

In practice, many varactors are neither exactly abrupt nor exactly graded. A typical diffused varactor has a doping profile so that, at low voltages, the capacitance is inversely proportional to the cube root of the voltage. At higher voltage it follows a square root law [8].

Variations of the depletion layer width, also affects the series resistance r_s, outside the bulk material. It can be shown [8] that

$$r_s = r_{s\,min} + \rho (S_{max} - S) \qquad (2.4)$$

Where

S = elastance.

ρ = resistivity of the lightly doped side.

2.2.2 Design Considerations

Varactor diodes are designed to exploit the property that the capacitance of a reverse-biased junction depends on the applied voltage. In practice there are three types of diode that exhibit this useful property i.e.

(i) simple p-n junctions whose operation is based on minority carrier conduction,

(ii) Schottky barrier or Hot carrier diodes based on the majority carrier operation and

(iii) Step recovery diodes [Boff] exploiting the minority storage effect.

In the design of varactor diode there are certain objectives which should normally be achieved. The depletion layer capacitance should decrease from a large value at near zero bias to a small value at the breakdown voltage. The value of the zero-bias capacitance is ordinarily specified according to the intended application. The V_B should be high enough to ensure that in use, the varactor is not driven into avalanche. Finally, the series resistance should be low enough to avoid dissipation losses.

Next, the following conditions of operation must be followed for a satisfactory performance. It is desirable in most cases not to allow the bias to swing past zero into

forward conduction. Since the driving current flows into the junction capacitance of the varactor diode and into the external circuit, the external resistance must be minimised to avoid losses. The larger the junction capacitance, the larger the driving current and the higher will be the circuit losses. As the quality of the varactor diode is obviously affected by the external circuitry, it is important in most applications to use lossless reactive components for filtering purposes.

One important design variable is the impurity concentration near the junction. If the concentration is very much larger on one side than on the other, the characteristics of the device will not be sensitive to the doping level on the high side. In such a case only the doping level on the low side has to be carefully controlled. This is the way p-n junctions are usually manufactured, heavy doping on one side, and light uniform doping on the other.

The doping level on the lightly-doped side of the junction determines the avalanche breakdown voltage of the junction [6]. As a practical consideration, it is usually difficult to make diodes with breakdown voltages consistently at or near the theoretical value. Depending on how well controlled and reproducible the diode processing will be, the design V_B should be chosen above the largest peak reverse bias voltage to be applied. The lightly doped layer is then adjusted to be just thick enough to

accommodate the depletion layer at breakdown.

The design area A is determined from the following expresssion [6]

$$A = C_o \left(\frac{2V_o}{q \epsilon_o \epsilon_r N} \right)^{1/2} \qquad (2.5)$$

where

C_o = total capacitance at zero bias,

q = charge at the junction,

ϵ_o = permittivity of free space,

ϵ_r = relative permittivity of the lightly dopped layer,

N = lower impurity concentration (numeric),

and V_o is given by

$$V_o = \frac{kT}{q} \ln \frac{n_n p_p}{n_i^2} \qquad (2.6)$$

where

n_n = electron density at the n side of the junction,

p_p = hole density at the p side of the junction,

and n_i^2 = the product of p and n

For a varactor diode with a Schottky barrier junction, the epitaxial layer thickness is made equal to the thickness required for the lightly-doped layer. The thickness of the heavily doped layer is around 0.2 μm.

2.3 Electrical Characterisation of Practical Varactors

2.3.1 The Equivalent Circuit

A varactor diode is fundamentally a semiconductor wafer which contains a junction of well-defined geometry. The equivalent circuit of the wafer includes junction capacitance C_J, junction resistance R_J in shunt with C_J which are functions of the applied voltage. Finally, the series resistance r_s which may also be a function of bias. This comprises the resistance of the semiconductor bulk material on either side of the junction through which the current flows and the resistance of the ohmic electrical contacts to the wafer.

Varactor diodes are normally operated under reverse bias, where the parallel junction resistance, which is usually 10 Mohm or more, may be neglected in comparison with the capacitive reactance of the junction at high frequencies. Therefore, the equivalent circuit of the reverse-biased varactor at microwave frequencies reduces to a capacitance and resistance in series. A forward-biased varactor on the other hand is more complicated, because it should also include the diffusion capacitance of the injected carriers, and their effect on the conductance of the semiconductor material.

At low frequencies, the varactor has, in general, forward and reverse characteristics of an ordinary

semiconductor diode. In the forward direction the diode current increases exponentially with the applied voltage, whilst for reverse bias theoretically a small saturation current, I_s, should exist. In practical diodes this does not happen because of surface effects around the junction. At breakdown voltage the diode reverse current increases rapidly, and is limited only by the resistance of the diode and any external resistance which may be present in the circuit [9].

Although the variation in junction capacitance is the most important characteristic of the varactor diode presence of parasitic resistances, capacitances, and inductances due to encapsulation and external circuitry may affect the operation.

2.3.2 The Depletion Capacitance

We have established that the most important operational parameter of the varactor diode is its nonlinear depletion capacitance and the series resistance and the breakdown voltage are the limiting factors [5].

The back-biased diodes do not conduct appreciable current because the mobile charge carriers are drawn away from the junction . Suppose that the voltage applied to a varactor is changed by a differential amount dV, with the respective change in stored charge dQ, then

$$dQ = A \frac{dV}{w} \tag{2.7}$$

where

A = design area of the varactor,

w = width of the depletion layer,

and ϵ = permittivity of the space-charge layer.

Now the incremental charge is given by

$$dQ = - AeN_a dx_1 = AeN_d dx_2 \tag{2.8}$$

where

N_a and N_d are the impurity concentrations on each side of the junction

dx_1, and dx_2 are the changes in position of the edges of the width on each side of the junction.

and e is the charge of the electron

As a consequence, the incremental depletion capacitance can now be expressed as

$$C = \frac{dQ}{dV} = A \frac{\epsilon}{w}$$

where

C = the incremental capacitance given by eqn. (2.2) i.e.

$$C = \frac{C_o}{\left(1 - \frac{V}{\phi}\right)^{1/2}} \tag{2.9}$$

2.3.3 The Series Resistance

Another important component of the varactor diode equivalent circuit is its series resistance. Physically, it represents the bulk resistance of the semiconductor material and the resistance of the contacts. Its value may be calculated [8] by integrating the bulk resistivity of the semiconductor over the path of the current i.e.

$$R_s = \frac{1}{A}\left[\int_0^{x_1} \rho_p(x)dx + \int_{x_2}^{x_n} \rho_n(x)dx\right] \qquad (2.10)$$

The p-type and n-type resistivities are functions of the acceptor and donor impurity densities. The series resistance is thus a function of x_1, x_2, which are in turn functions of the bias voltage. Hence, r_s is also a function of bias voltage. An increase in bias voltage causes a wider depletion layer which effectively lowers the series resistance.

It is important to point out that the a.c. series resistance is different from the d.c. resistance which is usually lower. The equivalent circuit of the varactor is shown in Fig. 2.3 in which R_j can be ignored because at radio frequencies it is shunted by the reactance of the capacitance C_j. Also in practice the inductance of the leads, L, and the case capacitance may be neglected, not

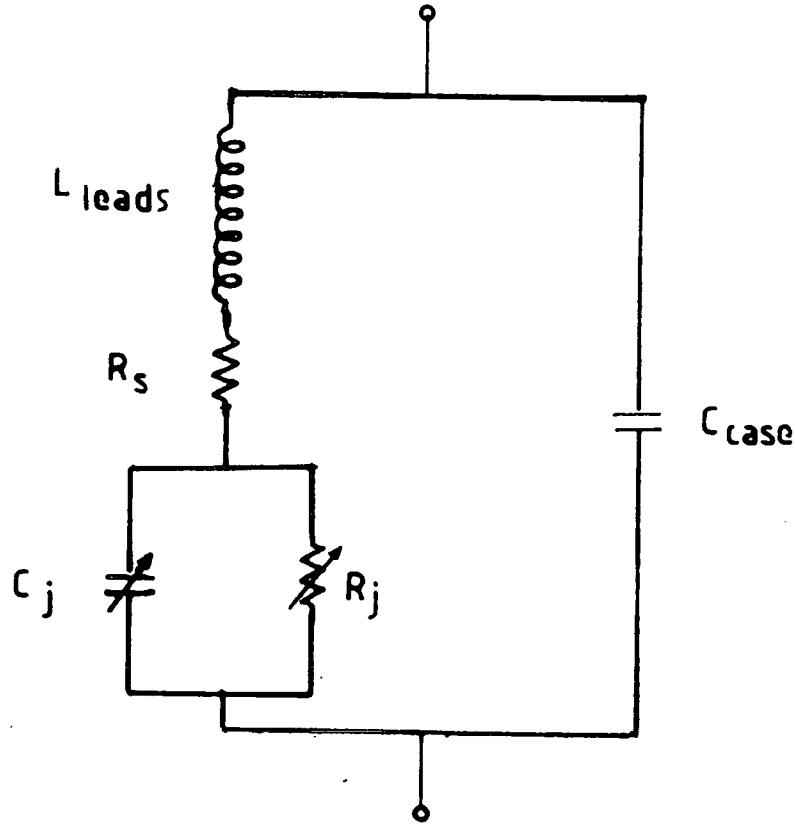

Fig. 23 Varactor Equivalent Circuit

Fig. 24 Simplified Equivalent Circuit

because they are unimportant but because their effect may be absorbed by external circuitry. Therefore, the simplified equivalent circuit is as shown in Fig. 2.4.

2.4 Applications

2.4.1 Introduction

Varactor diodes, because of their nonlinear low loss capacitance have become extremely useful elements in microwaves. A view of the varactor diode is presented in Fig. 2.5. Some of the most important and extensive applications are in low-noise parametric amplifiers, frequency multipliers or harmonic generators and, in general, other frequency-converting circuits. The operation of these circuits is dependent on the nonlinear phenomenon effect. The following paragraphs will outline the general principles of harmonic generators and parametric amplifiers, the two most useful applications.

2.4.2 Harmonic Generation

Harmonic generators and frequency multipliers may be used as direct sources of signals at high frequencies. Fig. 2.6 presents the diagram of a harmonic generator.

The nonlinear resistance of the semiconductor diode has been used at microwave frequencies as harmonic generator in the past. However, its efficiency according to Page's law [10] cannot exceed $1/n^2$, where n is the order of the harmonic. Greater efficiencies might be expected and

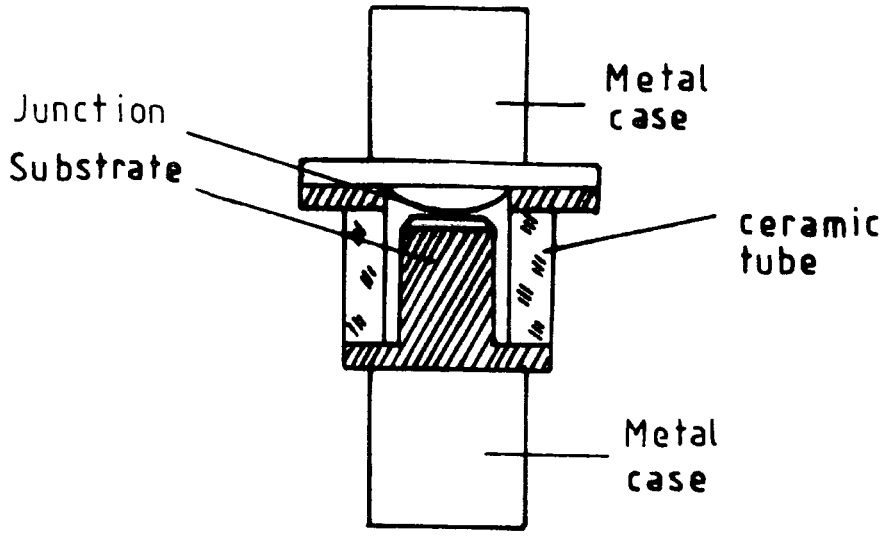

Fig. 2.5 Varactor Diode Pill

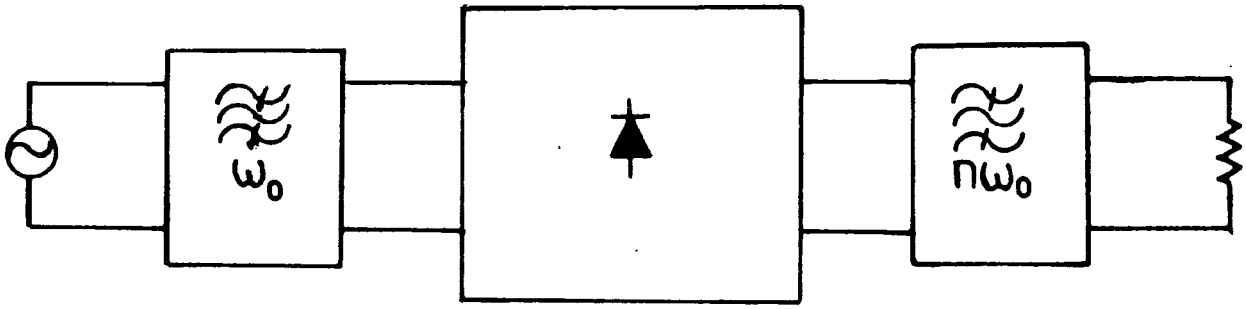

Fig. 2.6 Harmonic Generator

achieved from a nonlinear capacitance element used for harmonic generation. Theoretically, efficiencies of 100% are possible and values above 80% are achievable in practice for the second harmonic multiplication.

In a practical arrangement a sinusoidal generator drives a circuit, containing a nonlinear capacitance, at the frequency w_o through a bandpass filter. A load is connected to the output of the circuit through a bandpass filter around nw_o. If the circuit and filter networks are lossless, the input power introduced at w_o frequency may be transferred to the load at nw_o frequency with high efficiency.

Pumping the nonlinear capacitor with the charge at the fundamental frequency, w, harmonic voltages are produced across the diode. These harmonic voltages are approximately proportional to the amplitude of the driving charge raised to the power of the harmonic number [10]

$$V_n \approx \left(\frac{Q_1}{Q_o} \right)^n \qquad (2.11)$$

where

Q_o = average value of the stored charge,

and Q_1 = charge at the fundamental frequency.

As an example let us consider the simplest case when the varactor is abrupt with $\gamma = 1/2$, and the only two

currents flowing in the varactor are the input current at the frequency w_o and the output current at the frequency nw_o. The total charge and the current are then given by

$$q = Q_o + 2Q_1\sin(w_o t) + 2Q_n\sin(nw_o t) \qquad (2.12)$$

or

$$i = \frac{dq}{dt} = 2w_o Q_1\cos(w_o t) + 2nw_o Q_n\cos(nw_o t) \qquad (2.13)$$

The instantaneous value of the junction voltage may then be obtained from eqns.(2.2) and (2.3) leading to

$$v = \phi - \frac{\phi - V_B}{(q_\phi - Q_B)^2}\left(q_\phi - Q_o - 2Q_1\sin(w_o t) - 2Q_n\sin(nw_o t)\right)^2 \qquad (2.14)$$

2.4.3 Parametric Amplifiers and Converters

The varactor diode is one of the most promising nonlinear elements for low-noise parametric amplification. A parametric amplifier is a circuit based on the principle that when a resonant network is suitably coupled to an energy storage element, energy may be extracted from the source. This energy through the mechanism of the nonlinear capacitance is transferred to the fields of the resonant network. Thus in the parametric amplifier energy is normally taken from a driving source at high frequency to amplify an input signal at a lower frequency. However,

since a practical varactor diode has a small series resistance, this limits the minimum obtainable noise figures.

In the amplifier, the capacitance is modulated by the application of microwave power at the pump frequency,

$$\frac{1}{C_j} = \frac{1}{C_o}(1 + 2\gamma \cos 2\pi ft) \qquad (2.15)$$

where

f = the pump frequency

C_o = capacitance without the pump power

γ = diode capacitance modulation coefficient, which is a function of the voltage developed across the diode at pump frequency.

If only the pump and signal frequencies are present, there cannot be a steady flow of energy from one to the other, except when the pump frequency is exactly twice the signal frequency. For a steady flow of energy, it is necessary for the voltage across the capacitance to be maintained in the correct phase, and this can only be achieved by permitting power to flow at a third frequency. This the "idler" frequency which is equal to the difference between the signal and pump frequencies. The amplifier therefore contains three frequency-selective networks or filters which will permit power to flow only at these three frequencies, and the nonlinear capacitance forms the common

element between them. Manley-Rowe relations [5] represent the theoretical power into and out of an idealised nonlinear capacitance, i.e.

$$\sum_{m=0}^{\infty} \sum_{n=-\infty}^{\infty} \frac{m\, P_{m,n}}{mf_1 + nf_2} = 0$$

$$\sum_{n=0}^{\infty} \sum_{m=-\infty}^{\infty} \frac{n\, P_{m,n}}{mf_1 + nf_2} = 0 \qquad (2.16)$$

where

$P_{m,n}$ is the power flow into or out of the nonlinear capacitance, and f_1, f_2 the frequencies at which power is fed to the capacitance.

Some other varactor applications require three or more idlers frequencies. If a large current at frequency f_1 and a small current at frequency f_2 are put through a varactor sidebands with frequencies of the form mf_1+nf_2, for m,n positive or negative integers are generated. If the power flows at one of these frequencies to a load, the varactor is said to be a frequency converter. Frequency converters are classified according to whether the output frequency is greater than or less than the input frequency. They are known as upconverters or downconverters, respectively. Also according to the integer m in the formula mf_1+nf_2 for the output frequency, if m = 1 the device is called upper-sideband converter and if m = -1 lower-sideband converter.

CHAPTER 3

SPECTRAL EVALUATION

3.1 Introduction

In order to analyse frequency converting networks there is a need to have theoretical relationships, for the nonlinear behaviour based on the physics of the devices employed. Such relationships may be easily obtained if the precise laws of the devices are known. In many cases the laws are approximate due to the lack of knowledge and because other mechanisms affecting the performance may exist. As a consequence, to achieve closed-form equations for the devices we normally introduce severe approximations in the analysis, which makes the final relationships very often inaccurate. An alternative practical way of representing a nonlinear device which will include all these effects may be by its generated spectrum of harmonic components [11].

It is well known that if a nonlinear element is energised by a single-frequency sinusoidal source (V or I) the response will be a spectrum of harmonic currents or voltages. It is also logical to assume that the generated spectrum will contain all the necessary information to model the device. The resulting frequency spectrum is a unique representation of the device behaviour for the specified drive level and device parameters. It may be

considered as a device fingerprint which represents its characteristics and parasitic effects present implying as a consequence, that any changes in the law of the device characteristic will be reflected in the measured spectrum. It can therefore be useful and appropriate to employ generated harmonic spectra for the assessment of devices before they are used in frequency-converting applications.

3.2 Review of Fourier Analysis

3.2.1. Fundamental relations

An arbitrary function repeatable with a period of T seconds may be represented by the relationship f(t)=F(t+T). Let us consider that such a function is single-valued and has a finite number of discontinuities and a finite number of maxima and minima in one period of oscillation. Under these conditions, known as Dirichlet Conditions, the function f(t) may be represented over a complete period and anywhere between $t = -\infty$ and $t = +\infty$, except at the discontinuities, by a series of harmonic terms. The harmonic frequencies in the resulting spectrum are integral multiples of the fundamental. The series is called a Fourier series and may be obtained for any periodical waveshape using numerical or other analytical methods.

A general trigonometric Fourier Series for a periodic function may be written as [12]

$$f(t) = a_o + \sum_{n=1}^{\infty} a_n \cos(n w_o t) + \sum_{n=1}^{\infty} b_n \sin(n w_o t) \qquad (3.1)$$

or simplified to

$$f(t) = \sum_{n=0}^{\infty} C_n \cos(n\omega_o t + \phi_n) \tag{3.2}$$

where

$$C_n = (a_n^2 + b_n^2)^{1/2} \tag{3.3}$$

and

$$\phi_n = \tan^{-1}\left(\frac{b_n}{a_n}\right) \tag{3.4}$$

The coefficients C_n and ϕ_n give the amplitude and the phase shift, respectively for the n^{th} harmonic and ω_o is the fundamental frequency. The Fourier coefficients are obtained using orthogonality conditions and are given by

$$a_o = \frac{1}{T} \int_{-T/2}^{T/2} f(t)dt \tag{3.5}$$

$$a_n = \frac{2}{T} \int_{-T/2}^{T/2} f(t)\cos(n\omega_o t)dt \tag{3.6}$$

$$b_n = \frac{2}{T} \int_{-T/2}^{T/2} f(t)\sin(n\omega_o t)dt \tag{3.7}$$

Fourier Series, can also be expressed in an exponential form thus

$$f(t) = \sum_{n=-\infty}^{\infty} F_n e^{jn\omega_0 t} \qquad t_1<t<t_2 \qquad (3.8)$$

where

F_n is given as

$$F_n = \frac{1}{t_2-t_1} \int_{t_1}^{t_2} f(t)e^{-jn\omega_0 t}\, dt \qquad (3.9)$$

The Fourier series as represented by eqn. (3.8) is applicable to a periodic signal. The transition to an aperiodic signal representation is obtained by making the period approach infinity. This can be achieved by considering initially the exponential form of the Fourier series of a periodic function $f_T(t)$.

$$f_T(t) = \sum_{n=-\infty}^{\infty} F_n e^{jn\omega_0 t} \qquad (3.10)$$

where

$$F_n = \frac{1}{T} \int_{-T/2}^{T/2} f(t)e^{-jn\omega_0 t}\, dt \qquad (3.11)$$

In order that $|F_n|$ is convergent when T is increased, the following conditions must be satisfied, i.e.

$$\omega_n = n\omega_o \tag{3.12}$$

$$F(\omega_n) = TF_n \tag{3.13}$$

Eqns. (3.10) and (3.11) may now be written as

$$f_T(t) = \sum_{n=-\infty}^{\infty} \frac{1}{T} F(\omega_n) e^{j\omega_n t} \tag{3.14}$$

and

$$F(\omega_n) = \int_{-T/2}^{T/2} f_T(t) e^{-j\omega_n t}\, dt \tag{3.15}$$

If

$$T = \frac{2\pi}{\Delta\omega}$$

then

$$f_T(t) = \sum_{n=-\infty}^{\infty} F(\omega_n) e^{j\omega_n t} \frac{\Delta\omega}{2\pi} \tag{3.16}$$

In the limit, as T tends to infinity, $\Delta\omega \rightarrow d\omega$, the infinite sum in eqn. (3.16) may be written as

$$\lim_{T\to} f_T(t) = \lim_{T\to} \frac{1}{2\Pi} \sum_{n=-\infty}^{\infty} F(\omega_n) e^{j\omega_n t} \Delta\omega \qquad (3.17)$$

and therefore becomes the Riemann integral [12] i.e.

$$f(t) = \frac{1}{2\Pi} \int_{-\infty}^{+\infty} F(\omega) e^{j\omega t} d\omega \qquad (3.18)$$

Similarly eqn. (3.15) may be written as

$$F(\omega) = \int_{-\infty}^{+\infty} f(t) e^{-j\omega t} dt \qquad (3.19)$$

and is called the Direct Fourier Transform whilst eqn. (3.18) is called the Inverse Fourier Transform.

The Fourier Transform pair is one of the integral transforms that are commonly used in operational analysis. The frequency distribution of harmonics in a Fourier series is a line spectrum whereas in a Fourier Integral it is a continuous spectrum. Therefore, spectra of mathematically undefined and defined waveforms can be examined.

3.2.2 Sampling in Frequency Domain

In the frequency domain the sampling theorem states that if, a function f(t) equals zero outside the function period T, [13] i.e.

$$f(t) = 0 \qquad \text{for } t>T \tag{3.20}$$

then its Fourier Transform F(w) is defined from its values at F(nTT/T) equidistant points with distance TT/T apart. As a result F(w) can be expressed as

$$F(w) = \sum_{n=-\infty}^{\infty} F\left(n\,\frac{TT}{T}\right)\,\frac{\sin(wT-nTT)}{wT - nTT} \tag{3.21}$$

One method for evaluating the Fourier Transform is based on a Fourier series approach. Considering eqn. (3.19) let $t_1=-T/2$ and $t_2=T/2$. Then,

$$F_n = \frac{1}{T}\int_{-T/2}^{T/2} f(t)e^{-jnw_o t}\,dt = \frac{F(nw_o)}{T} \tag{3.22}$$

The eqn. (3.22) can now be expressed in terms of the coefficients of the Fourier expansion i.e.

$$F(w) = \sum_{n=-\infty}^{\infty} TF_n\,\frac{\sin(wT/2 - nTT)}{(wT/2 - nTT)} \tag{3.23}$$

As a result the evaluation of F(w) is reduced to a simple

problem of determining F_n. This method can also be used to give the Fourier transform, F(w), of an arbitrary function f(t) not satisfying f(t)=f(t+T) i.e. a non-periodic function [12].

3.3 Fingerprinting of nonlinear devices

Many nonlinar problems can be solved through the use of nonlinear differential equations. However, as their solutions cannot often be written in a closed form, development of other methods becomes necessary. A physical system is usually too complex and its analysis is not a simple process.

In the case of devices it is often necessary to establish a relationship between parameters and characteristics. A device is normally modelled into its simplest form and with an acceptable accuracy so that the performance of a particular circuit using this device, operating under specific conditions, can be predicted.

Modelling is a procedure which leads to the equivalent circuit of a device representing its approximate behaviour. A given device is initially expressed in terms of physical variables required for its design and the circuit applications. There are suitable techniques available to solve these problems and result in specific device parameters. It is important to know the physical mechanism of the operation of the device or a system so that satisfactory modelling can be realised.

The harmonic frequency spectrum generated by a nonlinear device is a unique representation of the device behaviour and therefore may be considered as its fingerprint. The basic difference between fingerprinting using harmonic spectrum and modelling is that the former will give the true nonlinearity of the device under particular working conditions. Modelling will always be approximate while the harmonic spectrum will presicely represent the device and its mechanism for particular levels. Such fingerprinting, within the measurement errors and perturbation effects, could provide a practical method of device indentification.

Most manufacturers supply data sheets with inadequate information. Quantities like noise figure, r.f impedance are usually given at a particular test frequency often without specifying the operating levels. In many applications sets or a matched pair of particular devices are required. By comparing the spectra, "fingerprints", of the devices, the required matching for particular applications may be achieved. It may also be possible, from such spectra, to predict the performance of a circuit.

3.4 Varactor Analysis

For a back biased diode the incremental capacitance as a function of voltage is given by [5]

$$C(v) = \frac{C_o}{\left(1 - \frac{v}{\phi}\right)^{\gamma}}$$

where

ϕ is the potential barrier,

γ is an index whose value depends on impurity profile of the diode junction,

and v is the applied voltage.

The current through the diode may be written as [5]

$$i = C(v) \frac{dv}{dt}$$

or

$$i = \frac{C_o \phi^{\gamma}}{(\phi - v)^{\gamma}} \frac{dv}{dt}$$

where

$$v = v_i - v_o + v_b \approx v_b + V_i \sin \omega t$$

or

$$v \cong v_b + v_i$$

and

v_i = input voltage

v_o = output voltage

v_b = bias voltage

then

$$i = \frac{C_o \phi}{(\phi - v_b)^{\gamma}} \frac{\omega V_i \cos \omega t}{(1 - v_i)^{\gamma}} = K (\omega V_i \cos \omega t) (1 - v_i)^{-\gamma}$$

where

$$v_i' = \frac{V_i}{(\phi - v_b)} \sin\omega t = \frac{v_i}{(\phi - v_b)}$$

or

$$v_i' = V_i' \sin\omega t$$

and

$$K = \frac{C_o \phi^{\gamma}}{(\phi - v_b)^{\gamma}}$$

Expanding binomially gives

$$i = K\omega V_i \cos\omega t \left\{ 1 + v_i' + \frac{\gamma(1+\gamma)}{2!} v_i'^2 + \frac{\gamma(1+\gamma)(2+\gamma)}{3!} v_i'^3 + \ldots \infty \right\}$$

Now [14]

$$\sin^{2n}x = \frac{1}{2^{2n}} \left\{ \sum_{k=0}^{n-1} (-1)^{n-k} \; 2\binom{2n}{k} \cos 2(n-k) + \binom{2n}{k} \right\}$$

and [14]

$$\sin^{2n-1}x = \frac{1}{2^{2n-2}} \left\{ \sum_{k=0}^{n-1} (-1)^{n+k-1} \; \binom{2n-1}{k} \sin(2n-2k-1)x \right\}$$

which on using for powers of v_i' in the equation results in

$$\begin{aligned} i = \; & K\omega V_i \left\{ \cos\omega t + V_i' \gamma \cos\omega t \sin\omega t + \right. \\ & + V_i'^2 \binom{1+\gamma}{2} \frac{1}{2} (1-\cos 2\omega t)\cos\omega t + \\ & + V_i'^3 \binom{2+\gamma}{3} \frac{1}{4} (3\sin\omega t - \sin 3\omega t)\cos\omega t + \\ & \left. + V_i'^4 \binom{3+\gamma}{4} \frac{1}{8} (3 - 4\cos 2\omega t + \cos 4\omega t)\cos\omega t + \right. \end{aligned}$$

$$+ V_1'^{5} \binom{4+\gamma}{5} \frac{1}{16} (10\sin\omega t - 5\sin 3\omega t + \sin 5\omega t)\cos\omega t +$$

$$+ \ldots\infty\}$$

Using the following trigonometrical identities, i.e.

$$\cos A \cos B = \frac{1}{2} \left(\cos(A-B) + \cos(A+B)\right)$$

and

$$\cos A \sin B = \frac{1}{2} \left(\sin(A-B) + \sin(A+B)\right)$$

and collecting the coefficients at each frequency finally produces

for the fundamental current i_1

$$K_w(\phi - V_b) \left\{1 + \frac{1}{2} \binom{1+\gamma}{2} V_1'^{3} + \frac{1}{2^3} \binom{3+\gamma}{4} V_1'^{5} + \right.$$

$$\left. + \frac{1}{2^5} \binom{5+\gamma}{6} V_1'^{7} + \ldots\infty \right\} \quad \cos\omega t$$

for the second harmonic i_2

$$K_w(\phi - V_b) \left\{ \frac{1}{2} \binom{\gamma}{1} V_1'^{2} + \frac{1}{2^3} \binom{2+\gamma}{3} V_1'^{4} + \right.$$

$$\left. + \frac{1}{2^5} \binom{4+\gamma}{5} V_1'^{6} + \ldots\infty \right\} \quad \sin 2\omega t$$

for the third harmonic i_3

$$K_w(\phi - V_b) \left\{ - \frac{1}{2^2} \binom{1+\gamma}{2} V_1'^{3} - \frac{3}{2^4} \binom{3+\gamma}{4} V_1'^{5} - \ldots\infty \right\} \quad \cos 3\omega t$$

for the fourth harmonic i_4

$$K_w(\phi - V_b) \left\{ - \frac{1}{2^3} \binom{2+\gamma}{3} V_1'^{4} - \frac{5}{2^5} \binom{4+\gamma}{5} V_1'^{6} - \ldots\infty \right\} \quad \sin 4\omega t$$

for the fifth harmonic i_5

$$K\omega(\phi - V_b) \left\{ \frac{1}{2^4} \binom{3+\gamma}{4} V_i'^5 + \frac{1}{2^6} \binom{5+\gamma}{6} V_i'^7 + \ldots\infty \right\} \cos 5\omega t$$

for the sixth harmonic i_6

$$K\omega(\phi - V_b) \left\{ \frac{1}{2^5} \binom{4+\gamma}{5} V_i'^6 + \frac{1}{2^7} \binom{6+\gamma}{7} V_i'^8 + \ldots\infty \right\} \sin 6\omega t$$

The objective for the above analysis was to show that even if the assumptions in the driving voltage function $v \approx v_b + v_i$ are made it produces still infinite series euations for the harmonics. These equations, depending on the drive level, provide approximate expressions for the actual current amplitudes of the frequency components.

CHAPTER 4

COMPUTER AIDED EXPERIMENTAL SPECTRAL CHARACTERISATION

4.1 Introduction

There are number of ways for evaluating nonlinear devices and the choice will normally depend on their final applications and operating conditions. Testing is time-consuming and the required equipment is usually expensive and therefore there is a need to develop quicker and cheaper techniques for device characterisation. In addition, to collect a comprehensive data over an extensive frequency range, requires a lot of measurements which is even more time consuming. The method of Numerical Fourier Analysis under consideration in this project offers an inexpensive means of assessing the devices in much shorter time [15].

On energising, the signal applied to a nonlinear device produces a distorted response which reflects the nonlinearity of the device characteristic and contains all the necessary information for its evaluation. The distorted voltage developed on the output can then be Fourier-analysed and hence provide the frequency spectrum for the device identification. In order, however, to increase the

speed of analysis computer facilities were employed. Furthermore, since the analysis in our project had to be carried out at high frequency there was a need to use a fast sampler for the distorted waveshapes with a low frequency display for our guidance as a bonus. In the following paragraphs, the method and the steps necessary to achieve these aims are discussed in some detail.

4.2 The Method

4.2.1 General

The method followed here aims to examine a distorted resulting response when a nonlinear system is driven by a single frequency signal source. The main objective was to determine the complete harmonic spectra of four nonlinear devices, varactors, by means of Numerical Fourier Analysis. Although, the amplitudes of the harmonics of a distorted waveform can be measured using a Spectrum Analyzer there are no high frequency instruments available which will determine the relative phases of the generated frequency components within the spectrum.

To carry out directly Numerical Fourier Analysis, on a high frequency waveform becomes difficult because such waveforms cannot be displayed. The method ivestigated in this project was made possible because a high frequency sampler manufactered by Bradley's was available. Further limitations would obviously be due to sampling techniques.

The accuracy of the sampling process used depended on

the risetime of the sampling step generated by the instrument used [16]. The sampling points in one period of the displayed waveform were read by a data acquisition system and the information was fed into a microprocessor for further analysis. The microprocessor was programmed to work in "Fast Fourier Transform" algorithm obtained from the computer library. Its purpose was to determine the amplitudes and phases of the harmonic components of the sampled data. To achieve this, the samples proportional to the analogue input signal were digitised using an analogue-to-digital converter, A/D, before being fed into microprocessor. It was also necessary to produce the external scanning voltage for the sampling unit and this was done by a digital-to-analogue converter, D/A, controlled by the processor. This divided the time-axis into an equal number of intervals and synchronised the reading of the sampled points. The resulting harmonic spectrum represented the nonlinearity of the device and could be used for its characterisation.

4.2.2 The Theory of Numerical Analysis

The response of a nonlinear device driven by a sinusoidal signal will be a periodic distorted waveform. This waveform can be subdivided into M equal sections over the period, T, along the time axis. If each section is represented by Δt, then [12]

$$T = M \Delta t \tag{4.1}$$

and if t_m be the time at the end of the m^{th} interval, then

$$t_m = m \Delta t \qquad \text{for} \quad 1 \leq m \leq M \tag{4.2}$$

and the ordinate at t_m, may be denoted as $f(t_m)$ or $f(m \Delta t)$

In order to proceed with numerical analysis, the distorted waveform is sampled at the points Δwt, $2 \Delta wt$, $3 \Delta wt$, ... , $m \Delta wt$, ..., up to $M \Delta wt = 2\pi$. Thus, there are M points and the spacing between adjacent points is uniform and equal to $2\pi/M$.

The approximate Fourier coefficients for a periodic case can now be deduced from eqns. (3.5), (3.6) and (3.7) and may be written as

$$a_o \approx \frac{1}{M} \sum_{m=1}^{M} f(m \Delta t) \tag{4.3}$$

$$a_n \approx \frac{2}{M} \sum_{m=1}^{M} f(m \Delta t) \cos[n(m \Delta wt)] \tag{4.4}$$

$$b_n \approx \frac{2}{M} \sum_{m=1}^{M} f(m \Delta t) \sin[n(m \Delta wt)] \tag{4.5}$$

where

$$\Delta wt = \frac{2\pi}{M}$$

and $$\Delta t = \frac{T}{M}$$, T is the period in seconds.

It can be seen from the above equations that the variables involved are M, m, Δwt, n and $f(t_m)$ with m representing all integer values from 1 to M. The Fourier coefficients numerically determined using the above equations and measured ordinates are finally used to calculate the amplitude and phase values of the harmonics from

$$A_n = (a_n^2 + b_n^2)^{1/2}$$ and

$$\phi_n = \tan^{-1} \frac{b_n}{a_n}$$

It is obvious that the higher the value of M, the closer is the approximation to the true values of the coefficients and hence the waveshape. The evaluation of the Fourier coefficients may be accelerated by using a microprocessor facility and an "F.F.T." algorithm.

4.2.3 The Aims of Programming

One of the advantages of digital electronic circuits is their ability to store and retrieve data easily. The

experimental research techniques are frequently computer-controlled in order to exploit this facility and minimise human errors.

It is convenient for a computer to use a binary, or base two, arithmetical system because only two digits are needed, i.e. one and zero. Since digital electronics have only two defined logic states, i.e. high and low, it is possible to let one state represent a binary one and the other represent a binary zero, respectively [18].

The largest binary number that may be accepted here has a decimal value of 256, which is the equivalent of an 8-bit word i.e. the computer is capable of reading from 0 to 255 points maximum.

The process of describing a programming procedure, to a computer is therefore based on a binary number sy The commands of a Fast Fourier Transform programme, "F.F.T.", which was the only technique available for Fourier Analysis, was obtained from a computer library, and used in this project. The programme was stored in RAM memory and was executed when needed by entering the data. The procedure, initially, was for the programme to read the data, i.e. 256 different sampling points of the waveform, which were next stored in memory in the form of an array. These sampling points were needed to operate the "F.F.T." algorithm and produce the fourier coefficients, a_0, a_n and b_n. From the coefficients the magnitudes and phases of the harmonics were then calculated [19].

4.3 Practical System

The block diagram of the practical system used in the project is shown in Fig. 4.1 . It was decided, as the impedance of the sampling adapter was 50 ohm, it would be advisable to insert some attenuation in series with the device under test to achieve a better match. The device was placed in the inner conductor of a coaxial holder. The experiment consisted of measuring the distortion of the output waveform, caused by the device nonlinearity.

4.3.1 Sampling Adapter

For the sampling process , Bradley Sampling Adapter type 158 was used capable of accepting signals with risetimes just below 1 nsec. or an equivalent passband from zero frequency to just over 1 GHz. The output from this unit can be displayed on a monitor [16].

In a conventional oscilloscope, the waveform of the signal, which is observed, is drawn during a single horizontal sweep in a time equal to the period of the input signal. The sampler, on the other hand, builds the input waveform up as a low frequency display by sampling its high frequency value many cycles apart. The input signal is applied to a sampling gate which opens for approximately 350 pS in each cycle by a sampling gate pulse. Each time the gate is opened the sampler measures the input signal and then generates an equal value at about the time the

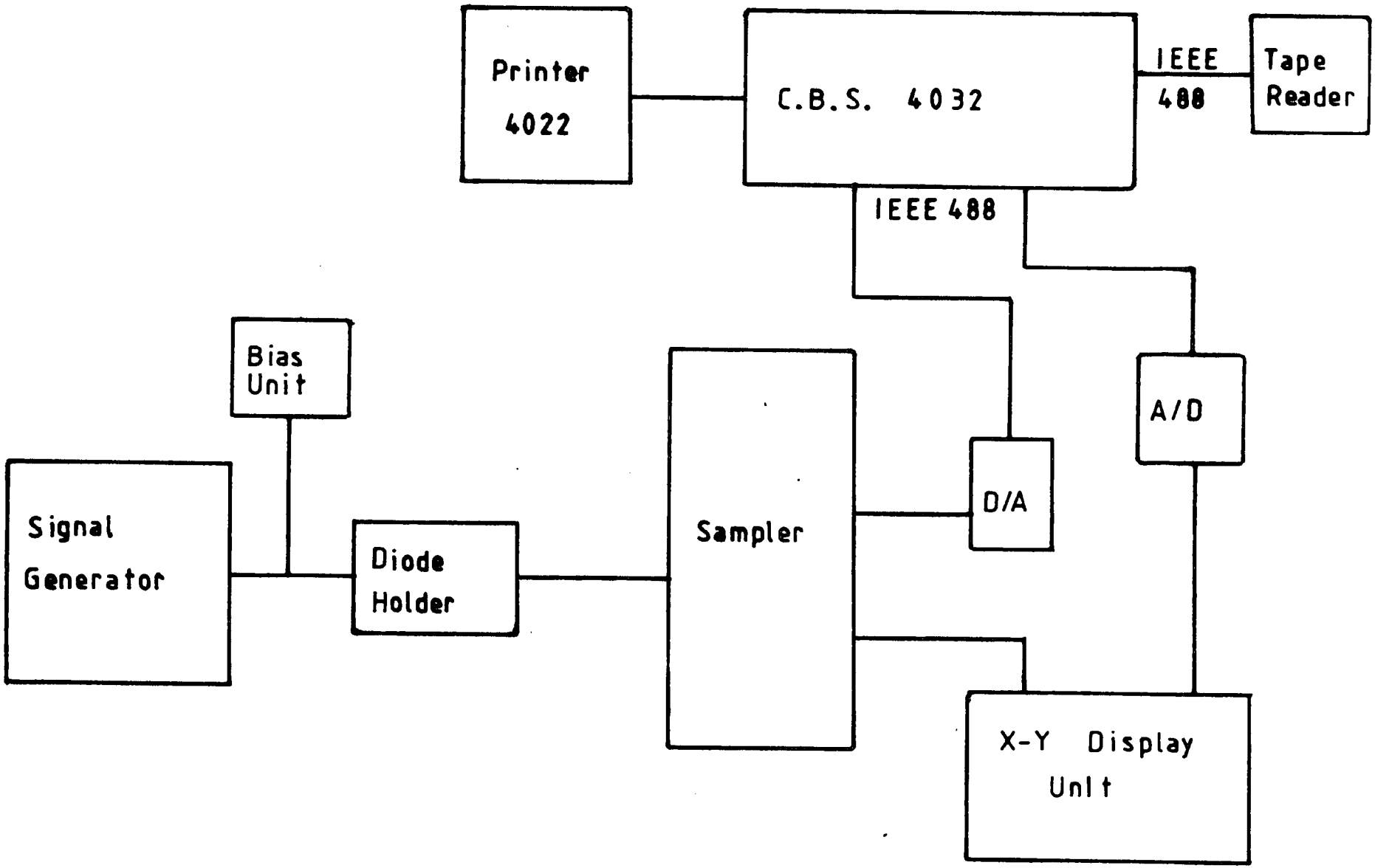

Fig. 4.1 Block Diagram of the Sampling Method

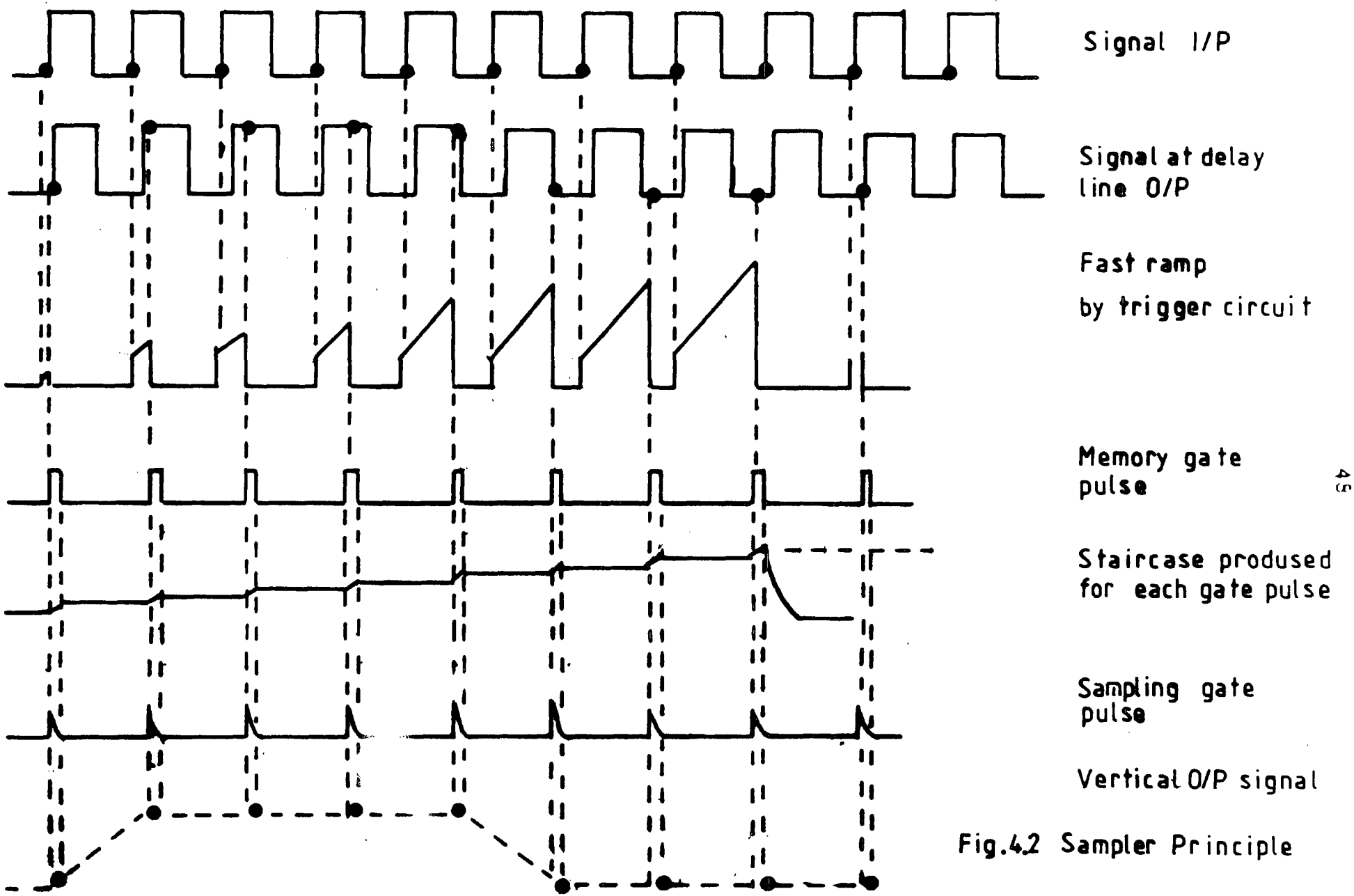

Fig.4.2 Sampler Principle

Fig. 4.3 Block Diagram of the Sampling Adaptor

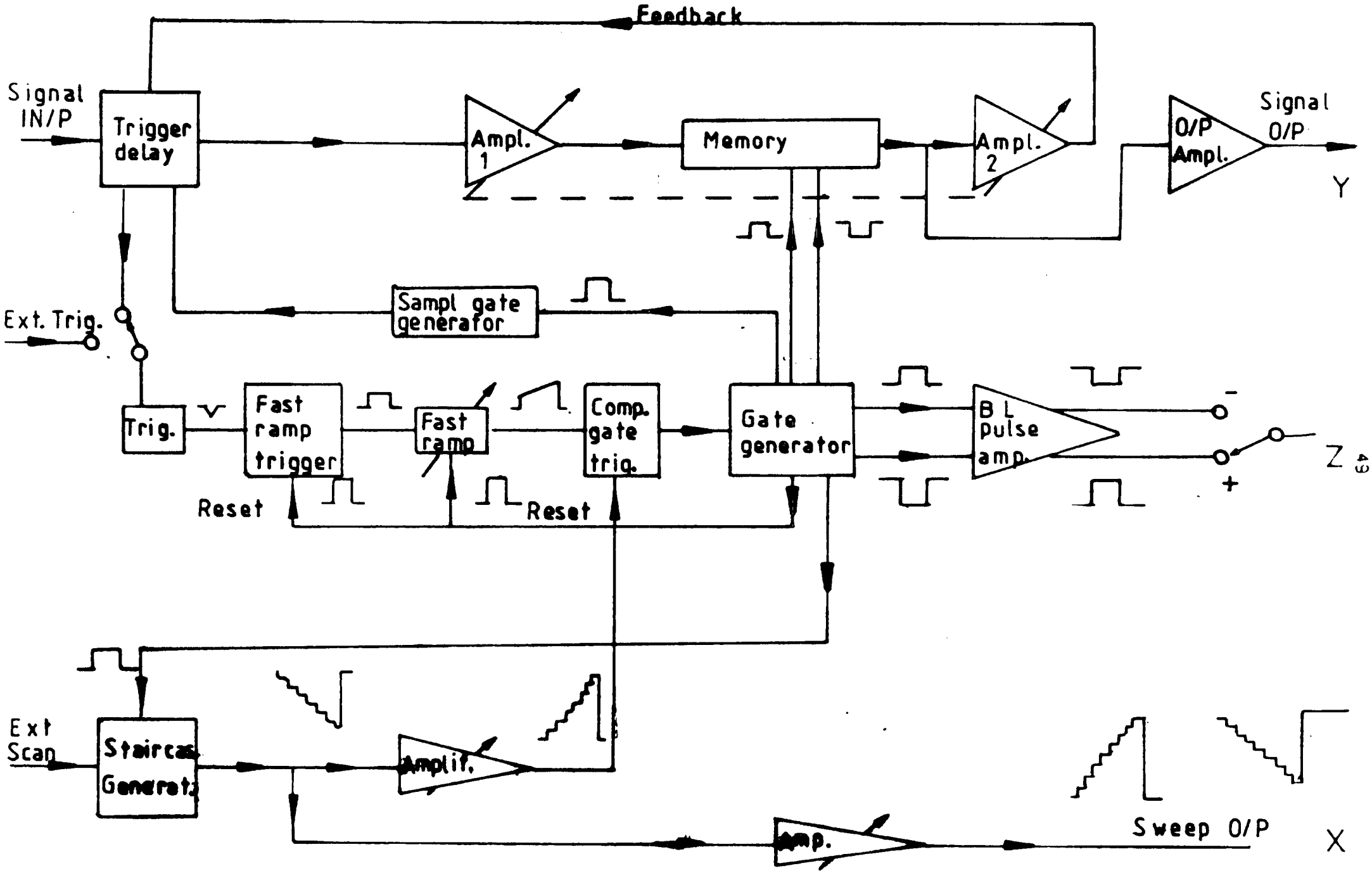

sample is taken. Aliasing errors could occur in this process bue since we do not consider high order harmonics then six the effects would be negligible according to the formula $n < M/2$.

The sampler has a memory circuit so that each sample point, dot, is displayed during a small interval of 2 μS before the next sample is taken [16]. It also provides a scanning signal which places each dot at the correct position on the horizontal axis. The gate opens at a frequency lower than the input frequency so that each sample represents a different and latter part of the input signal. Therefore the waveform is rebuilt from a number of samples taken over a period equal to many cycles of the signal. The principle of the reproduction process of the waveform is illustrated in Fig. 4.2. The block diagram of the sampler is also presented in Fig. 4.3.

4.3.2 D/A, A/D, Converters

Analogue signals via A/D converter were used as inputs to a computer. Since a microprocessor could only handle digital information, an analogue-to-digital conversion was required for interfacing. Similarly, the digital-to-analogue converter, may deliver a current or a voltage output that is proportional to the value of the digital applied input. The information can be in a coded form and may represent positive or negative quantities or both [20].

The ZN425E is an 8-bit D/A converter, shown in

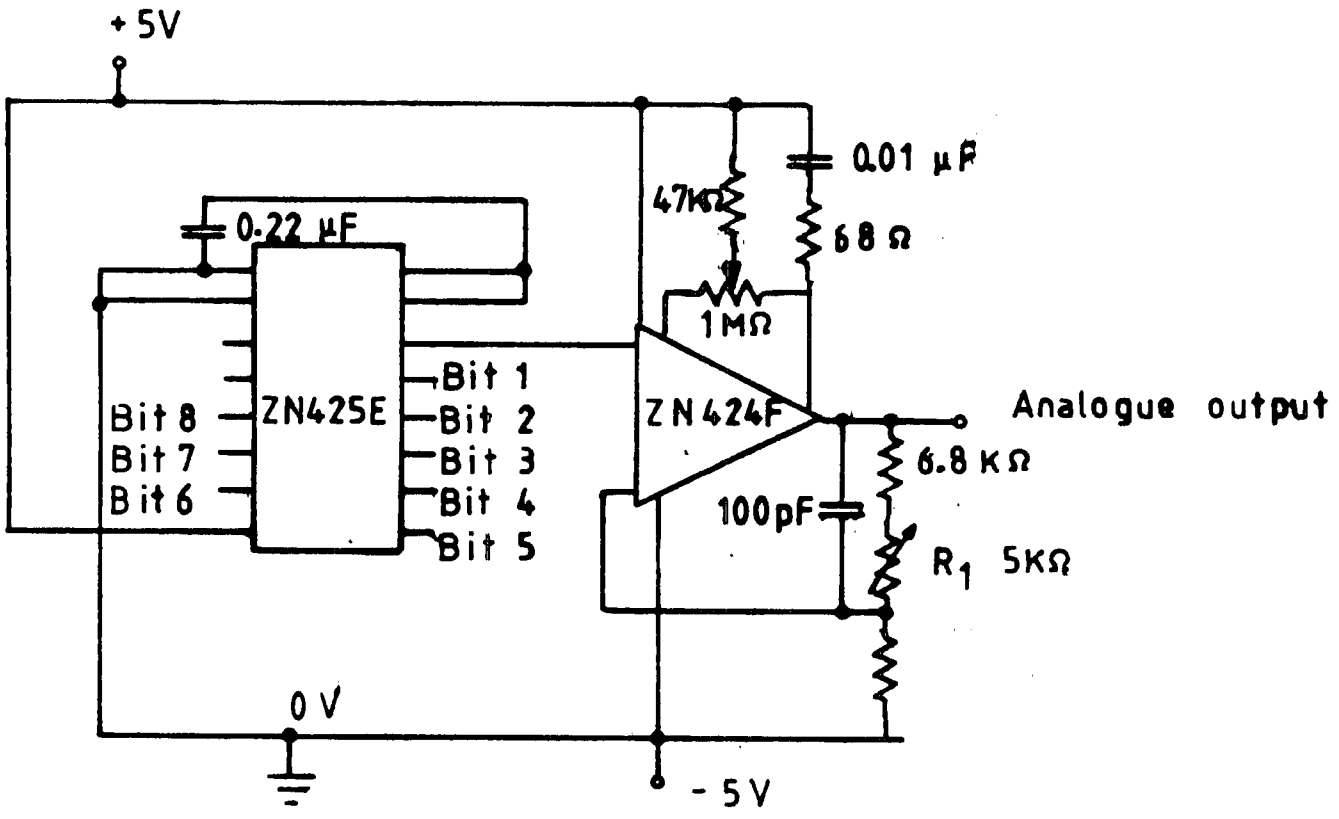

Fig. 4.4 D/A Converter

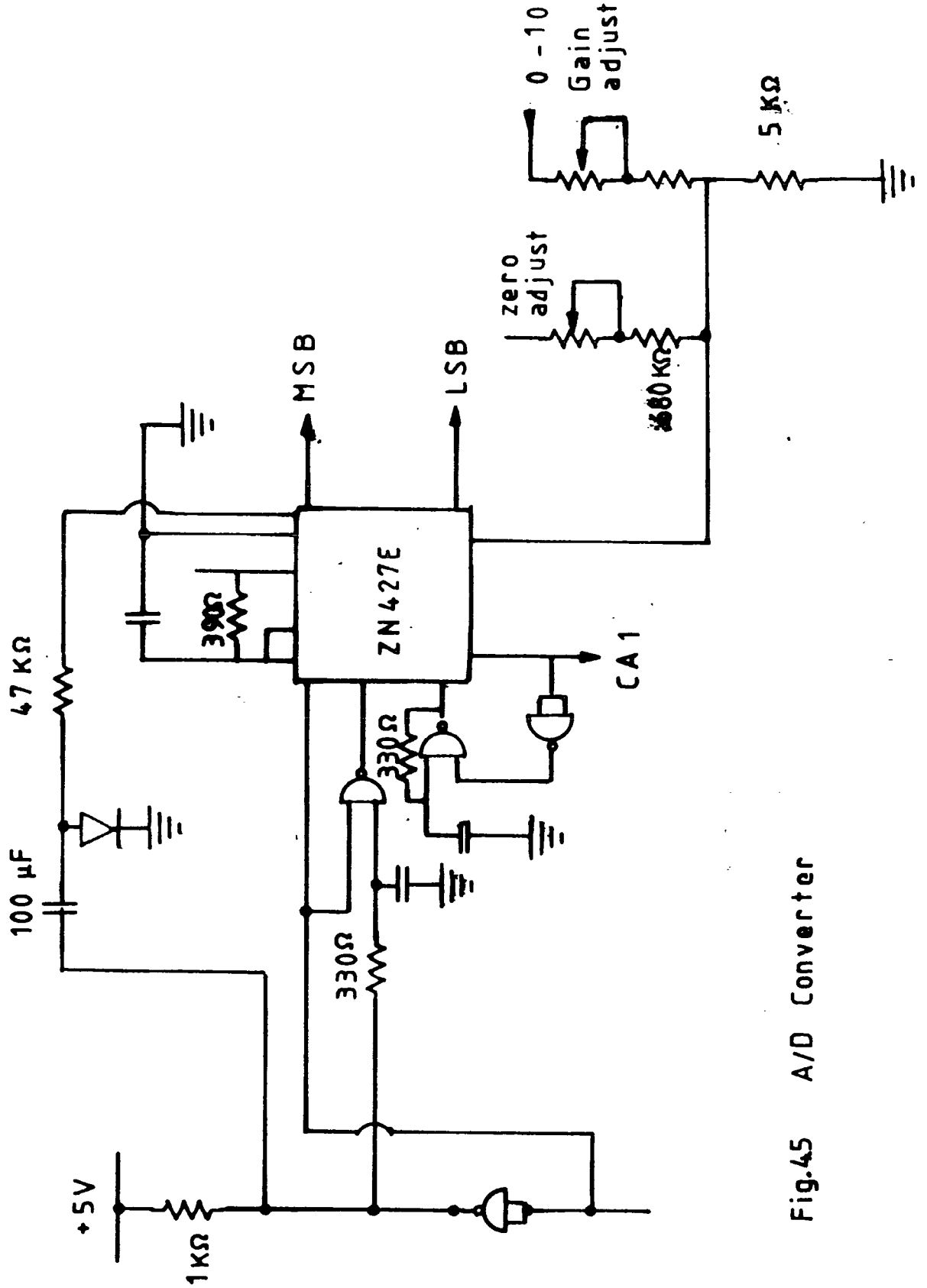

Fig.45 A/D Converter

Fig. 4.4 , whose major components are an (R-2R) ladder network, an array of precision bipolar switches, an 8-bit counter and a reference voltage unit of 2.5 V. It gives an analogue voltage output, and thus the usual current to voltage converting amplifier is not required. The accuracy of the D/A converter depends on the components used in the converter, and also on the electrical noise and leakage in the circuit. A reason and an advantage of having D/A conversion is to keep information in digital form, so that it is independent of time and temperature [21].

An A/D converter will read at various points the amplitude of the signal and its value will be allocated in a particular code using binary system. For this purpose the ZN427E was used, shown in Fig. 4.5 which is an 8-bit bipolar Successive Approximation A/D converter. The term Successive Approximation means that the operation of this converter is based on "n" successive comparisons between the analogue input, V_{in}, and the feedback voltage, V_f. The ZN427E consists of a fast comparator , (R-2R) ladder network, analogue voltage switches, successive approximation register and 2.5 V reference voltage circuit. It provides a fast conversion at a speed of 10 sec [22].

4.3.3 The Microprocessor

The initial waveform generated by the nonlinear element, energised with a sinusoidal drive, was fed into the sampler, and converted to a digital form. The

microprocessor, loaded with the "F.F.T." programme (see Appendix B) was then able to read the information and produce an output of amplitudes and phases of constituent harmonics in the distorted waveform. Here, a Commodore Business System Computer was used , and peripheral devices i.e. a printer and a tape reader were connected through the IEEE 488 port. This was a bidirectional port which allowed the peripheral devices to be interfaced simultaneously to the computer.

The computer consisted of three self-contained units. The first, was the central processor with all the necessary arithmetic and logic operations. The second, was the memory where the programme was stored and gives the computer the ability to, temporalily, save the information for future use. The third unit consisted of peripheral devices attached to the computer.

4.3.4 Diode holder

As the project involved the investigation of diode properties, the construction of a proper diode holder was essential. The holder was manufactured in a coaxial form and adapted for use with General Radio (GR) system having the characteristic impedance of 50 ohm. The main requirement for a properly designed holder was to ensure that it retained the characteristic impedance of the line. It had to meet the test that when the diode holder was short-circuited and terminated with the characteristic

impedance it produced no or negligible standing waves. Under these conditions, the dimensions of both the inner and outer conductors of the diode holder would meet the specifications required for matching purposes [11].

For a coaxial lossless transmission line, the characteristic impedance is given by [23]

$$Z_o = \frac{1}{2\pi} \sqrt{\frac{\mu}{\epsilon}} \ln \frac{a}{b} \qquad (4.6)$$

where

μ = permittivity of the medium,

ϵ = permeability of

a = internal diameter of the outer conductor

and b = diameter of the inner conductor.

It was found that the diode holder had a very satisfactory VSWR of 1.02 at 1GHz.

4.4 Testing

It was the intention that the spectral information acquired obtained by means of this method will be helpful in the selection of nonlinear devices for the best performance in particular applications. Although, the method was simple in principle, many practical difficulties had to be overcome before reliable results were obtained.

The experimental set up consisted of both analogue and digital units. Its accuracy, therefore, depended on precision of the measurements at the analogue stage and on the performance of the intervening digital units. The basic quantity to be analysed and displayed for information using the sampling unit, was the distorted output waveform from the device. A low pass filter was inserted between the source and the diode to ensure that the distorted displayed output was the true waveform from the device. The accuracy of the sampling unit was of the most importance since the validity of the method depended to a large extent on the sampling process. Furthermore, it had to be ensured that there was no loss of information because of the A/D and D/A converters.

The software, i.e. the programme, was tested by feeding in the theoretical values of a known waveform and comparing them against the practical observed values on the output of the system. The theoretical values of an ideal waveform were generated by a subroutine of the programme.

The accuracy of the complete system was also tested by feeding directly known generated signals, square pulse and triangular repetitive waveforms, and recording their output spectra. The computed readings were then compared against the expected theoretical values.

The validity of this technique was also partially confirmed by means of another method. The spectrum analyser was the alternative since it can measure the harmonic

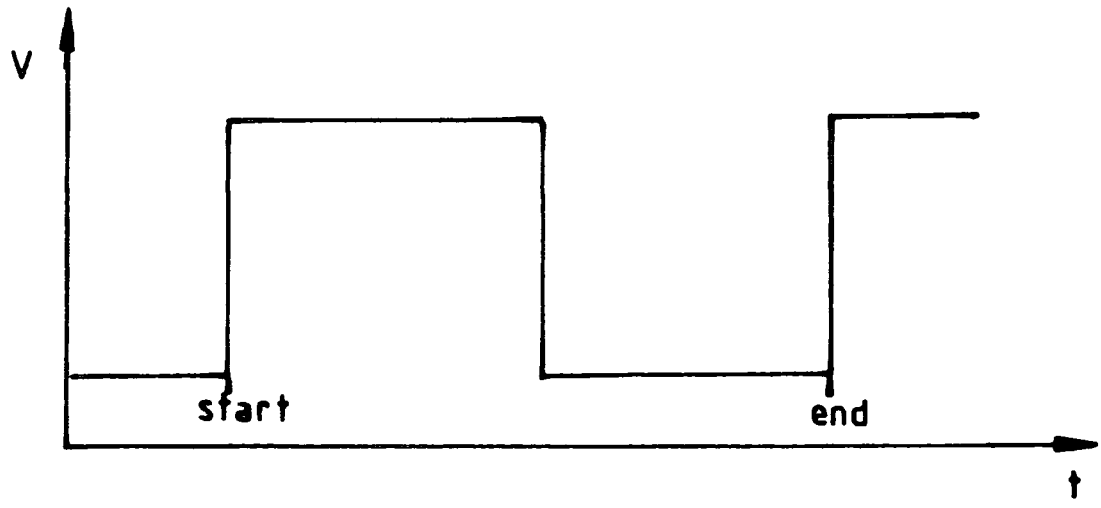

Waveform shown on display unit

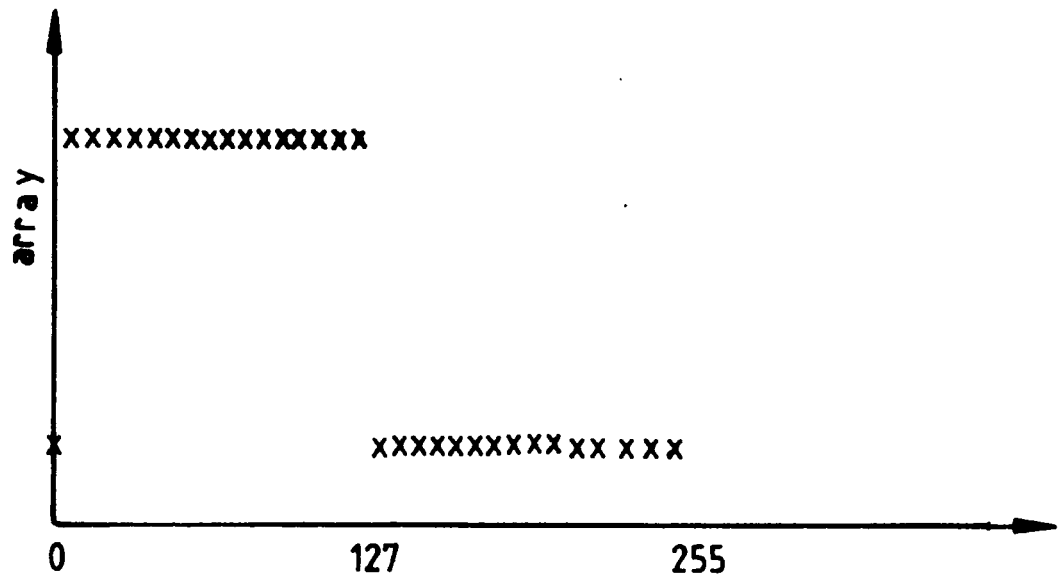

Fig.4.6 Computer Reading

amplitudes, however not the phases.

An ideal square wave pulse is shown in Fig. 4.6 . The first 63 points of the pulse represent the maximum value 10, from the 64th to 190th the minimum value of 0 and from the 191st to 253rd the value of 10. Since the ratio is one-to-one the d.c. value should be half of the height of the pulse. The "sine" components should be zero because of the even symmetry and the "cosine" components only for odd harmonics [24]. Its Fourier Coefficients given by the programme are shown in table (4.1).

Table 4.1

$a_o = 5$				
Harmonics	a_n	b_n	C_n	ϕ_n degs.
1	6.39	0	6.39	0
2	0	0	0	90
3	-2.13	0	2.13	0
4	0	0	0	90
5	1.28	0	1.28	0
6	0	0	0	90
7	-0.91	0	0.91	0
8	0	0	0	90
9	0.71	0	0.71	0
10	0	0	0	90
11	-0.58	0	0.58	0
12	0	0	0	90
13	0.49	0	0.49	0
14	0	0	0	90
15	-0.42	0	0.42	0

A theoretical square wave is represented by the following equation [25]:

$$f(t) = \frac{1}{2} + \frac{2}{TT}\left(\cos t - \frac{\cos 3t}{3} + \frac{\cos 5t}{5} - \ldots\right) \qquad (4.7)$$

and the expected values X10 are presented in table (4.2).

Table 4.2

Harmonics	a_n	b_n
1	6.36	0
2	0	0
3	-2.12	0
4	0	0
5	1.27	0
6	0	0
7	-0.91	0
8	0	0
9	0.71	0
10	0	0
11	-0.58	0
12	0	0
13	0.49	0
14	0	0
15	-0.42	0

The values of an ideal sinusoidal waveform generated within the program are given in tables (4.3) and (4.4).

Table 4.3

$a_o = 0$				
Harmonics	a_n	b_n	C_n	ϕ_n degrees
1	0	1	1	90
2	0	0	0	90
3	0	0	0	90
4	0	0	0	90
5	0	0	0	90
6	0	0	0	90

Table 4.4

$a_o = 1$				
Harmonics	a_n	b_n	C_n	ϕ_n degrees
1	0	1	1	90
2	0	0	0	90
3	0	0	0	90
4	0	0	0	90
5	0	0	0	90
6	0	0	0	90

The values of an ideal triangular waveform generated within the program are given in table (4.5).

Table 4.5

$a_o = 0$				
Harmonics	a_n	b_n	C_n	ϕ_n degrees
1	25.7	0	25.7	0
2	0	0	0	90
3	2.9	0	2.9	0
4	0	0	0	90
5	1	0	1	0
6	0	0	0	90
7	0.5	0	0.5	0
8	0	0	0	90
9	0.3	0	0.3	0
10	0	0	0	90
11	0.2	0	0.2	0
12	0	0	0	90
13	0.2	0	0.2	0
14	0	0	0	90
15	0	0	0	90

A known sinusoidal waveform was fed into the system and the results are shown in table (4.6). The tested frequency is 0.5 GHz. The maximum value of the waveform is 2 and the minimum 0.

Table 4.6

a_o = 1.004				
Harmonics	a_n	b_n	C_n	ϕ_n degrees
1	-0.0122	1.0058	1.0058	-89.3
2	0	0	0	90
3	0	0	0	90
4	0	0	0	90
5	0	0	0	90

All the harmonics should be zero except for the fundamental because if the waveform is a pure sinusoid. Also, a_1=0 because it is sinusoidal signal and hence cosine components should not exist. The overall percentage error was found to be less than 0.5%.

To test the error of the diode holder a generated sinusoidal waveform was applied through the empty holder at a frequency of 0.5 GHz . The maximum value of the waveform was 0.738 and the minimum 0. The results are shown in table (4.7).

Table 4.7

a_o = 0.3362				
Harmonics	a_n	b_n	C_n	ϕ_n degrees
1	-0.0248	0.3565	0.3573	-86.0206
2	-0.0209	0.0189	0.0281	-42.12
3	-0.0152	-3.2E-03	0.154	11.8886
4	1.2E-03	6.3E-03	6.4E-03	79.12
5	-3.4E-03	6E-03	3.4E-03	-61.6

A square wave generated from a source was analysed with this method. The results are shown in table (4.8). The frequency tested was 25 MHz, the maximum value of the waveform 10.336 and the minimum 0.

Table 4.8

a_o = 5.18				
Harmonics	a_n	b_n	C_n	ϕ_n degrees
1	-0.36	6.59	6.59	-86.88
2	-0.09	0.02	0.09	-12.53
3	-0.35	2.21	2.23	-81.01
4	-0.1	0.01	0.1	- 5.72
5	-0.38	1.32	1.37	-73.95
6	-0.41	0	0.1	0
7	-0.1	0.88	0.97	-65.02
8	-0.14	0	0.14	0
9	-0.4	0.65	0.76	-58.4
10	-0.12	-0.05	0.13	22.61

4.5 Summary

It was shown that the determination of the harmonic spectrum generated by a nonlinear device, energised by a high frequency fundamental source was possible. The method, based on Numerical Fourier Analysis used a closed-loop system incorporating a sampling unit which also translated high frequency distorted waveform to a low frequency display. The process of the analysis would have been tedious and lengthy but with the aid of a microprocessor it was reduced to a simpler and quicker procedure.

Nonlinear devices are extensivly used in high frequency

applications and it is an essential phenomenon to the operation of many circuits. In these applications the aims are usually to accentuate the nonlinearity of the device so that the basic harmonic-generated process is initiated. In addition, the generated spectrum offers a means of characterising the device, as fundamental V-I plots, at these frequencies lose their meaning. Spectral characterisation represents the actual nonlinearity of the device under normal working conditions. The method also offers a possibility of comparison between the devices of the same type and their capabilities in particular applications.

It was found that the errors in the harmonic measurements were lower at frequencies below 1GHz. This was because the sampling unit limiting frequency of operation was about 1.2 GHz caused by a risetime of the sampling pulse of about 0.5 nsec. Even in the case of a low frequency, the errors were in the order of 10%. To improve the accuracy it was necessary therefore, to use a high precision equipment and higher power source to cover a bigger range of drive levels.

The resulting spectra or "fingerprints" of the devices introduced a new method of characterisation. Evaluation of devices may next be carried out by examining and interpreting the patterns of the spectra.

CHAPTER 5

MEASUREMENTS AND PROCEDURES

5.1 Introduction

The testing of the system and the behaviour of the diode holder were considered in the previous chapter. The measurement procedures described here are connected with the computer-aided experimental technique used in the determination of generated spectra of nonlinear elements. Since the nonlinear element response is dependent on the input level there is a need first to decide, which parameter should be chosen to represent the drive. The difficulties involved in carrying out the measurements of the input quantities forced us to consider the current at the fundamental frequency measured in the load as the drive parameter. The values of this fundamental drive current are important and should be stated with any measurements of C-V and Q-V characteristics. The available instruments and the experimental arrangements for the measurements and the results obtained will be discussed in this chapter.

5.2 Choice and Measurement of Drive Level

The characteristics of nonlinear diodes or elements are level-dependent and therefore the actual drive conditions must be specified. The quantity selected for the drive level must be reliable and repeatable. Applied power,

voltage and current at the fundamental frequency were considered for the representation of the drive level. Voltage could not be used because no voltmeter of [11] sufficiently high impedance was available. In addition, the measurement of the voltage at the end of a mismatched line creates problems because of the standing waves. Power was not a suitable quantity because the power-meter normally employes a 50 ohm thermistor and there are no frequency selective instrument available of high enough impedance.

It was finally decided that the drive level should be represented by the current, I_1, at the fundamental frequency. The components of the generated harmonic spectra can then be recorded with reference to this level. It was also noted that the upper limit of the drive current should be restricted to avoid the burn-out level of the diode.

The measurement of the drive current was carried out by measuring the voltage on the outpute by means of a spectrum analyser, assuming that the current at the input of 50 ohm load will be the same as the current through the diode.

5.3 Measurements with Slotted Line

A slotted line is a section of uniform lossless transmission line with a longitudinally-oriented slot which provides access to a pick-up probe that detects voltage variations on the line as it moves along it. The voltage induced in the probe circuit is proportional to that

existing between the inner and the outer conductors of the line at any probe position [26].

One of the most informative measurements that can be carried out on a slotted line, is the measurement of the Voltage Standing Wave Ratio (VSWR). The block diagram of the slotted line assembly is shown in Fig. 5.1. From the value of the VSWR, the capacitance of the diode can be deduced, following a series of calculations. Knowing the capacitance which is a function of the applied bias the C-V characteristic of the diode may be obtained.

Using the VSWR, the impedance of a load terminating the line may be calculated. In this case the load is the diode, and its impedance is given by [27]

$$Z_L = Z_o \frac{1 + \rho}{1 - \rho}$$

or

$$Z_L = Z_o \frac{1 - jS_v \tan(\beta X_{min})}{S_v - j\tan(\beta X_{min})} \qquad (5.1)$$

$$\beta = \frac{2\pi}{\lambda} \qquad (5.2)$$

where

β = phase constant,

S_v = VSWR,

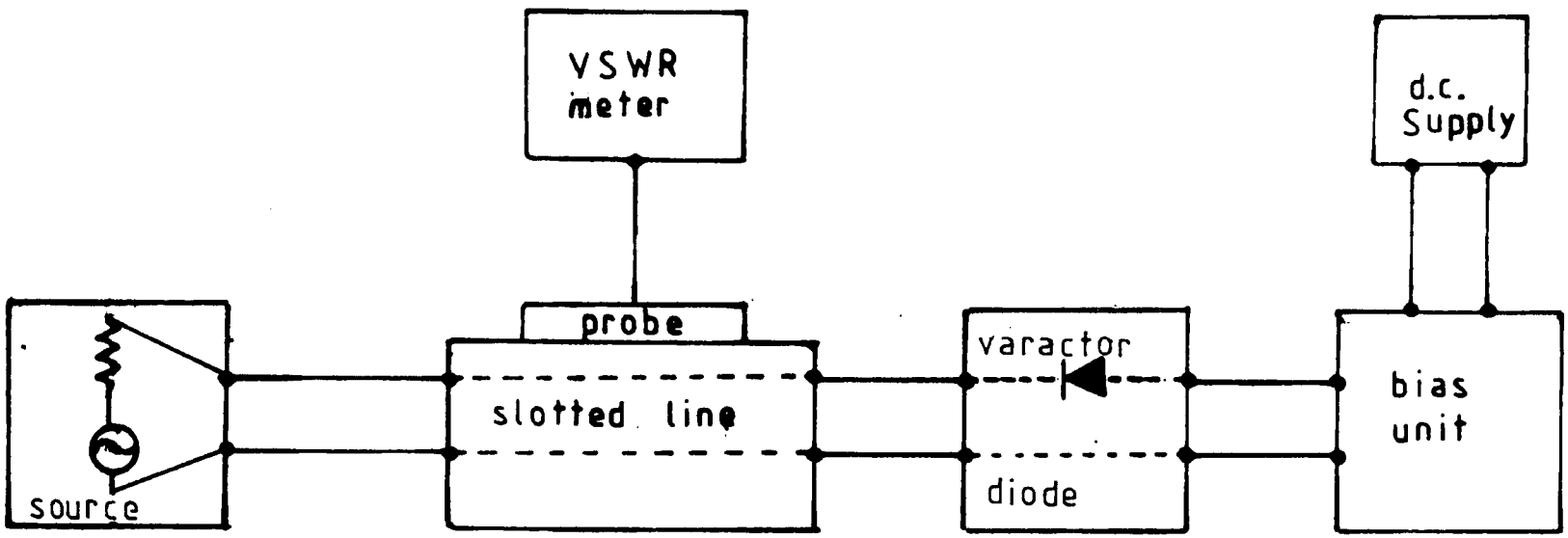

Fig.5.1 Block Diagram of Slotted Line Measurements

λ = wavelength,

and ρ = reflection coefficient of the line due to the diode.

From the impedance of the diode its capacitance may be calculated [27].

$$X_c = \frac{1}{wC}$$

or

$$C = \frac{1}{2\pi f X_c} \qquad (5.3)$$

Knowing the capacitance and the applied bias voltage on the diode its C-V characteristic can be drawn.

Using the obtained capacitance from eqn. (5.3) and the following relation

$$Q = CV \qquad (5.4)$$

the Q-V characteristic of the diode can also be obtained.

A DC4303A GaAs No.3 diode was tested at 0.45 GHz and different bias levels. The C-V and Q-V characteristics are presented in Fig. 6.1 in chapter 6.

The measurements were carried out according to the

following steps:

(i) The frequency was verified by measuring the wavelength along the slotted line,

(ii) Using a VSWR-meter the VSWR of the diode was measured.

(iii) The position of X_{min} was recorded,

(iv) Varying the applied bias voltage, via the bias unit, values of VSWR were measured, together with the positions of minima, X_{min}, of the standing wave pattern.

5.4 Spectrum Measurements

As the aim of the work is to assess the harmonic generating properties of a diode, the method of spectral characterisation becomes appropriate. The spectra of interest will be those of the amplitude and relative phases.

The quantities that can be determined are the voltage measured across a known impedance at n^{th} harmonic and the drive level which was stated earlier to be the current at the fundamental.

For the Sampling Method Measurements, the experimental block arrangement for the spectrum measurement is shown in Fig. 4.1. It consists of analogue and digital parts. The analogue part includes signal generator, bias unit, diode holder, sampler and a display unit. The digital part includes A/D, D/A, converters, microprocessor and the

peripheral instruments, e.g. printer, tape reader.

The signal source type HP3200B VHF oscillator used in this method, covers the frequency range from 10 to 500 MHz. Its frequency accuracy is within 2%. Across the 50 ohm external load it can deliver a maximum power output greater than 200 mW in the frequency range 10 to 130 MHz, greater than 150 mW from 130 to 260 MHz and greater than 25 mW from 260 to 500 MHz. Initially, the frequency of the oscillator was set accurately to 475 MHz by calibrating it against the spectrum analyzer.

The bias unit type GR874-FBL was connected between the signal generator and the diode holder. This unit has impedance of 50 ohm and a satisfactory VSWR of less than 1.25 between 300 MHz and 5 GHz. It provided a reverse bias voltage, necessary to set the operational point of the varactor diode and comprised a blocking capacitor in series with the line, an isolating choke, and a low pass filter. The bias unit was inserted at the source end of the line, in order to avoid reflections at the measurement terminals.

Driving the signal from the source through the diode holder to the sampler as it was described in chapter 4 the amplitudes and relative phases for each harmonic of the diodes were obtained. The V-I plots of these results are presented in Figs. 6.6 - 6.45 where I_1 is the drive current and V is the voltage output of the diode developed across the known impedance of the sampler which was 50 ohm [11].

In order to confirm these results, another method had to be used. In this method a spectrum analyzer was connected after the diode holder, in place of the sampler, and the same sets of measurements were carried out under the same conditions. The Spectrum Analyzer (type TR4131/E) used in this method covered a wide frequency range from 10 kHz to 3500 MHz. The results are presented in Figs. 6.46 - 6.65.

The above results were obtained for the 2nd to 6th harmonics. The experimental set-up for the V-I characteristics of the fundamental, is shown in Fig. 5.2. A high impedance voltmeter was connected after the generator to measure the voltage at the input to the diode. Measuring the output voltage through the spectrum analyzer and subtracting this value from the input voltage, the diode voltage was obtained. The drive current was measured by the method described in para. 5.2. The results are presented in Figs. 6.2 - 6.5.

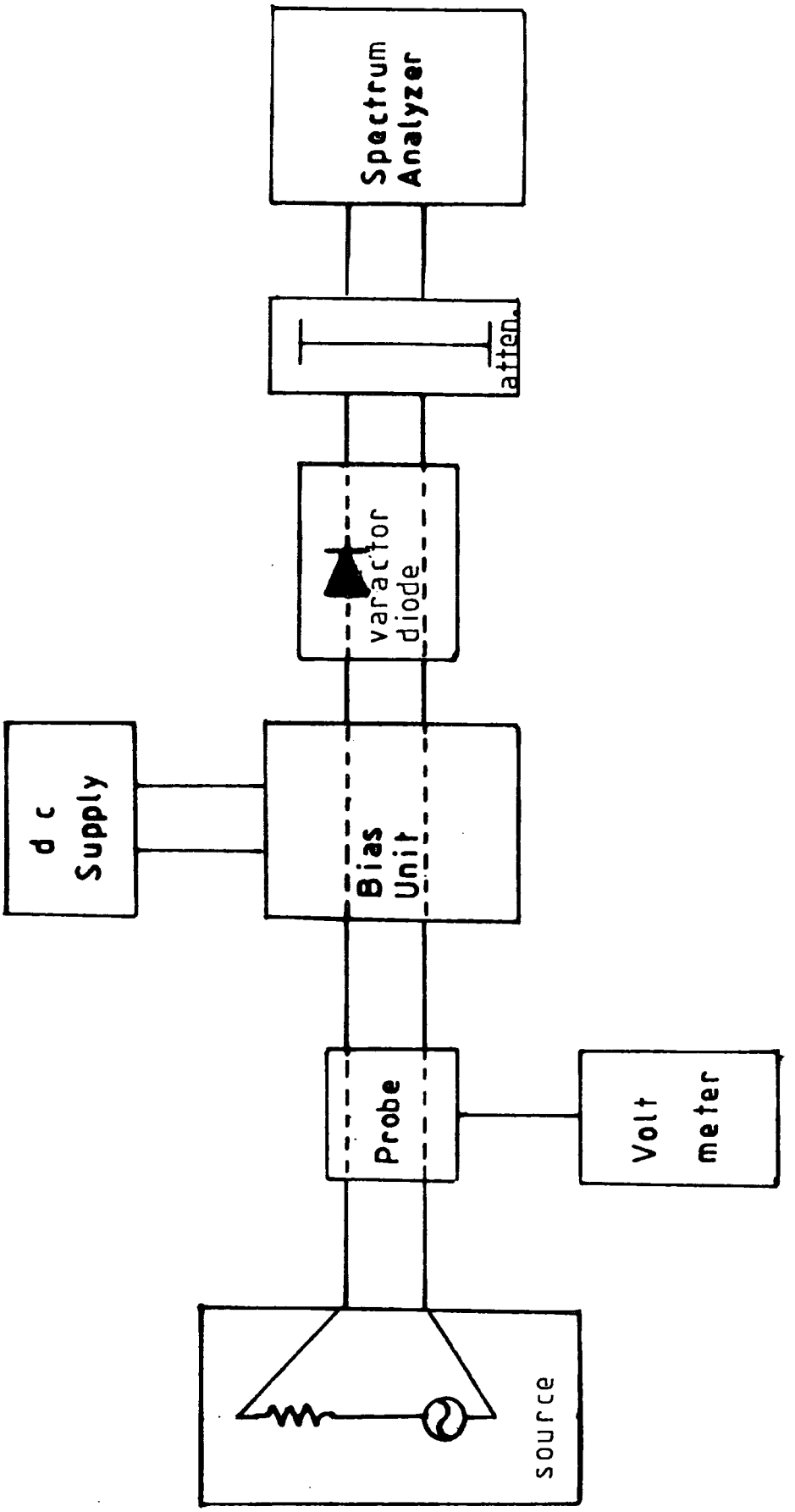

Fig. 5.2 Measurements Assembly

CHAPTER 6

RESULTS

6.1 Introduction

The results of the spectrum measurements carried out on four diodes are presented in this chapter. As it was mentioned before these results are shown in form of graphs, from which the diode harmonic generating properties can be found. The experimental methods and procedures were already discussed in chapter 5.

In order to overcome the need for a large number of plots, an alternative method of representing the amplitudes and phases of harmonics against the drive level was introduced. This was done by combining the harmonic spectra of a diode at different drive levels on a single plot. Each complete display contains therefore the "fingerprint" at every energised level which can be extracted at will. In addition, the dynamic behaviour of the diodes may be compared for different levels and particular harmonics.

6.2 C-V, Q-V Measurements

Fig. 6.1 presents the C-V and Q-V characteristics of a DC4303A GaAs Varactor diode which was tested at 0.45 GHz and different biases levels at a drive level of 4.2 mA. The lowest value of the capacitance at -10 V bias was 0.48 pF and at -1 V bias it reached 1.07 pF.

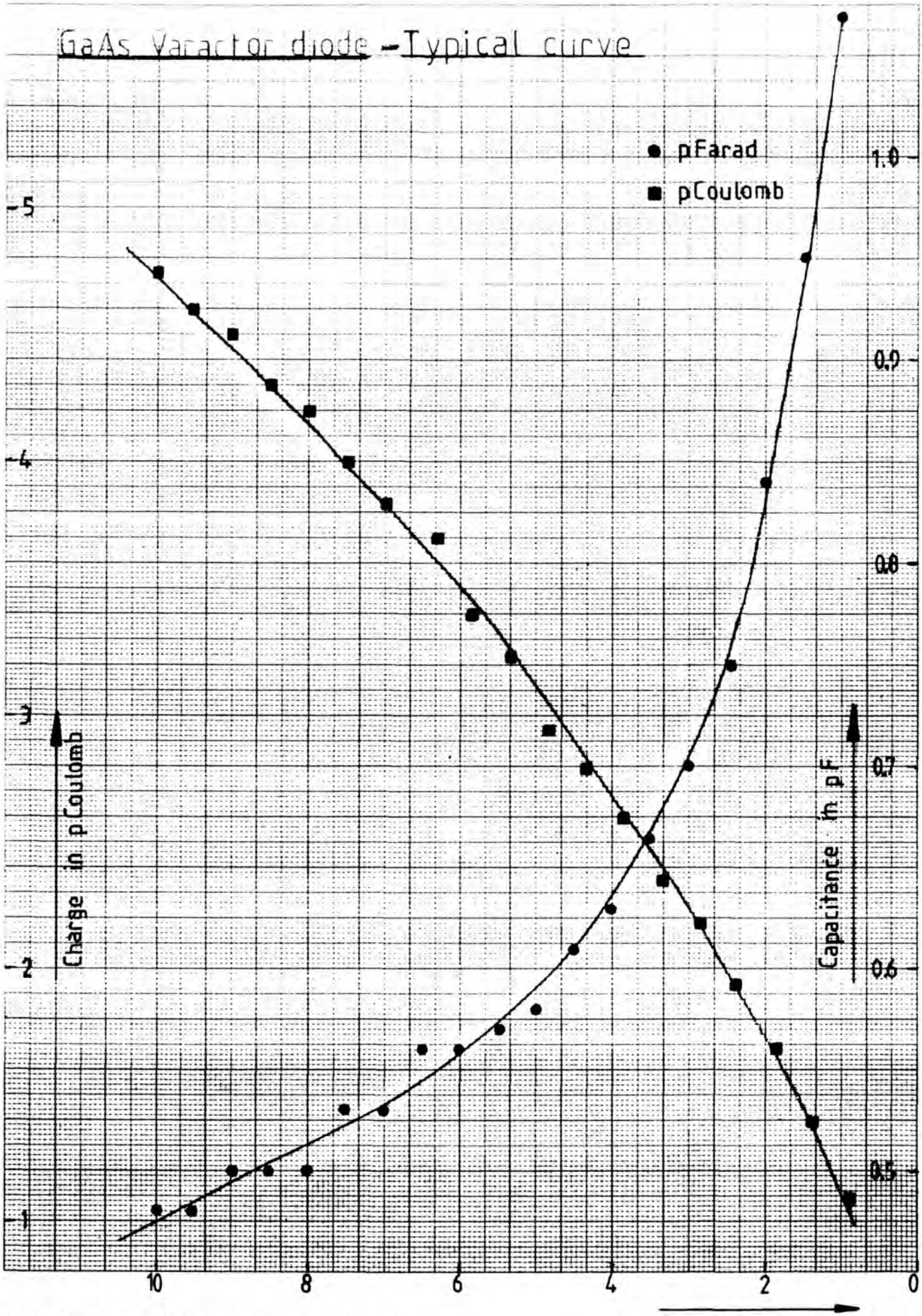

Fig. 6.1 C-V, Q-V Characteristics

6.3 I-V of the Fundamental

The input voltage, V_{in}, of the diode is sinusoidal and at the fundamental frequency, but in actual fact it may contain some of the harmonics. On the other hand the output voltage, V_1, was at the fundamental frequency because it was measured selectively using spectrum analyzer. The voltage across the diode is the difference between the two i.e. $V_{in} - V_1$ assumed to be at the fundamental frequency. The plots representing the fundamental V-I relationships are shown in Figs. 6.2, 6.3, 6.4 and 6.5. When the diode is driven higher the error of the measurements increases as the assumption that the diode voltage is at the fundamental frequency may not strictly hold. The curves at higher level may be extrapolated.

6.4 Sampling Method Results

The fundamental drive frequency chosen for the mesurements was 0.475 GHz in order to maintain the maximum power output from the particular source used. Four diodes of the same type, DC4303A GaAs, were examined against the drive current up to 16 mA, for three different bias conditions, i.e. -2, -4, -6 volts. Comparing the amplitude spectra it can be seen that the changes due to different biases do not vary significantly. It was decided, therefore, that only one plot will be adequate to show the diode behaviour.

The patterns for the second and third harmonics appear

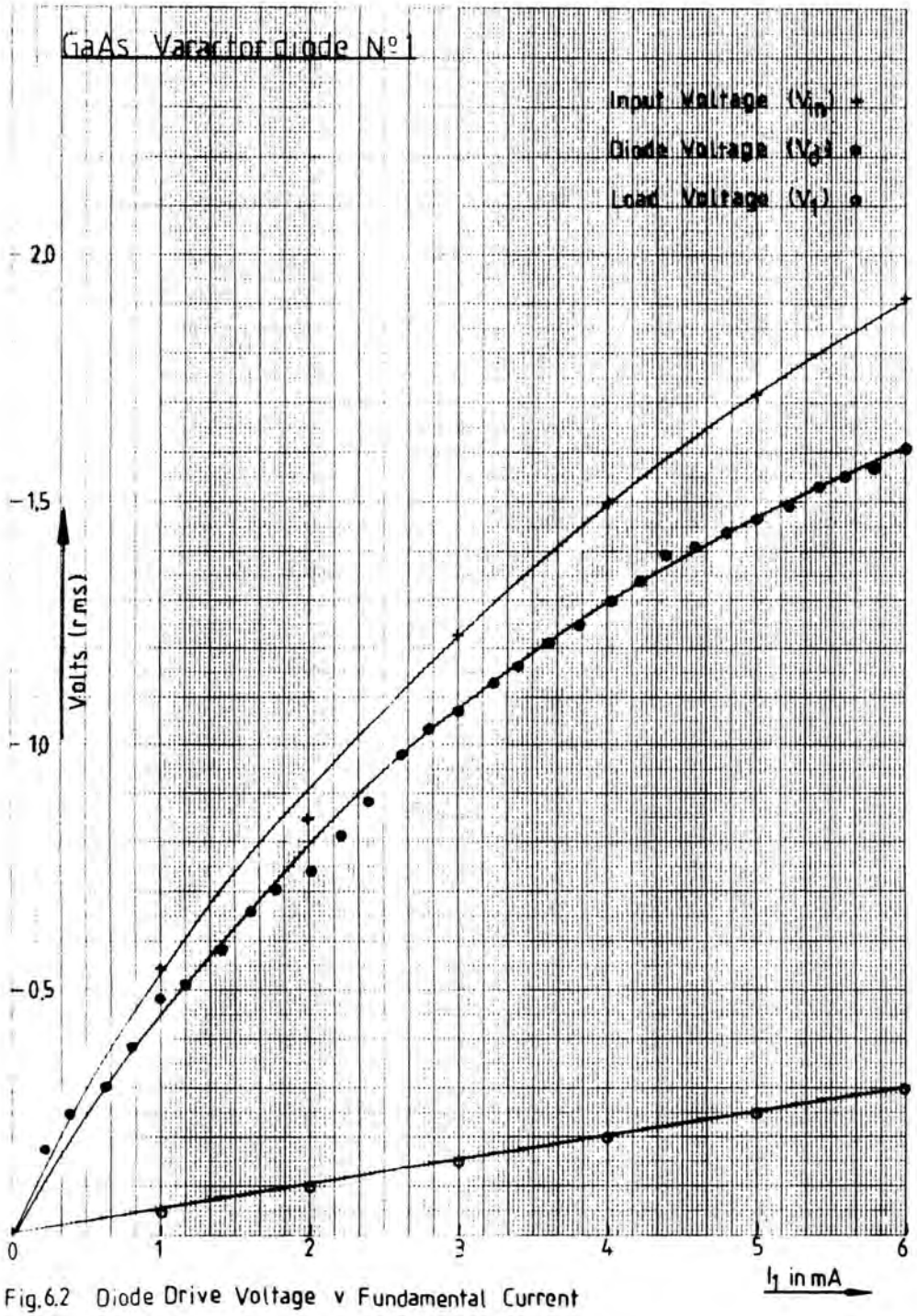

Fig. 6.2 Diode Drive Voltage v Fundamental Current

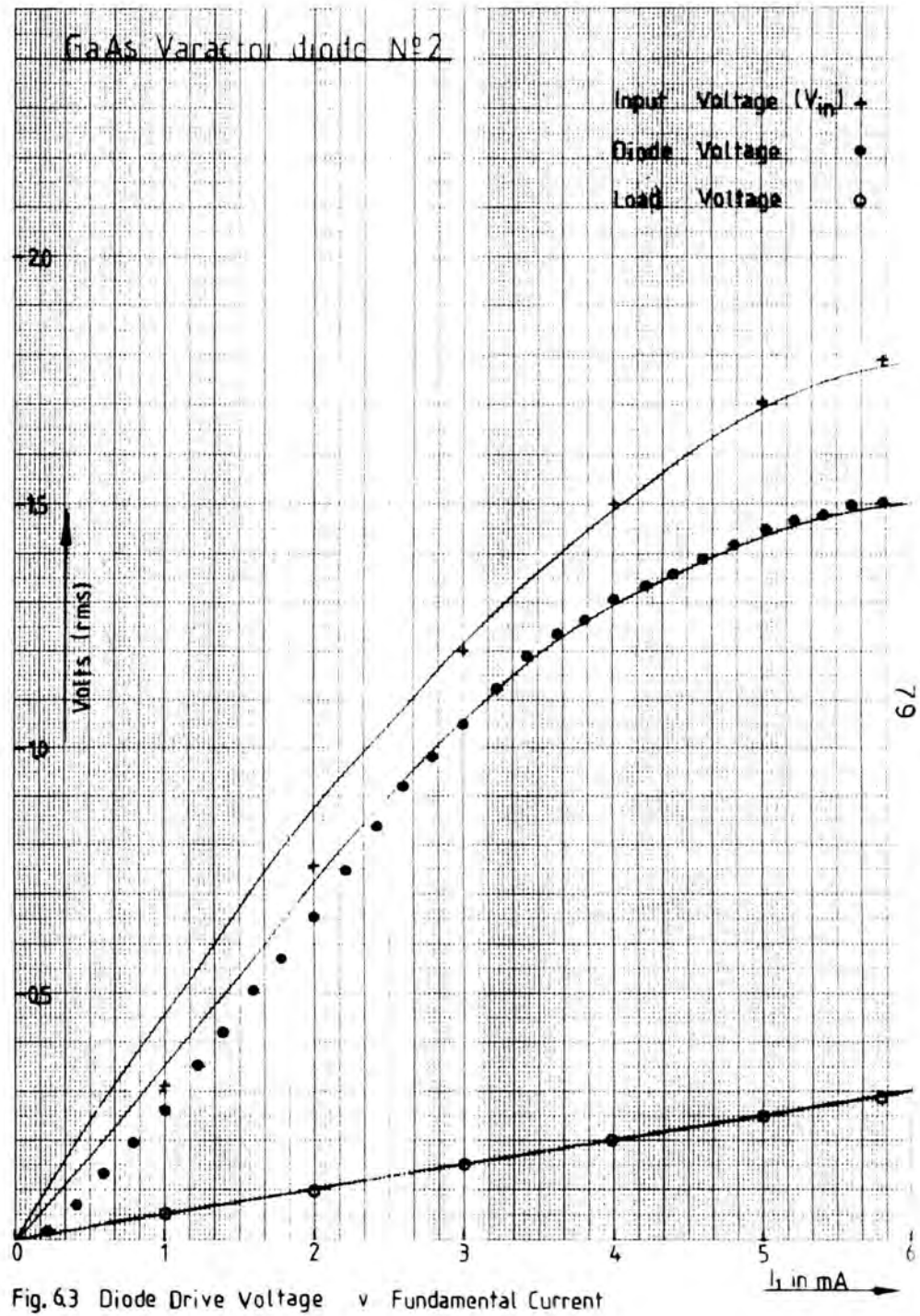

Fig. 6.3 Diode Drive Voltage v Fundamental Current

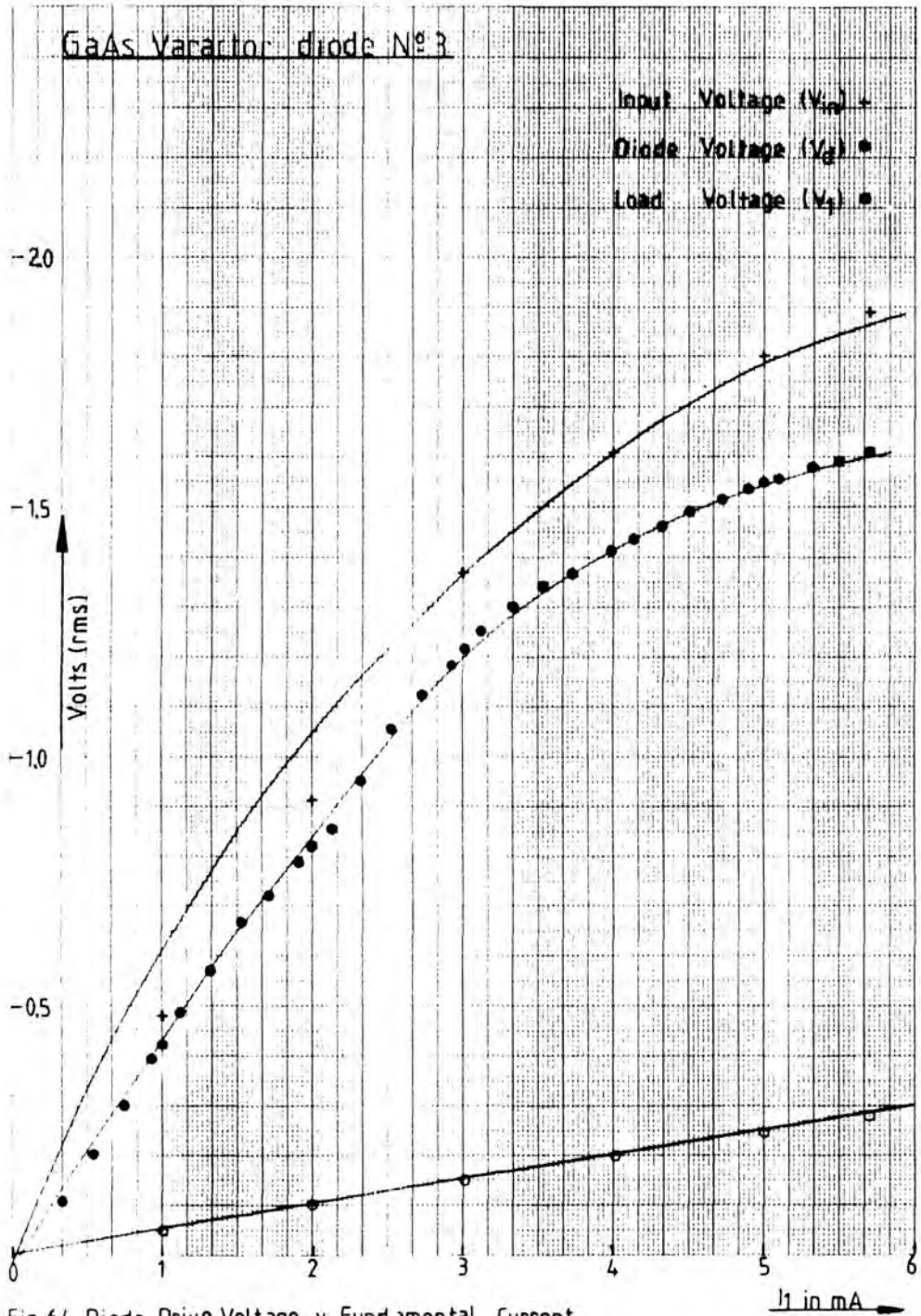

Fig. 6.4 Diode Drive Voltage v Fundamental Current

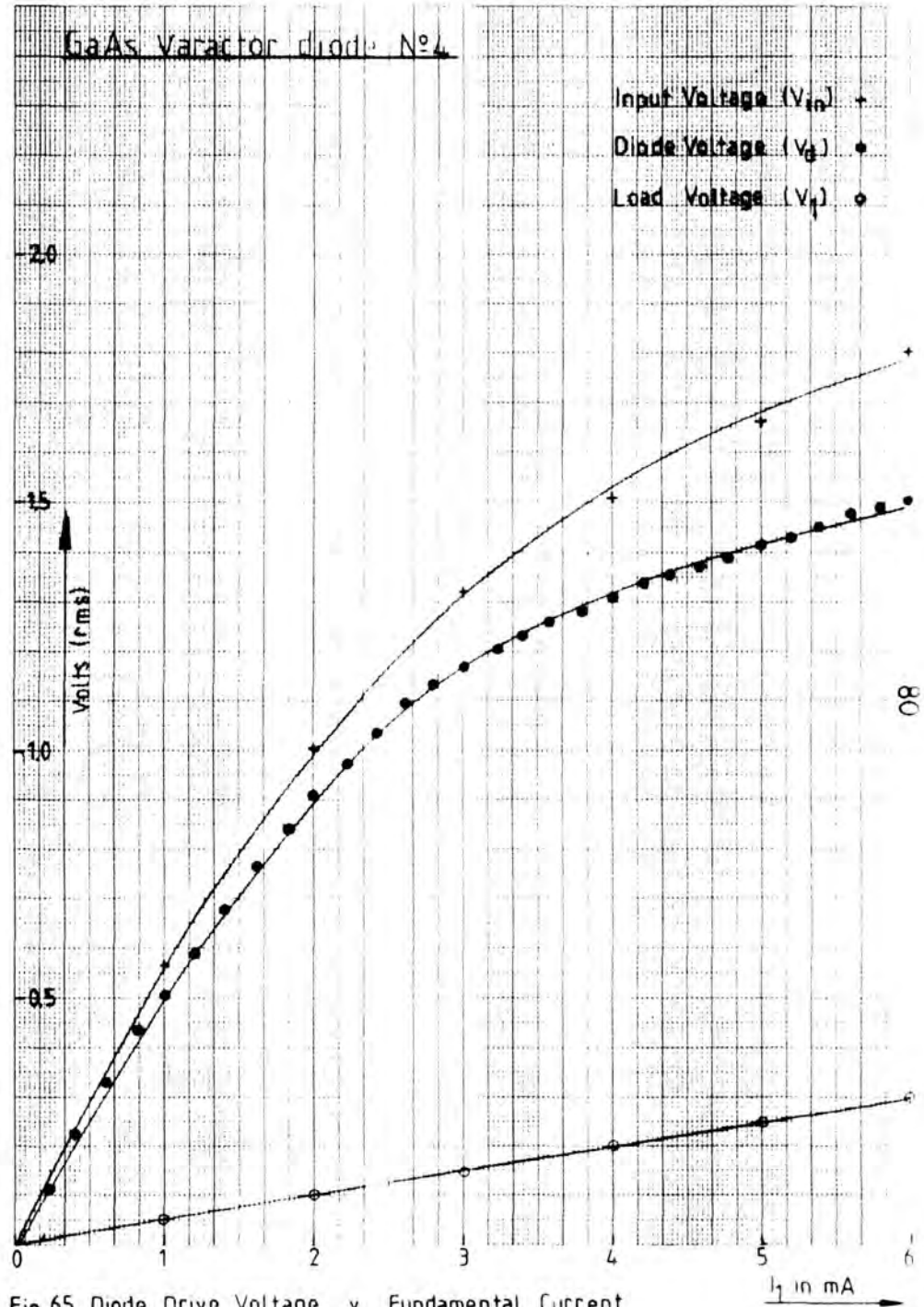

Fig. 6.5 Diode Drive Voltage v Fundamental Current

to be similar for the four diodes as shown in Figs. 6.6, 6.11, 6.16 and 6.21. If the level is increased the input pulse becomes narrower and most harmonics tend to occur in the first lobe of the spectrum envelope. The theoretical plot of the envelope is shown in Fig. 6.66. It was found that the second harmonic has appeared in the first lobe for all the used drive levels. Slight variations with bias are observed for the second harmonic in all the diodes and the plot drawn attempted to show the overall average tendency.

Similar behaviour was observed for the third harmonic, which increased with increasing drive level, as shown in Figs. 6.7, 6.12, 6.17 and 6.22. It was also noticeable that the slope for the third harmonic in diodes Nº 3 and 4 was smaller than in diodes Nº 1 and 2. The third harmonic for all the diodes was of a lower level than the second harmonic and still occurred in the first lobe.

The plots for the fourth harmonic amplitudes, in all the diodes, had a dip close to around 8 mA of drive current as shown in Figs. 6.8, 6.13, 6.18 and 6.23. The amplitudes were found to be lower than those of the second and the third for all the diodes. The dip indicated that the fourth harmonic below 8 mA drive level occurs in the second lobe and with increased drive level shifts into the first lobe.

Similar pattern was also observed for the behaviour of the fifth harmonic for each of the diodes. This is presented in Figs. 6.9, 6.14, 6.19 and 6.24. The values of

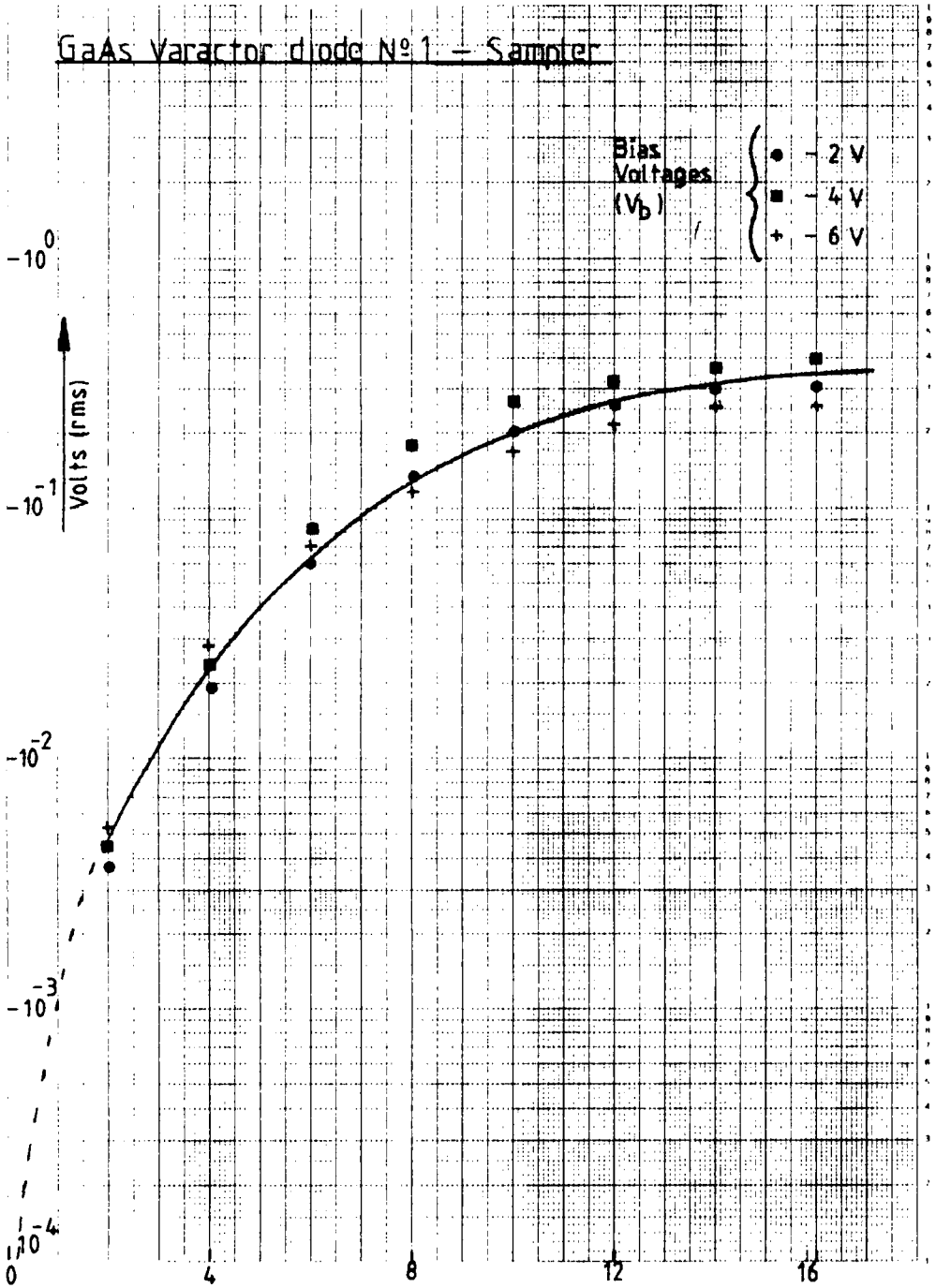

Fig. 6.6 2nd Harmonic Amplitudes v Drive Level

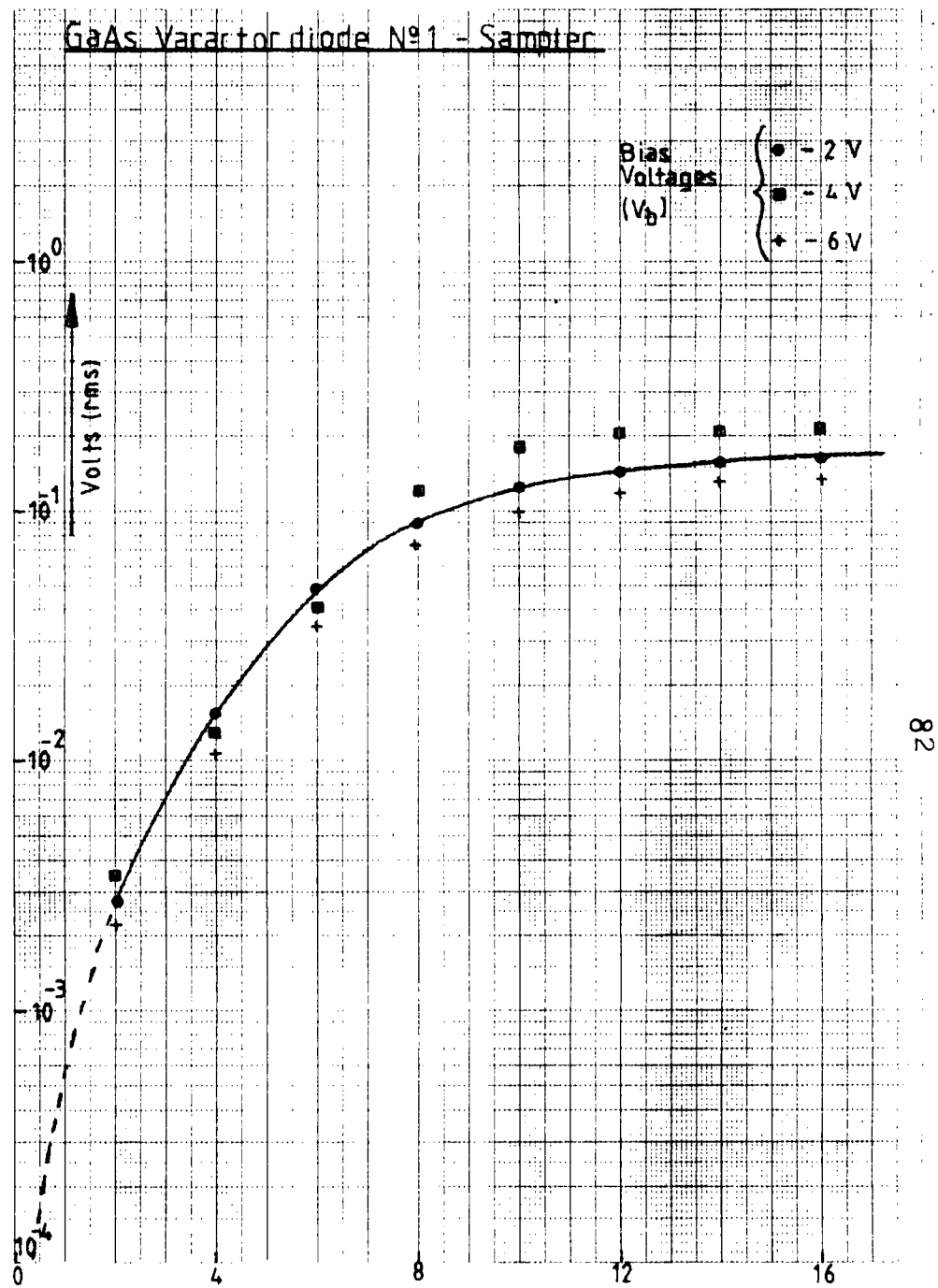

Fig. 6.7 3rd Harmonic Amplitudes v Drive Level

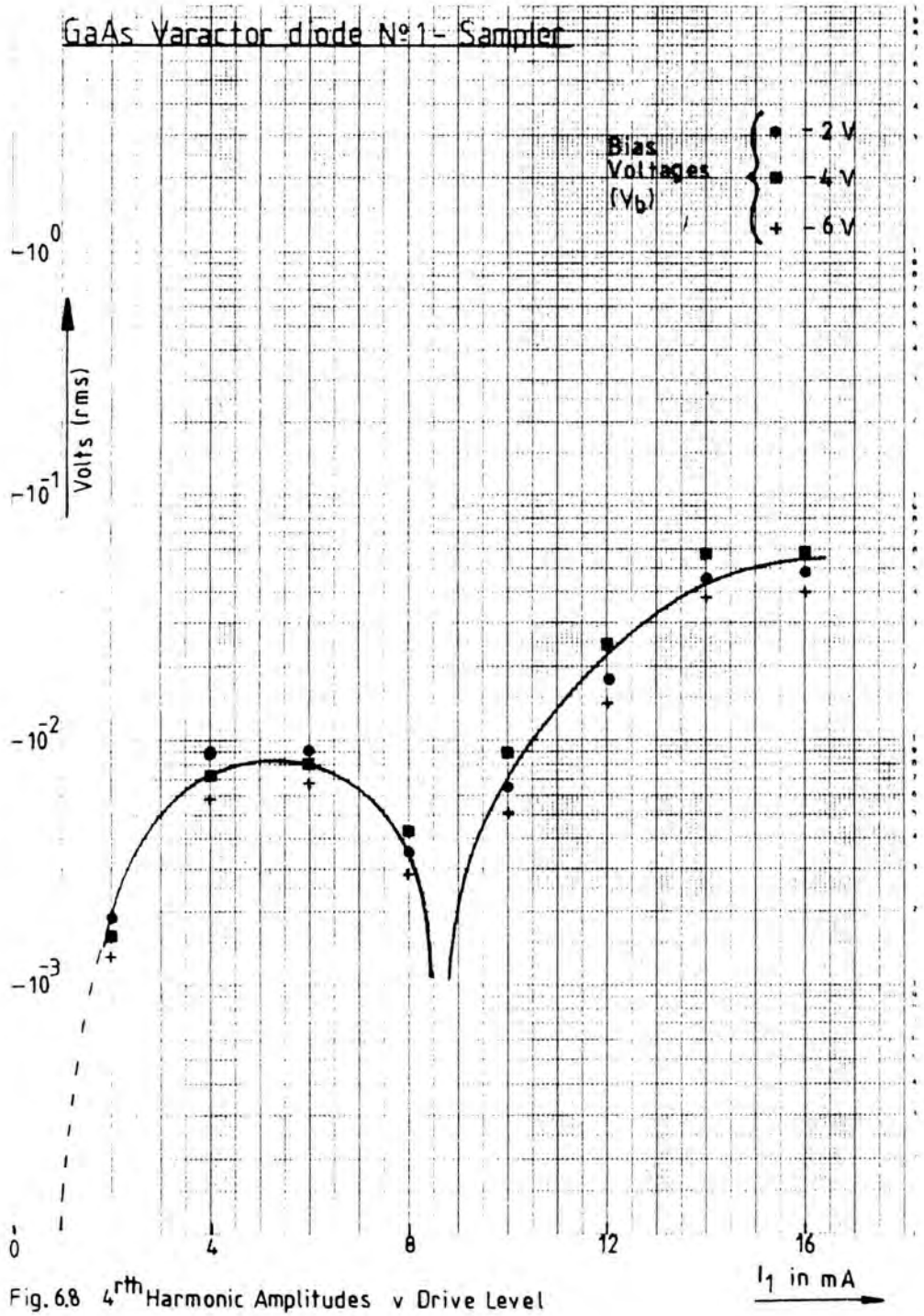

Fig. 6.8 4rth Harmonic Amplitudes v Drive Level

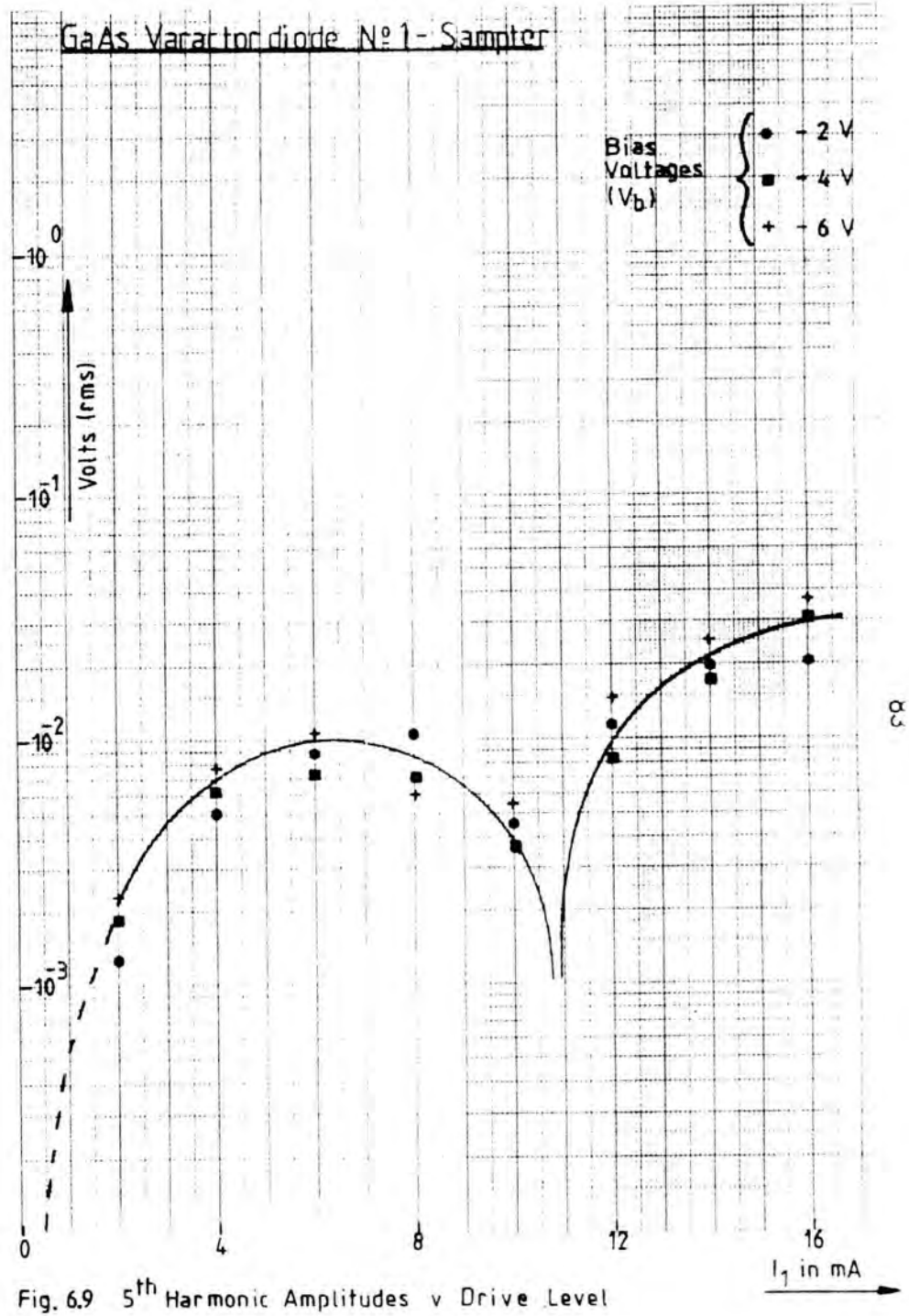

Fig. 6.9 5th Harmonic Amplitudes v Drive Level

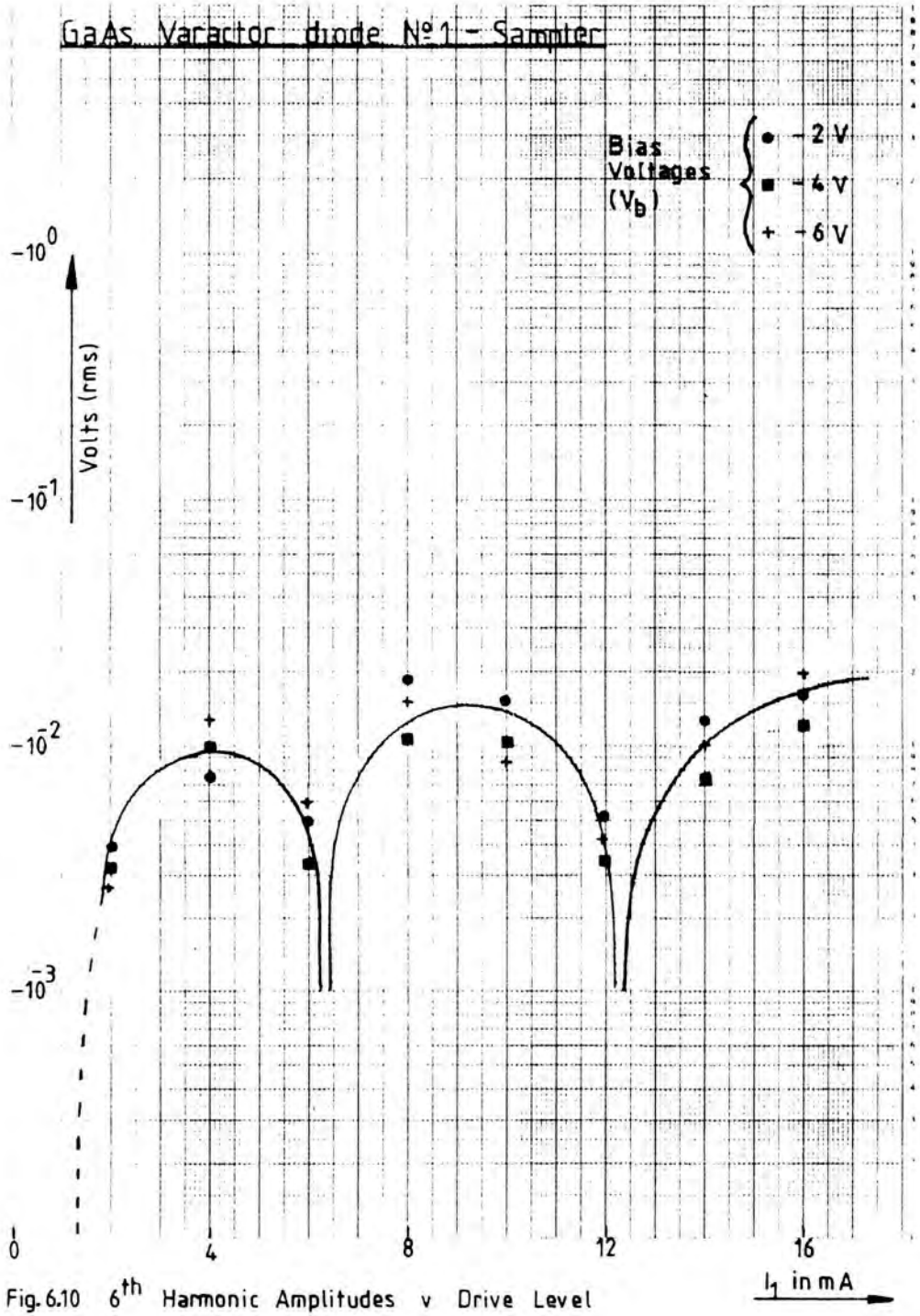

Fig. 6.10 6th Harmonic Amplitudes v Drive Level

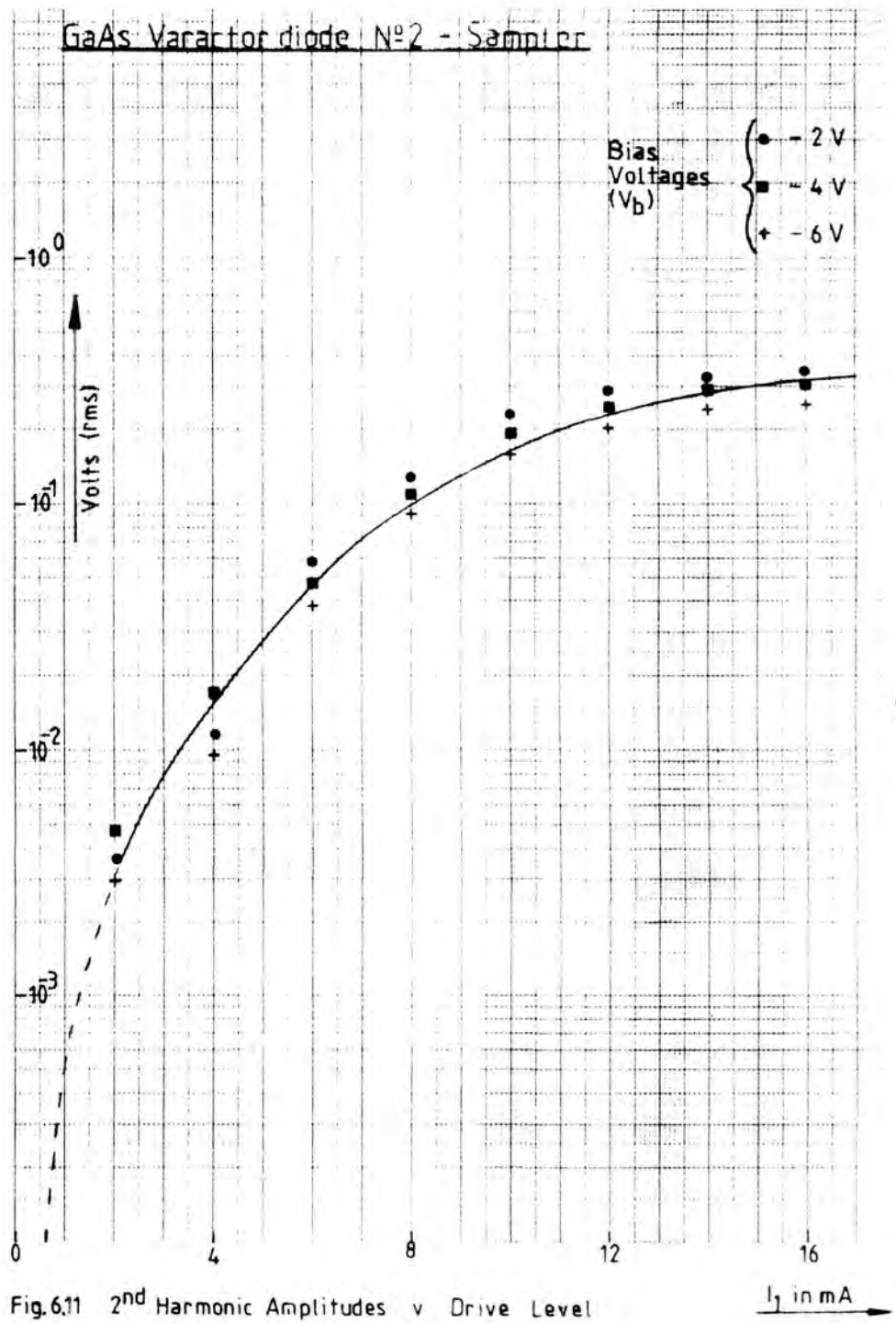

Fig. 6.11 2nd Harmonic Amplitudes v Drive Level

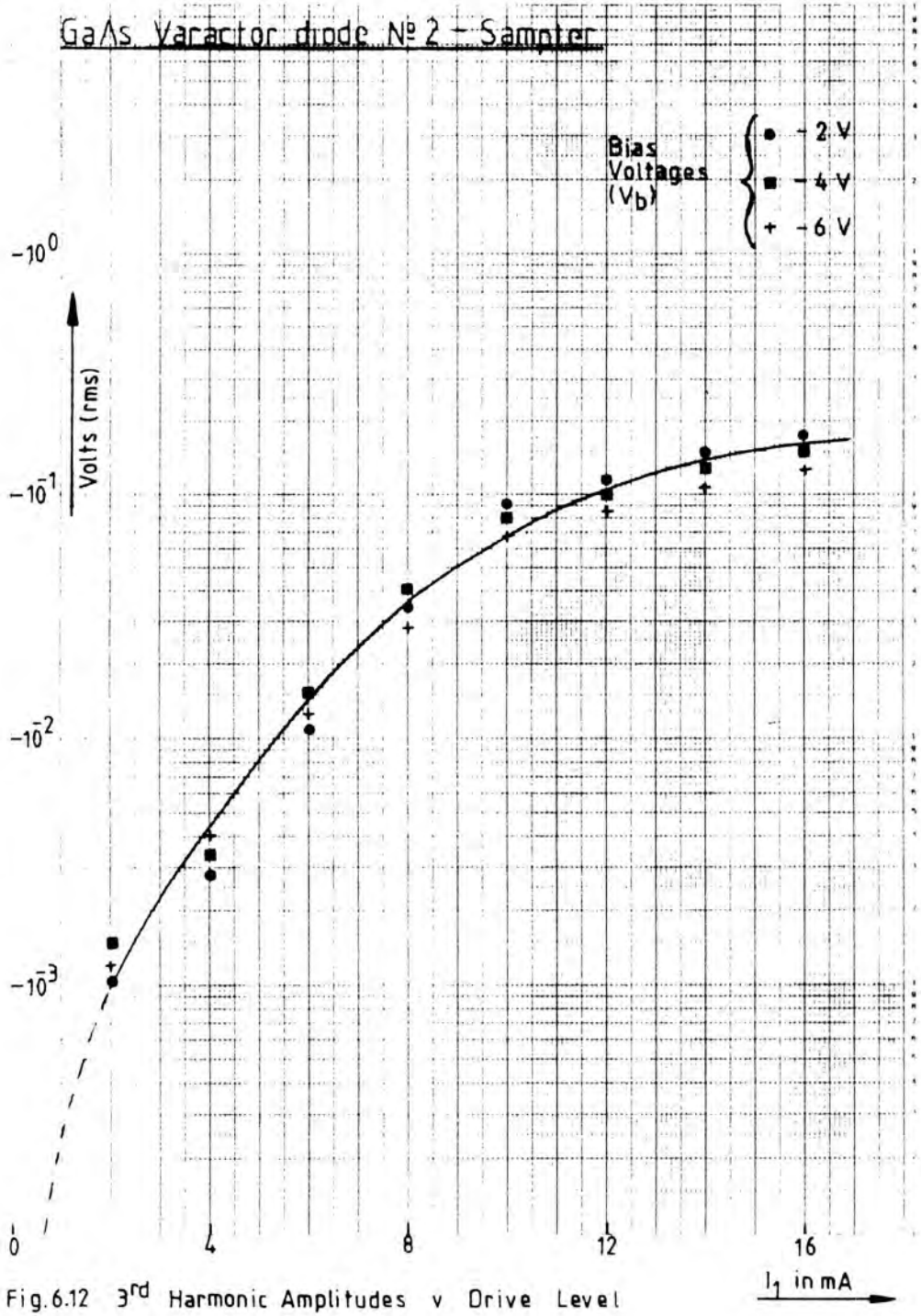

Fig.6.12 3rd Harmonic Amplitudes v Drive Level

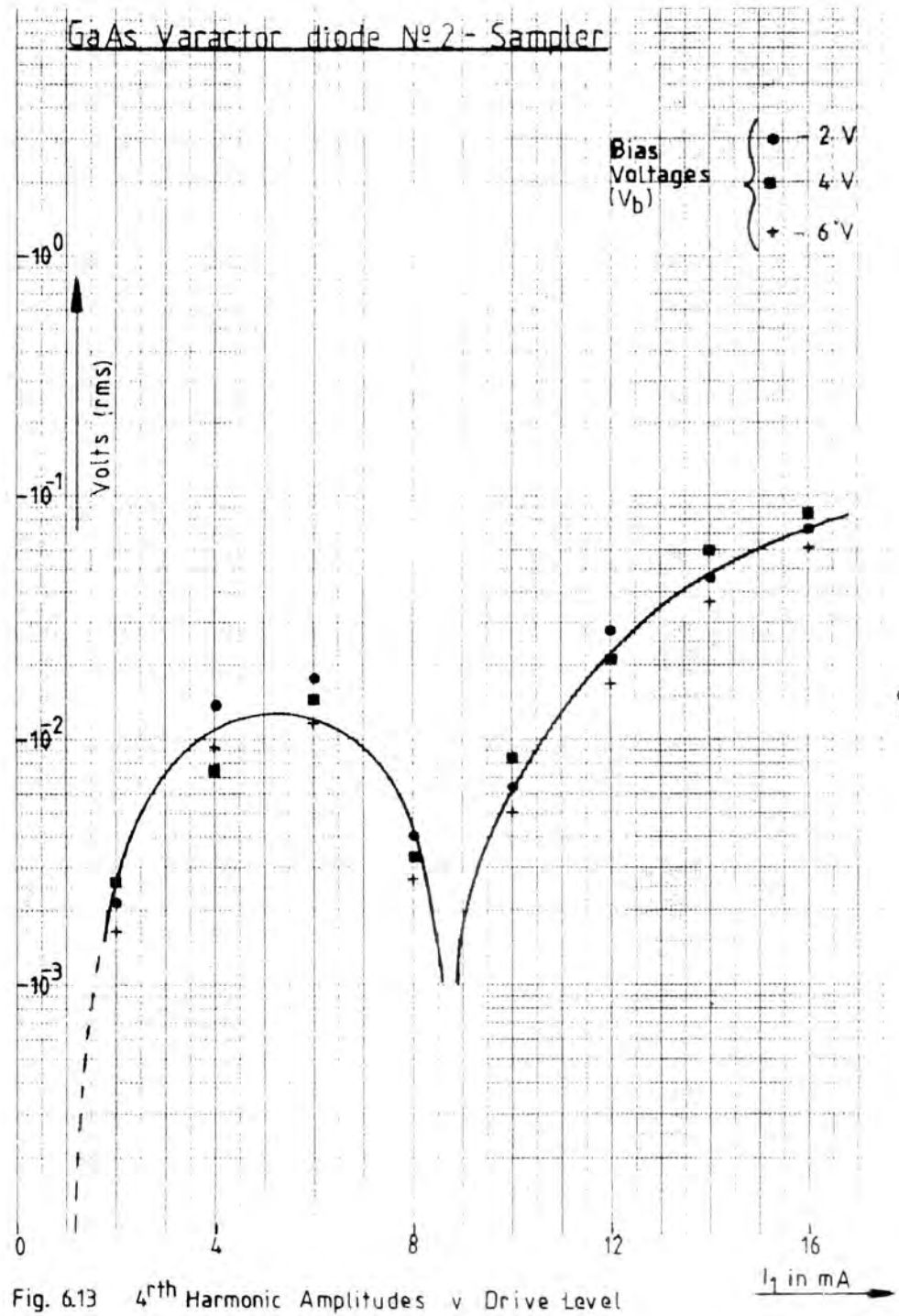

Fig. 6.13 4rth Harmonic Amplitudes v Drive Level

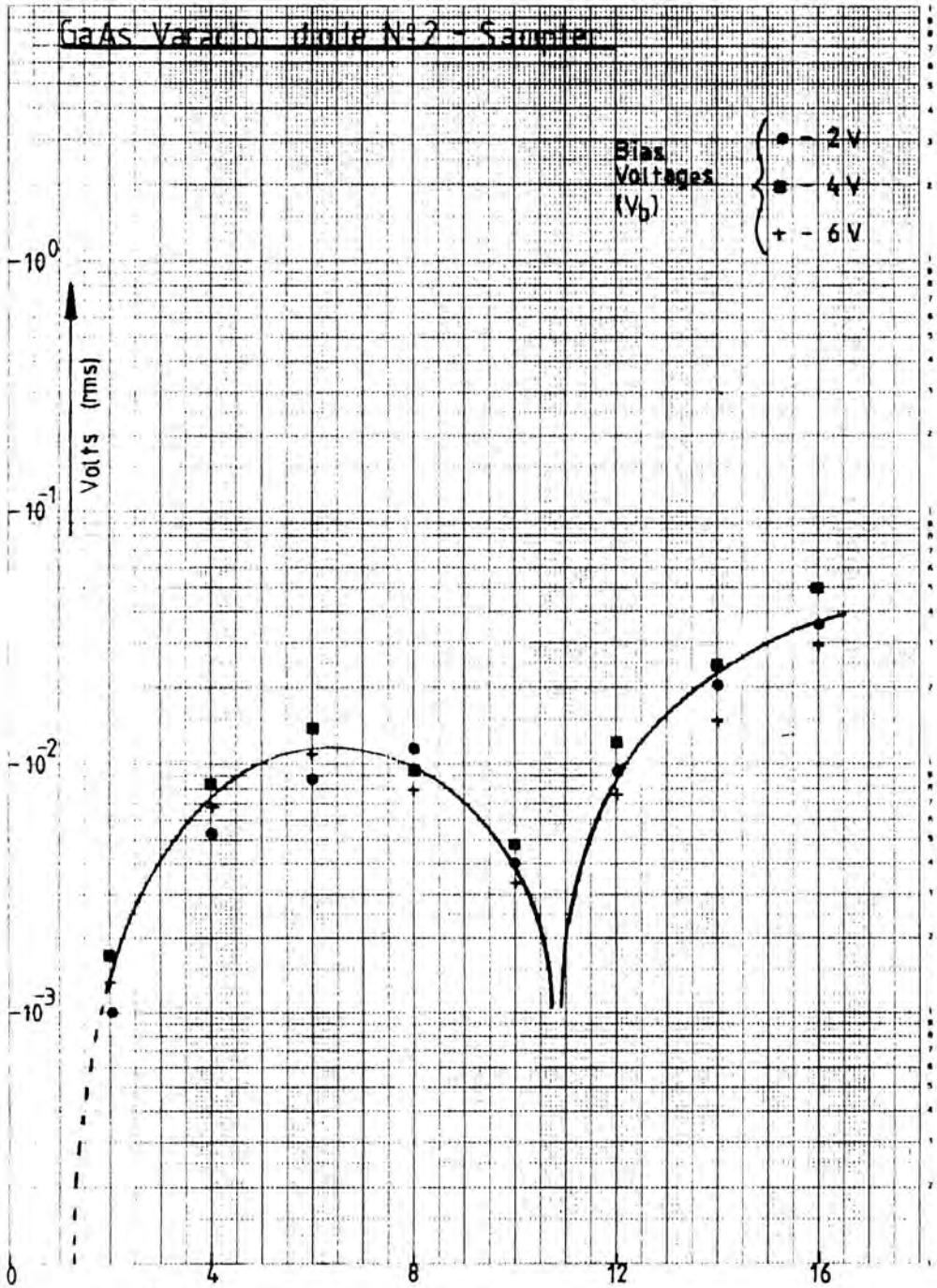

Fig. 6.14 5th Harmonic Amplitudes v Drive Level

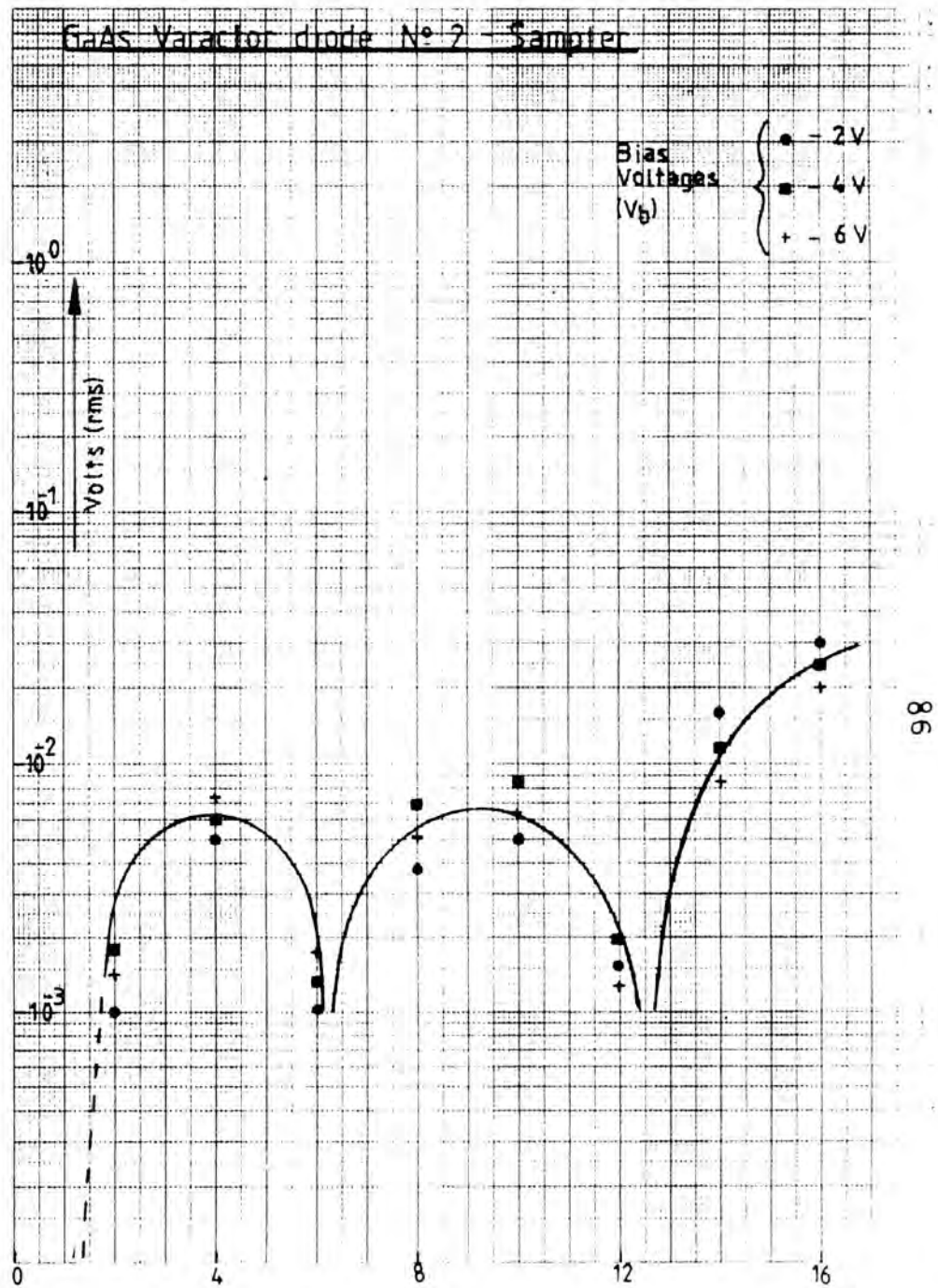

Fig. 6.15 6th Harmonic Amplitudes v Drive Level

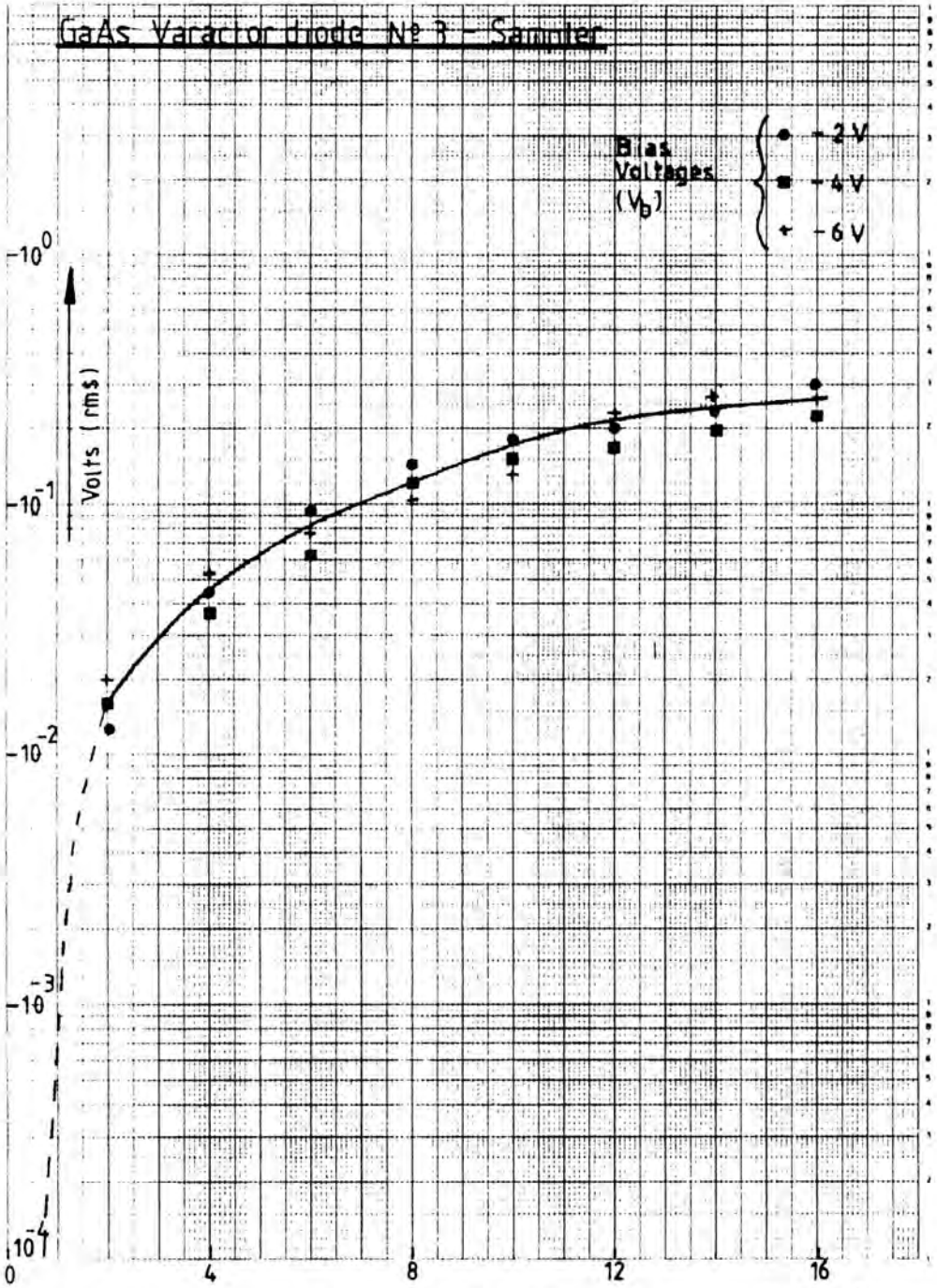

Fig. 6.16 2nd Harmonic Amplitudes v Drive Level

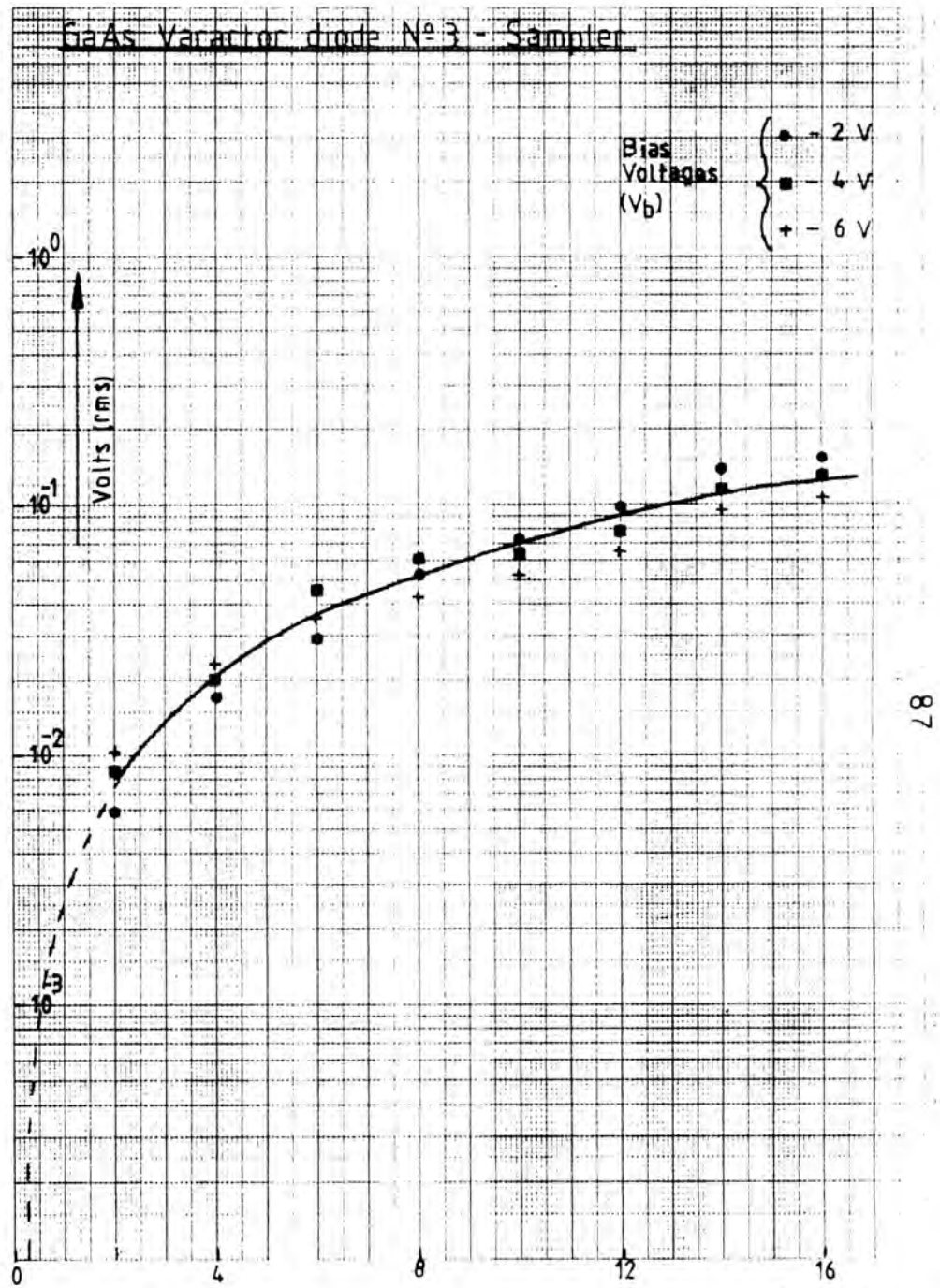

Fig. 6.17 3rd Harmonic Amplitudes v Drive Level

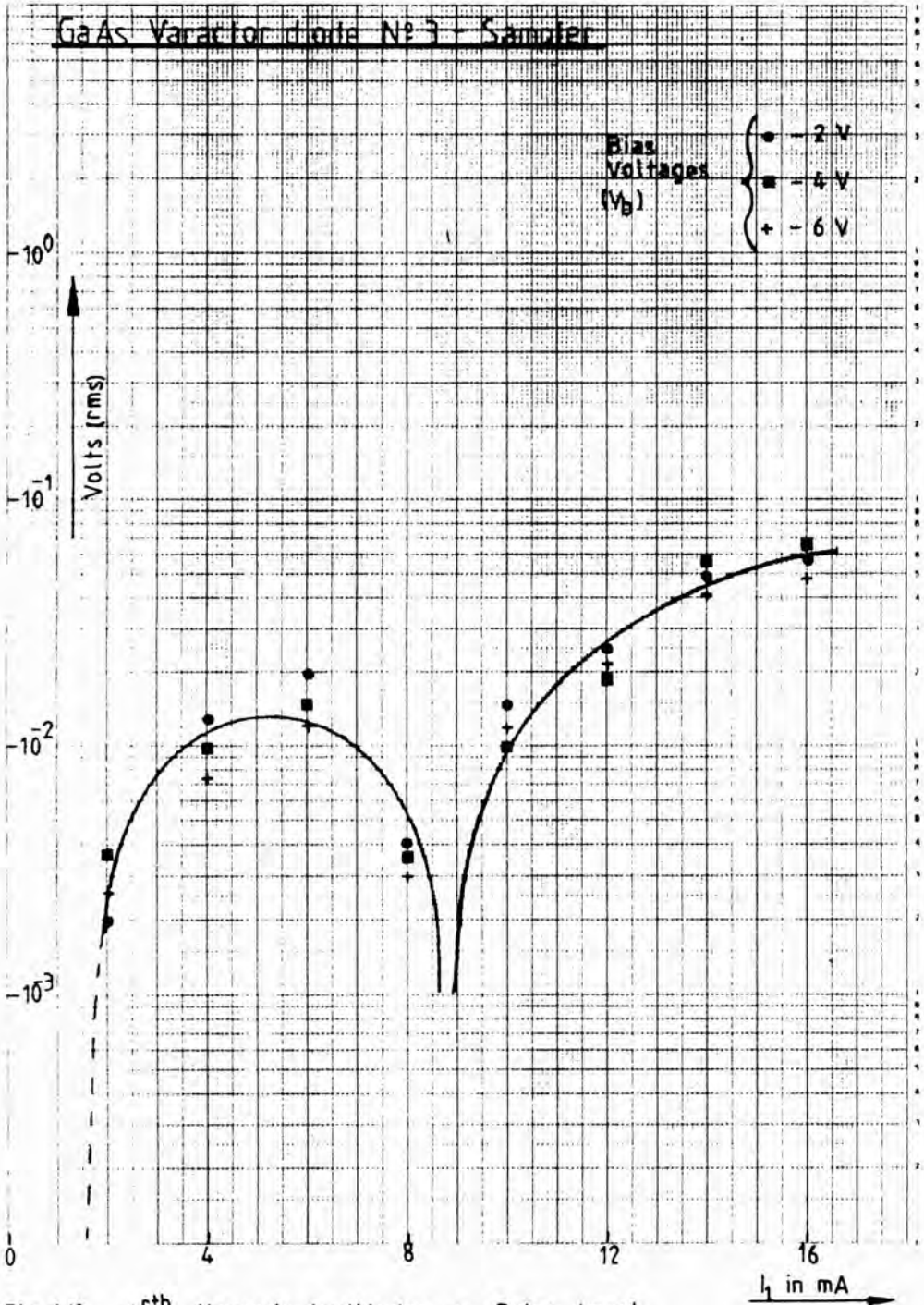

Fig. 6.18 4rth Harmonic Amplitudes v Drive Level

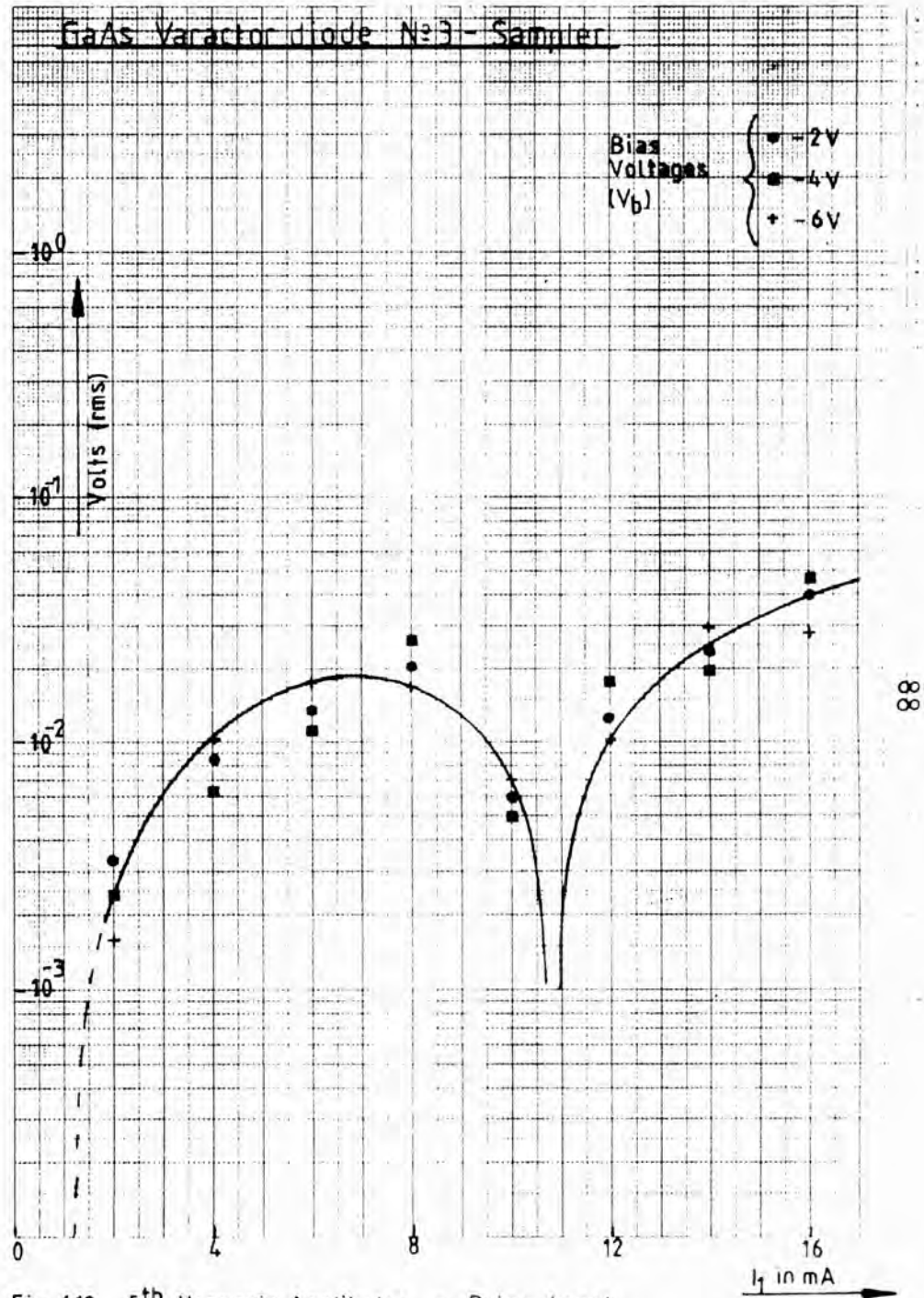

Fig. 6.19 5th Harmonic Amplitudes v Drive Level

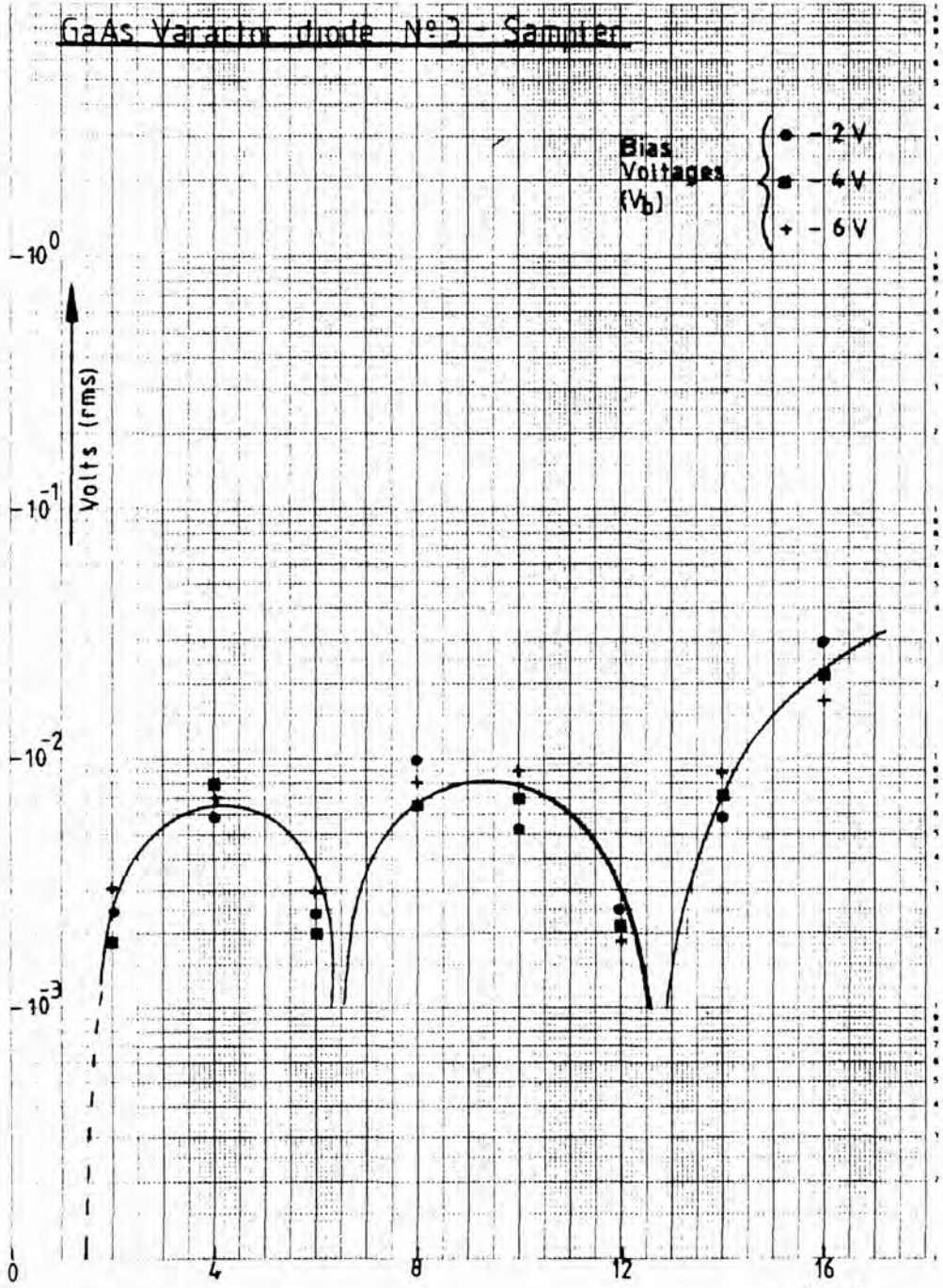

Fig. 6.20 6th Harmonic Amplitudes v Drive Level

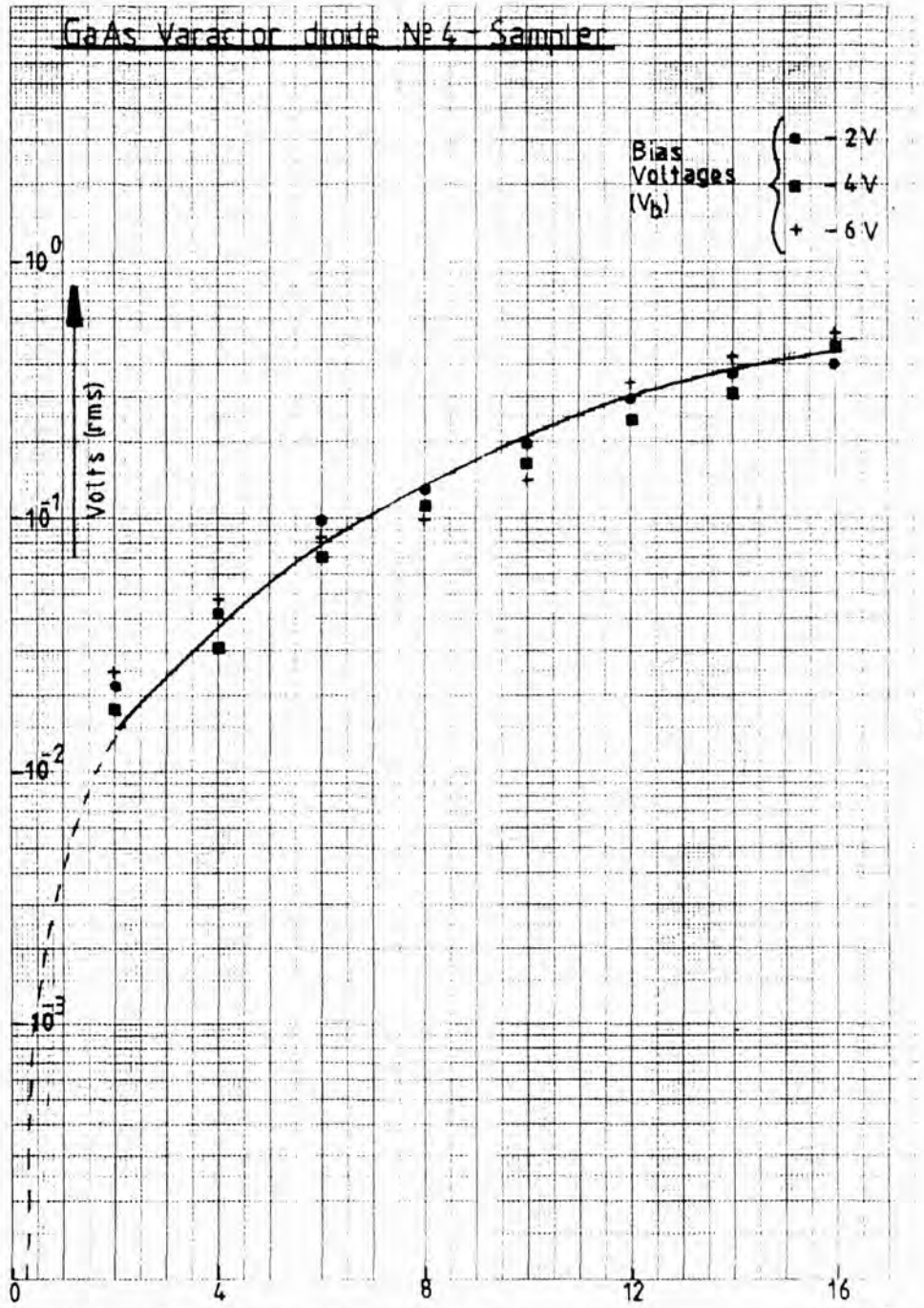

Fig. 6.21 2nd Harmonic Amplitudes v Drive Level

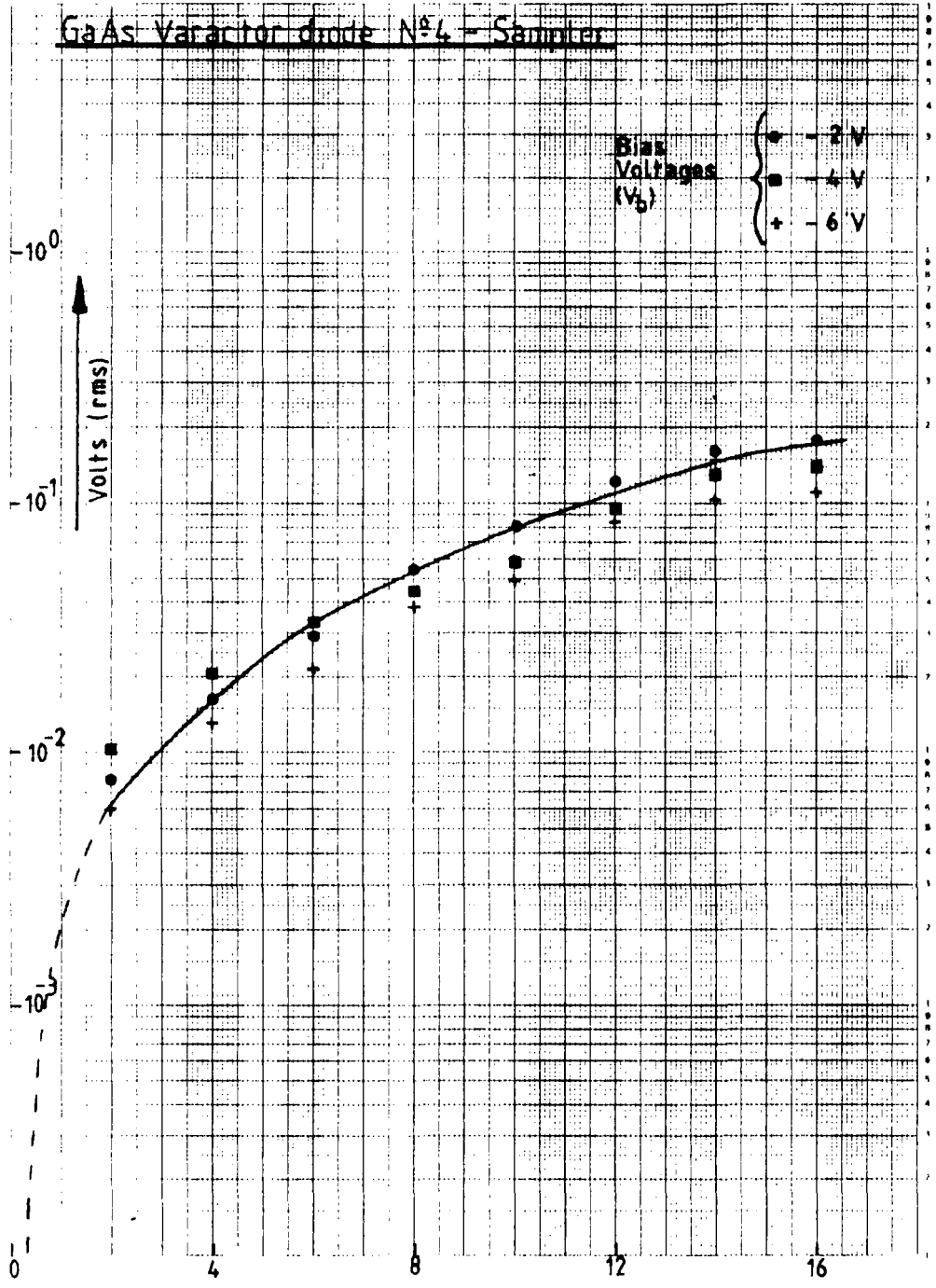

Fig. 6.22 3rd Harmonic Amplitudes v Drive Level

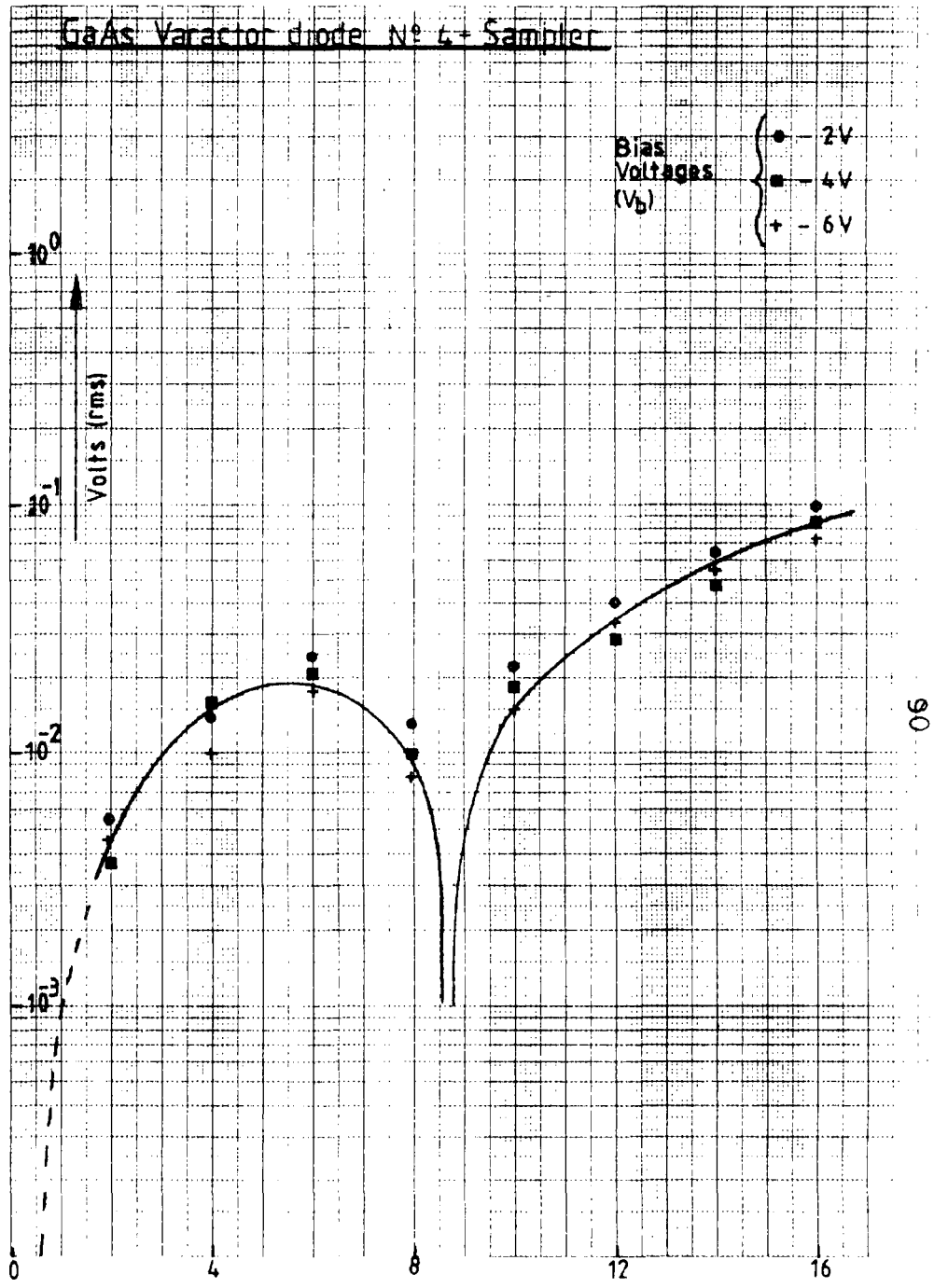

Fig. 6.23 4rth Harmonic Amplitudes v Drive Level

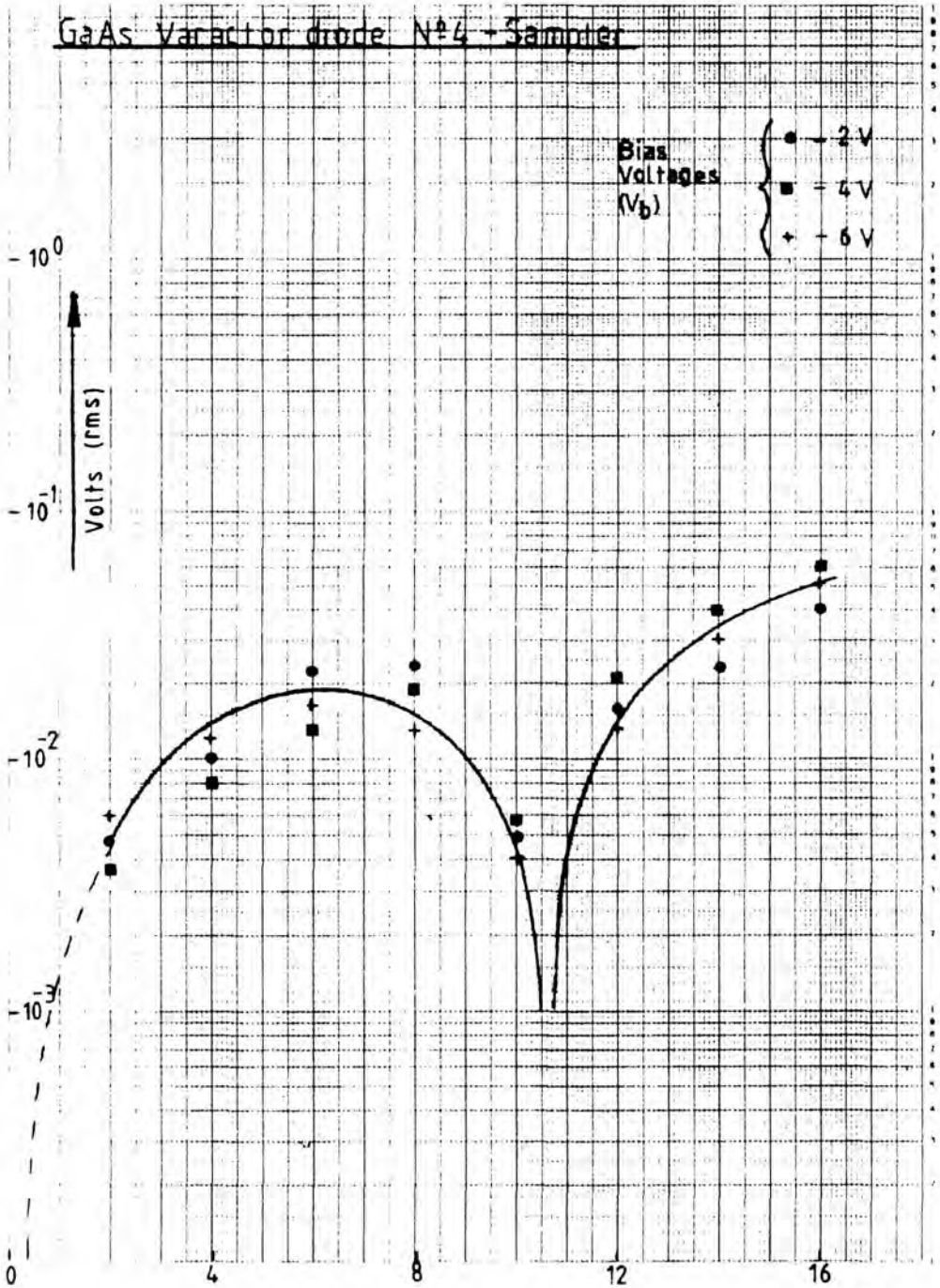

Fig. 6.24 5th Harmonic Amplitudes v Drive Level

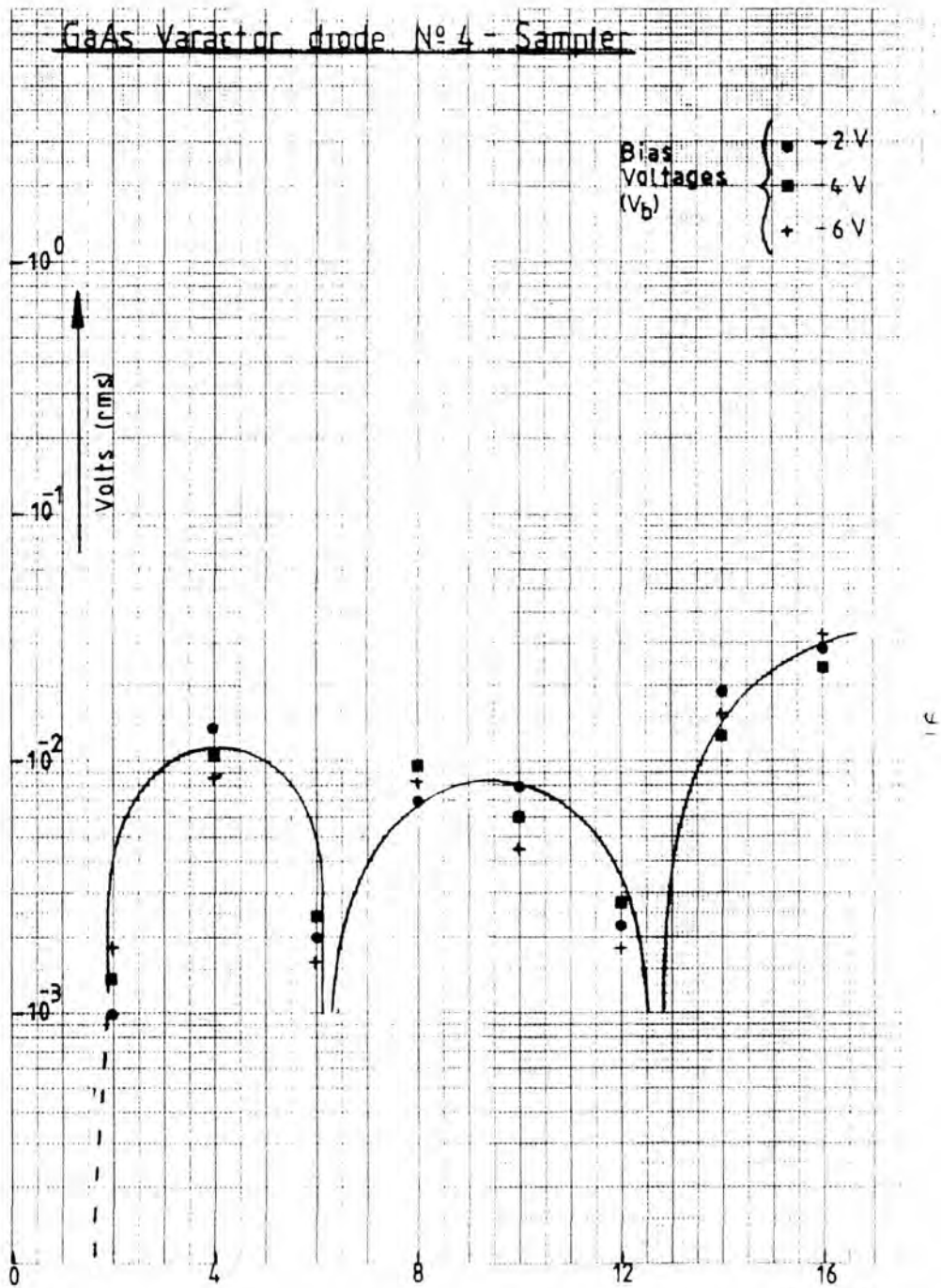

Fig.6.25 6th Harmonic Amplitudes v Drive Level

the fifth harmonic amplitudes were slightly lower than those of the fourth and there was a dip at around 10 mA indicating the transition between the two lobes.

In the case of the sixth harmonic, presented in Figs. 6.10, 6.15, 6.20 and 6.25 it was found that two dips occur. The first was between 5 and 6 mA and the second around 11 mA. This implies that the sixth harmonic at low drive level occurs in the third lobe and then as the level is increased moves into the second and finally into the first lobe. The amplitudes are lower level than those of fifth harmonic

The variations of the harmonic phases with respect to the fundamental are presented in Figs. 6.26-6.45. If the distorted waveform was symmetrical, this would suggests that the relation between the fundamental and the harmonics can only be 0 or 180 degrees, as only cosine components would be present. If, however, the waveshape was asymmetrical the phases would be within 90 degrees and sine and cosine components would be present.

In the case of the first diode, the second harmonic relative phase was found to increase with the drive level, then had a peak and later decreased. On the other hand, for the second diode, it started to increase and then remained at the same level as shown in Fig. 6.31. The third and fourth diodes behaved in a similar manner as in Figs. 6.36 and 6.41.

The remaining harmonics behaved in the same way and

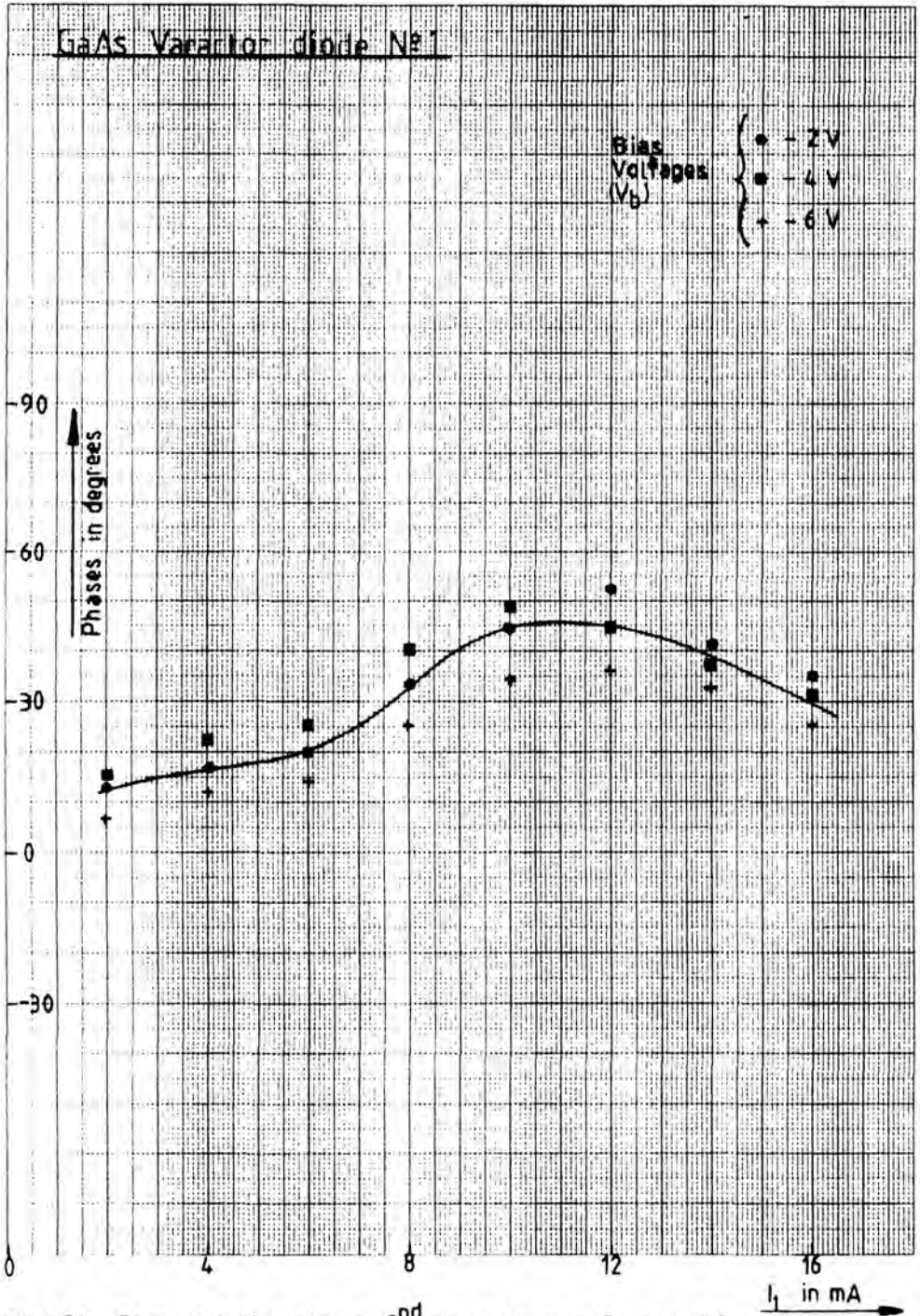

Fig. 6.26 Phase Relationship of 2nd Harmonic w.r.t. Fundamental

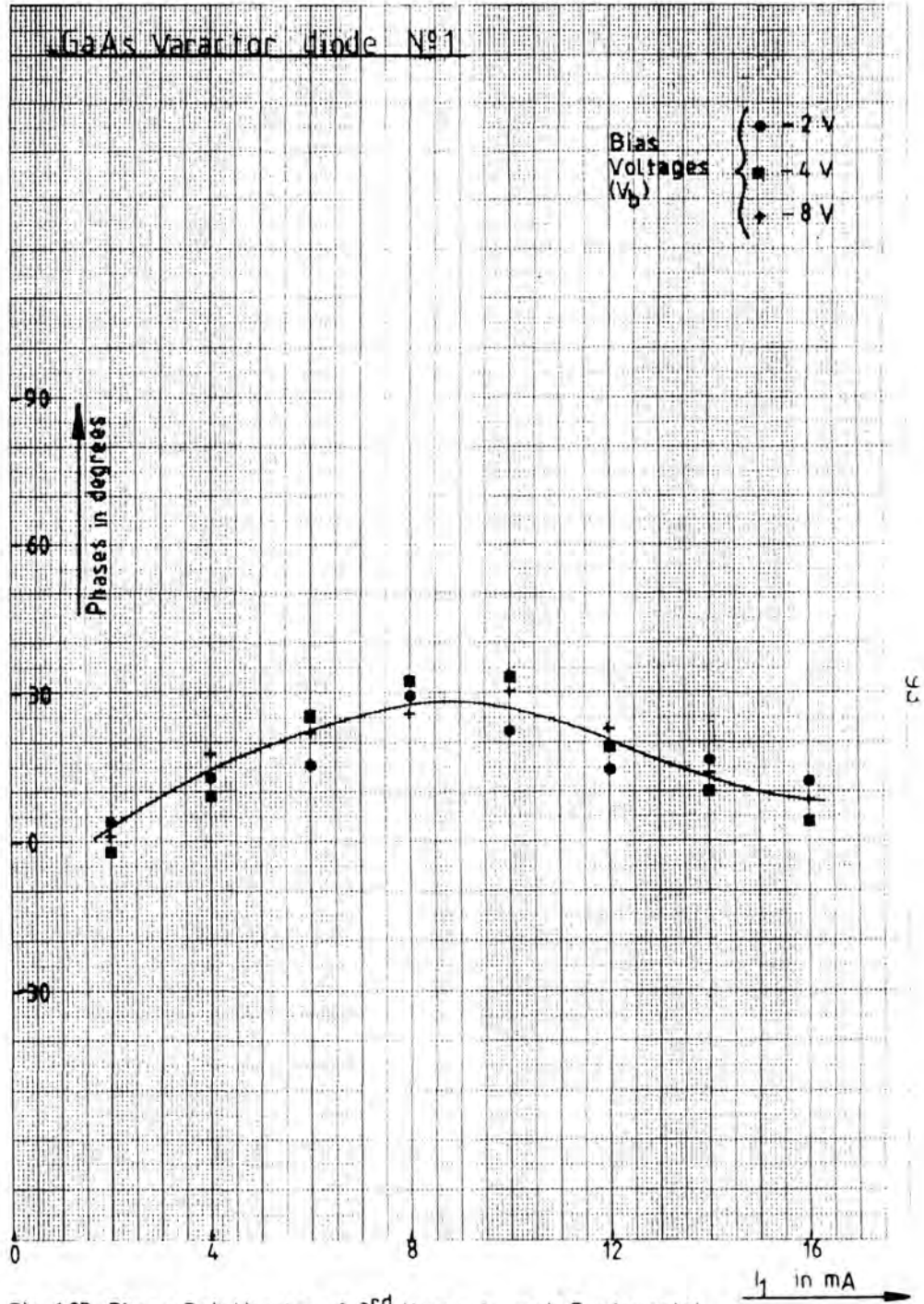

Fig. 6.27 Phase Relationship of 3rd Harmonic w.r.t. Fundamental

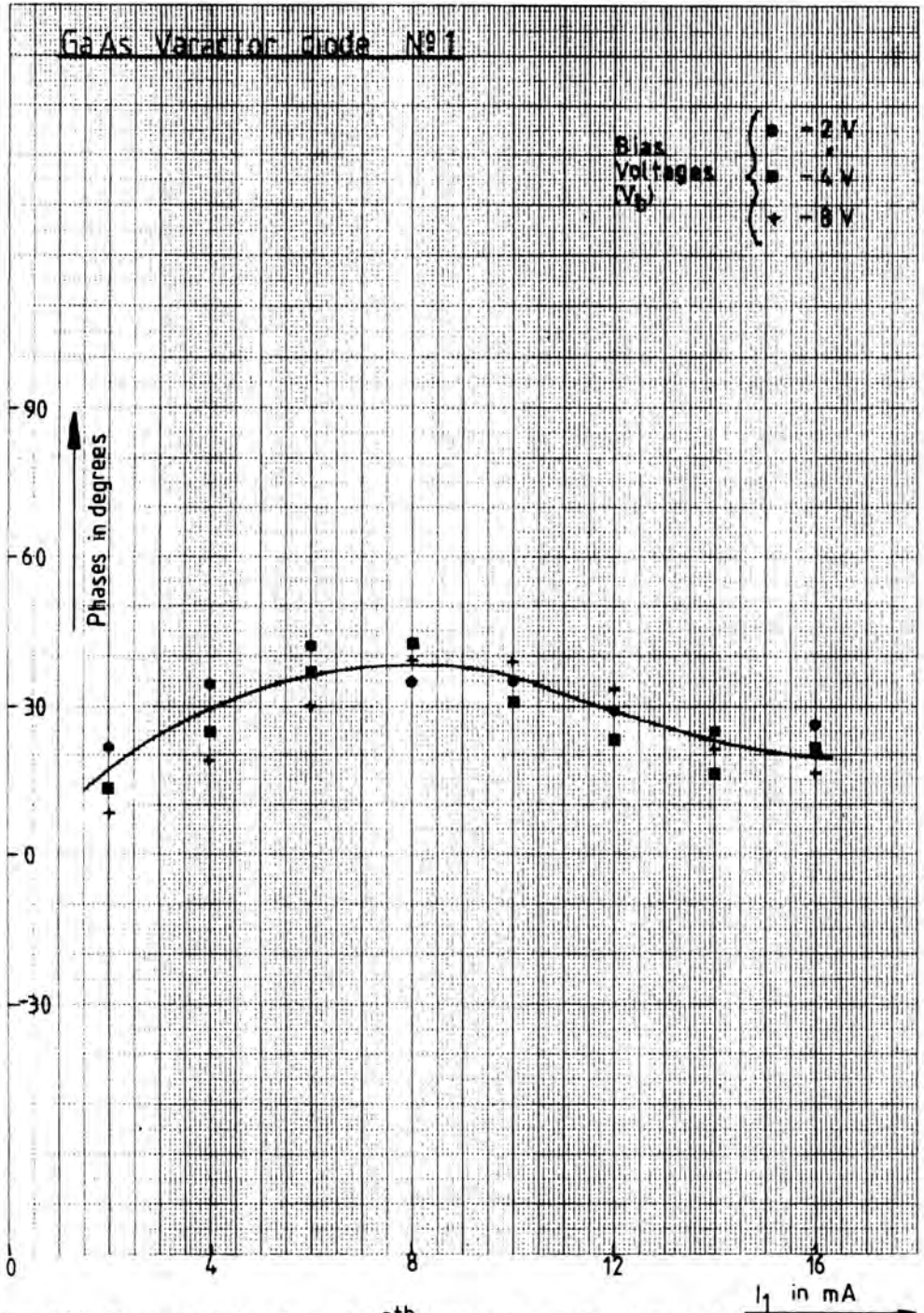

Fig. 6.28 Phase Relationship of 4^{rth} Harmonic w.r.t. Fundamental

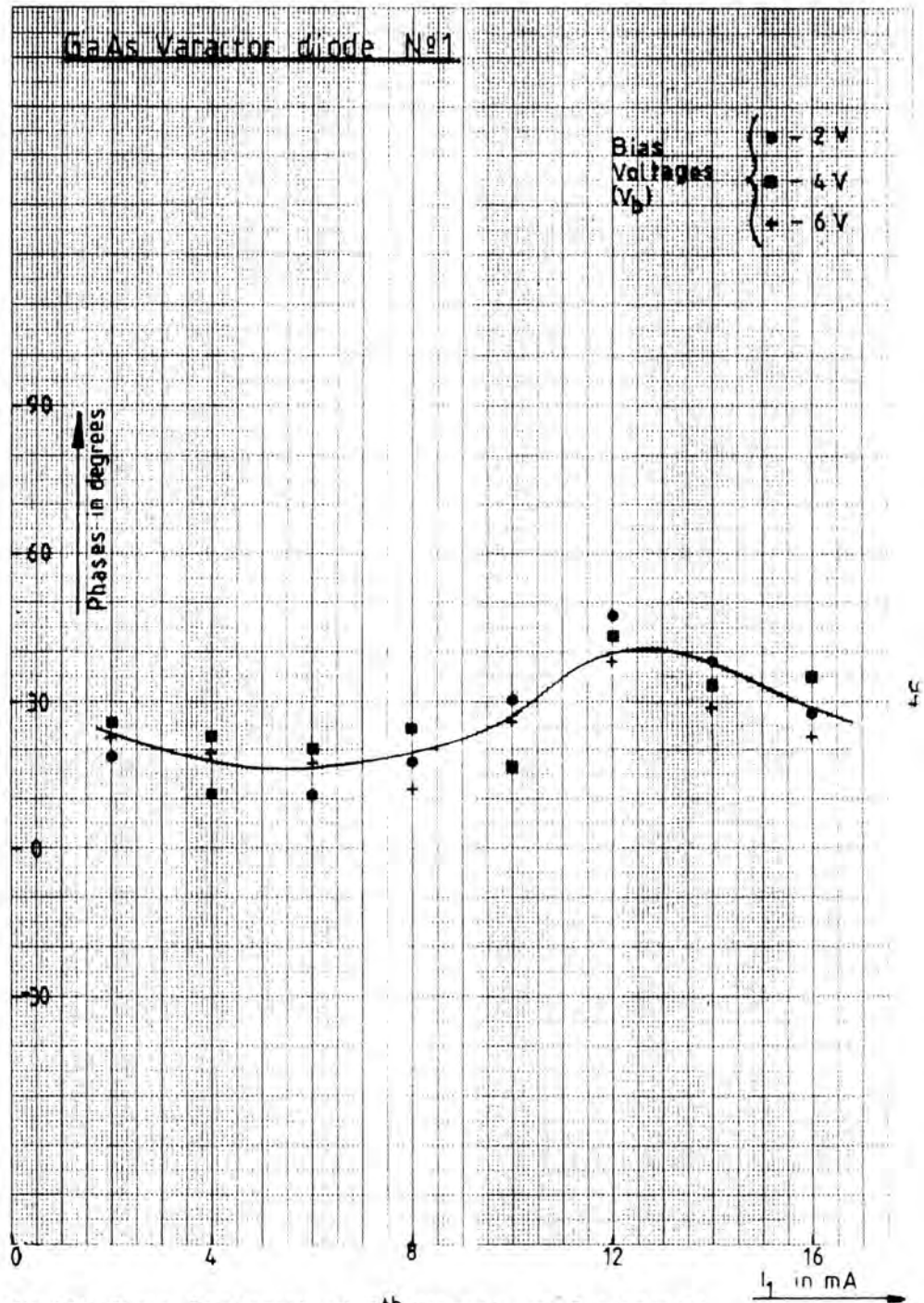

Fig. 6.29 Phase Relationship of 5th Harmonic w.r.t. Fundamental

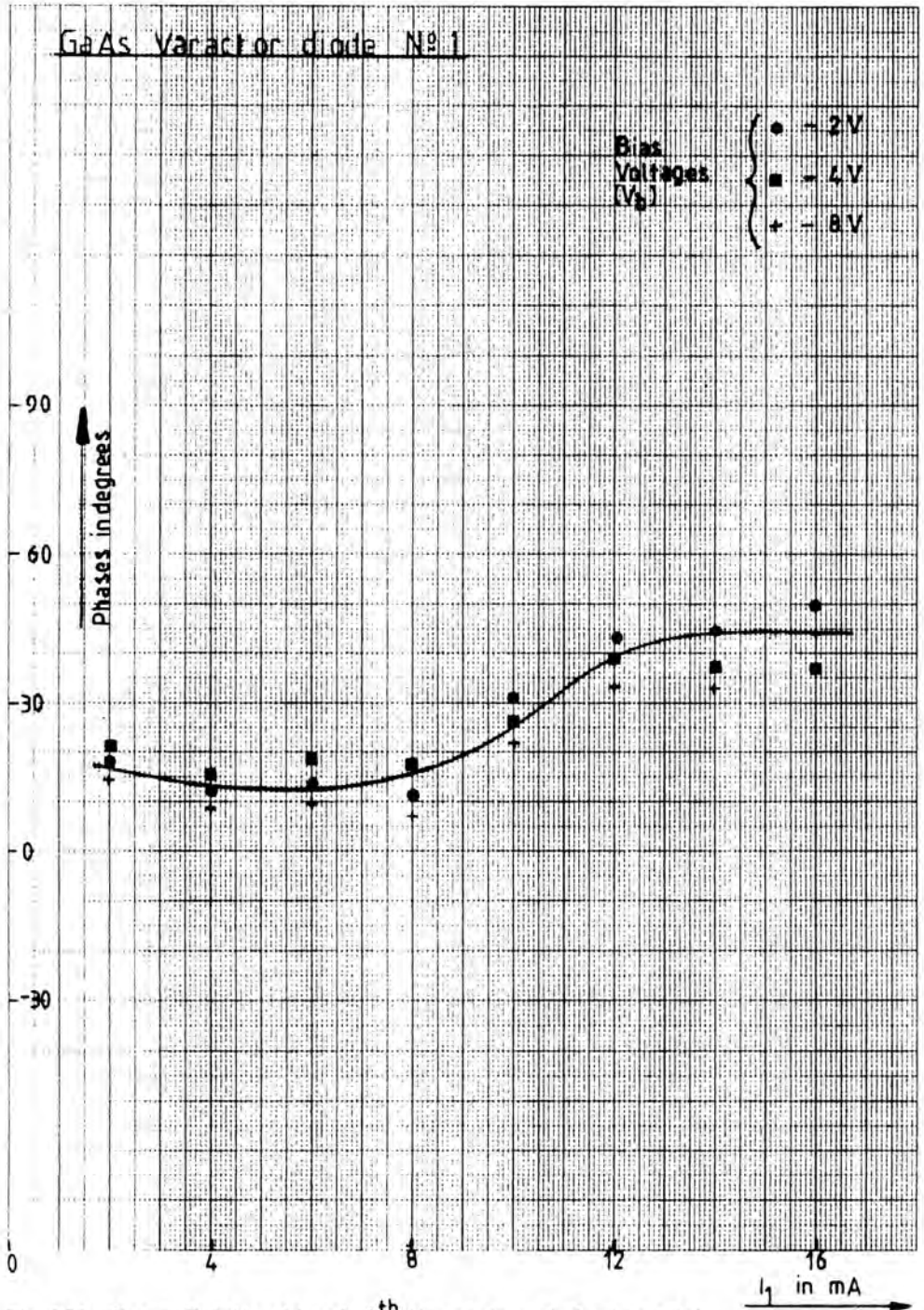

Fig. 6.30 Phase Relationship of 6th Harmonic wrt Fundamental

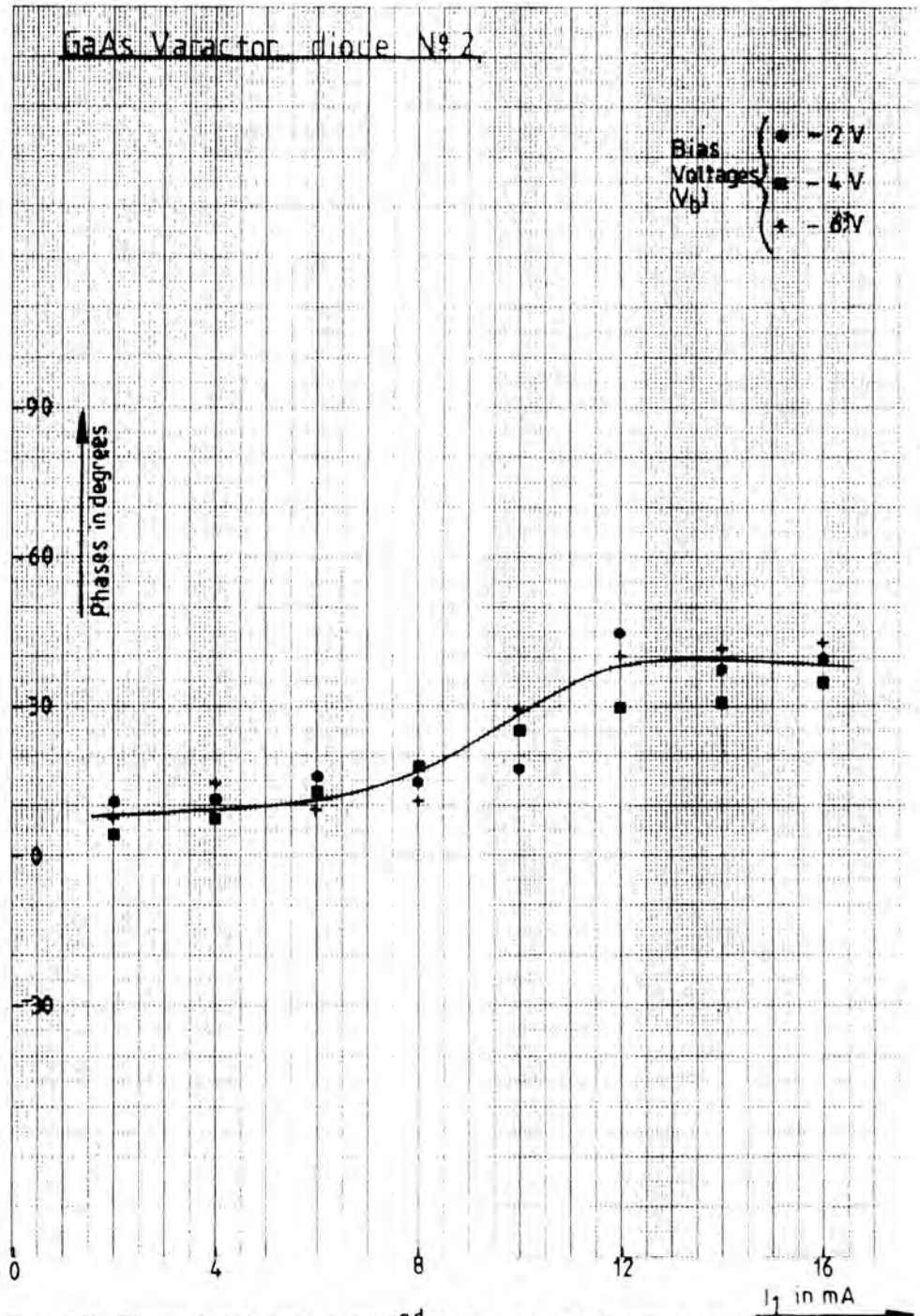

Fig. 6.31 Phase Relationship of 2nd Harmonic w.r.t. Fundamental

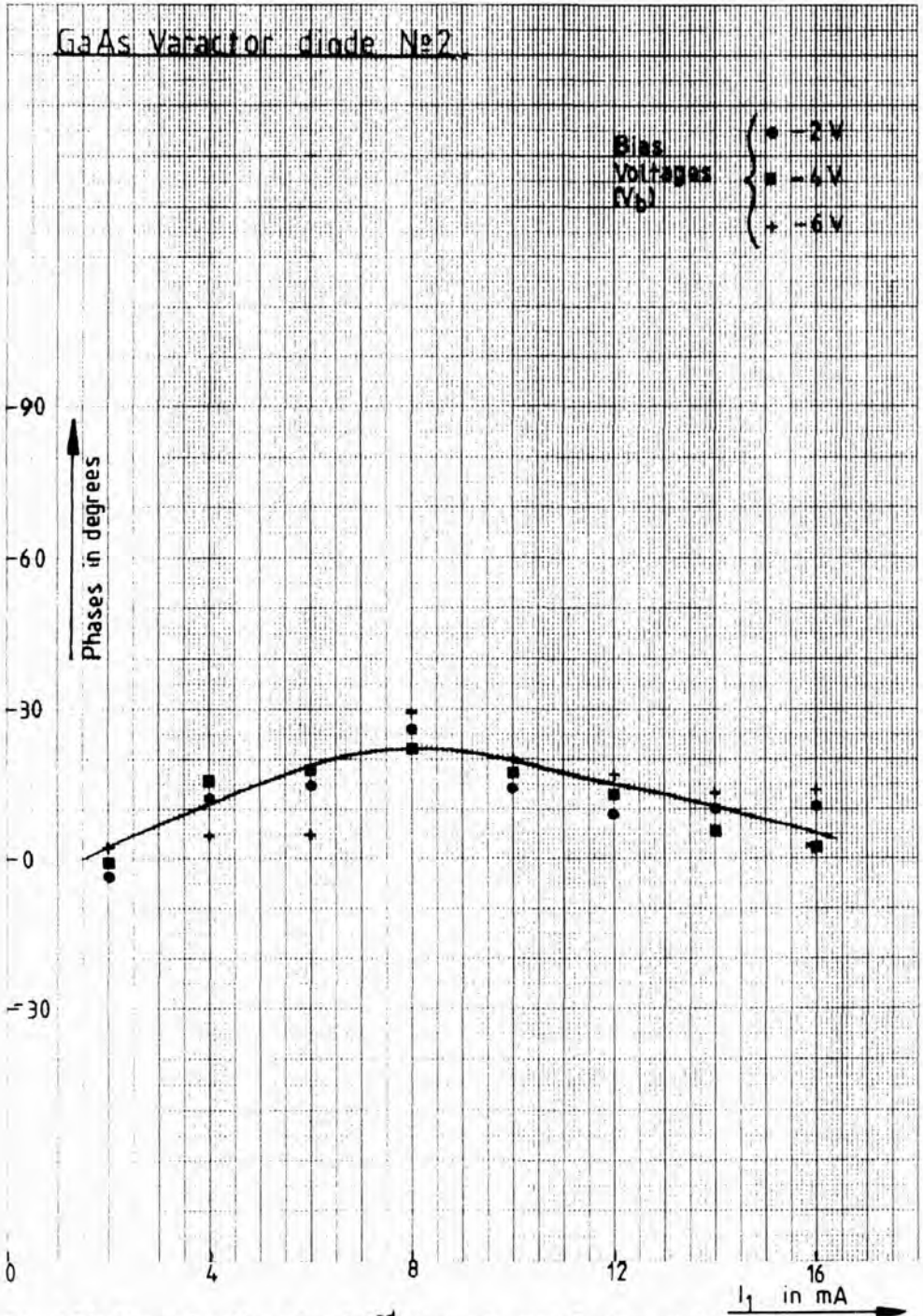

Fig. 6.32 Phase Relationship of 3rd Harmonic w.r.t. Fundamental

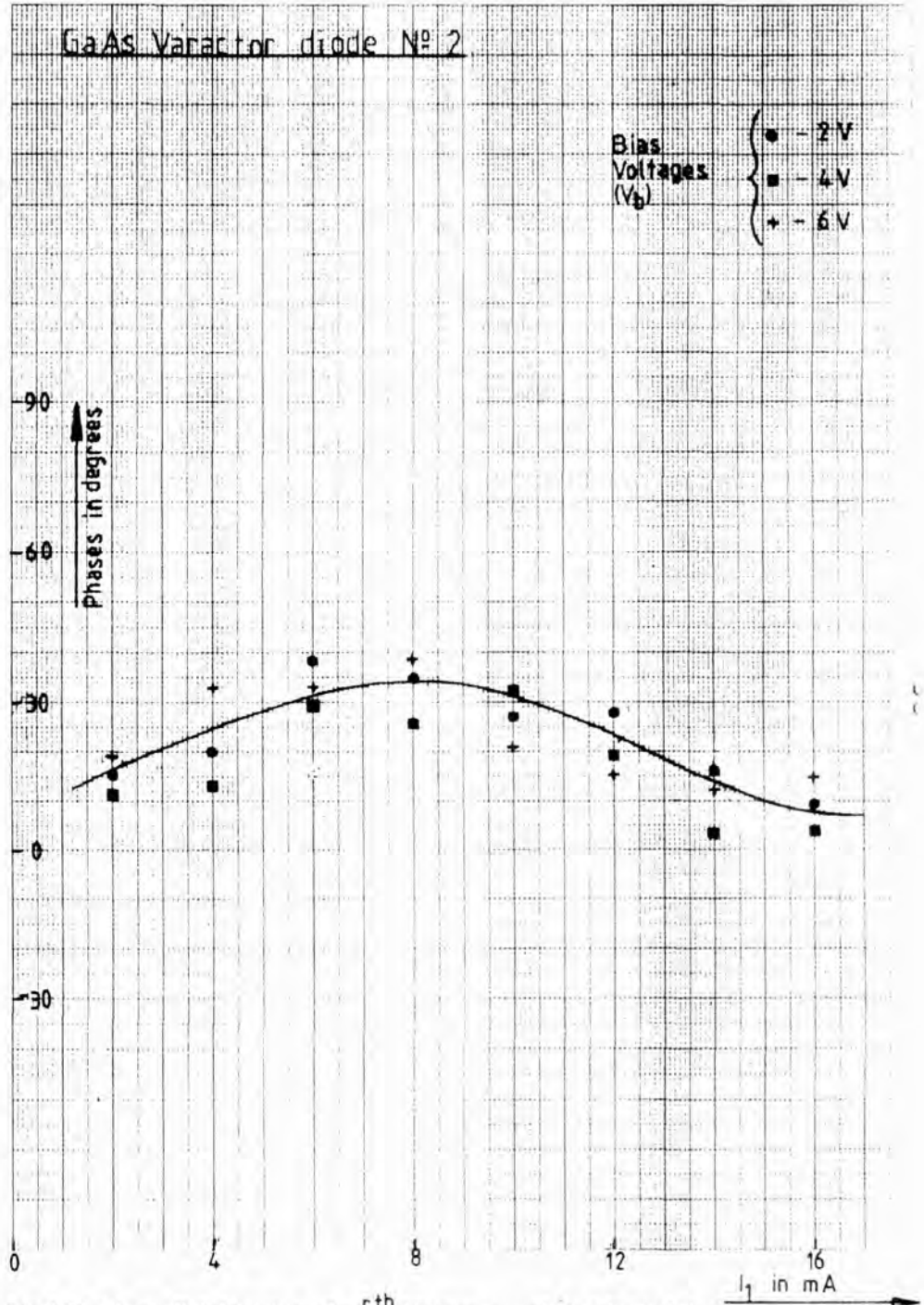

Fig. 6.33 Phase Relationship of 4rth Harmonic w.r.t Fundamental

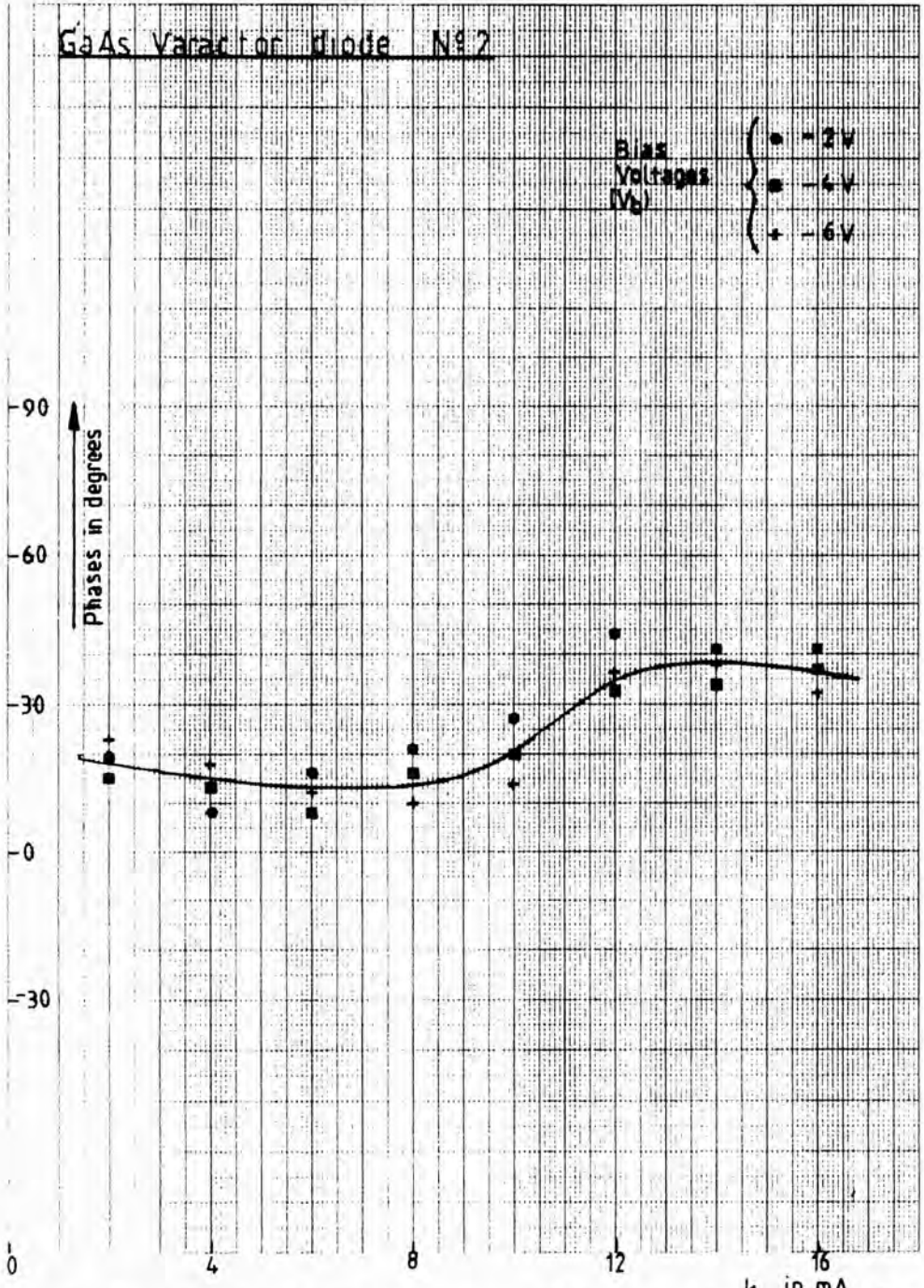

Fig. 6.34 Phase Relationship of 5th Harmonic w.r.t. Fundamental

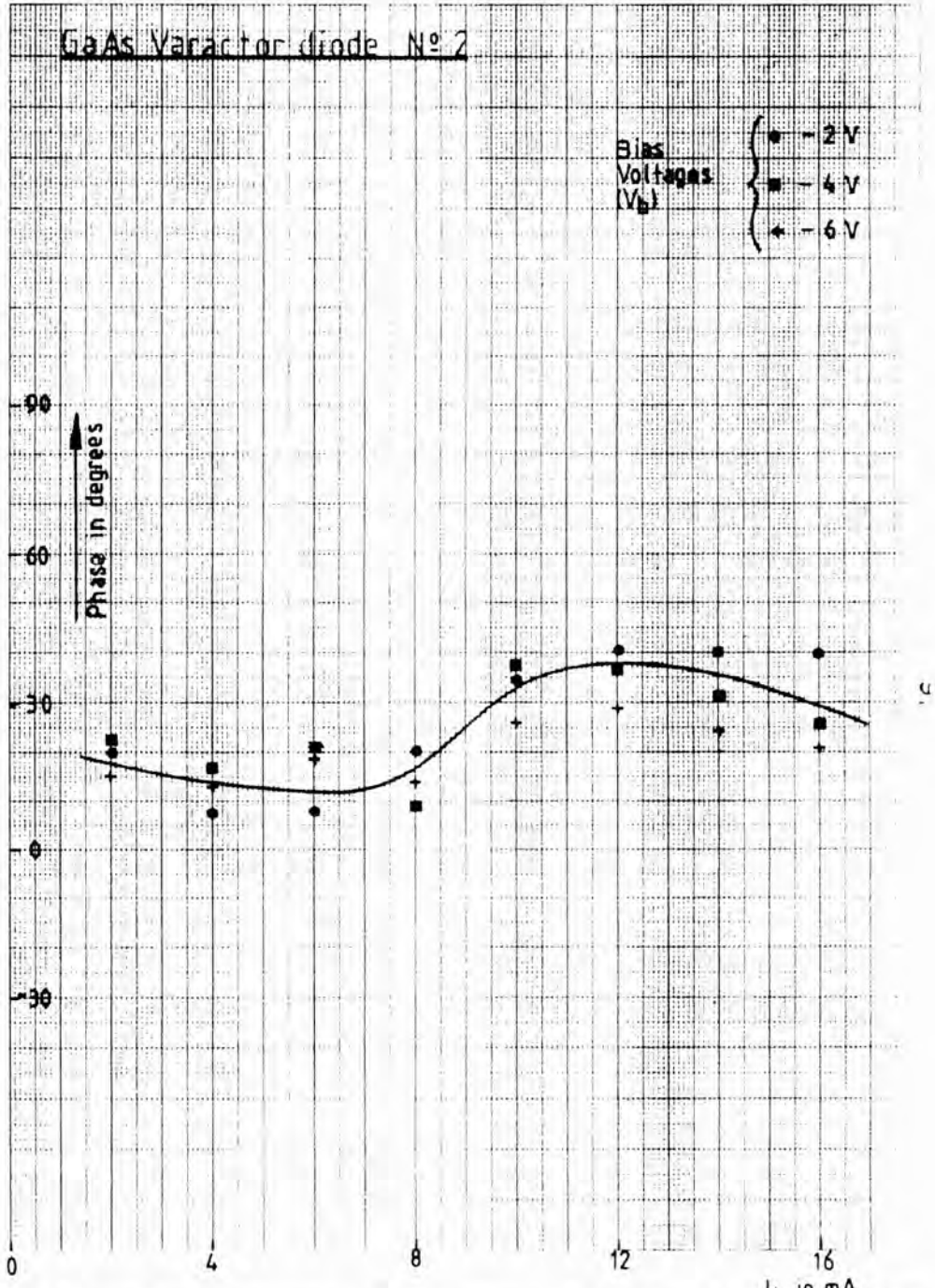

Fig. 6.35 Phase Relationship of 6th Harmonic w.r.t. Fundamental

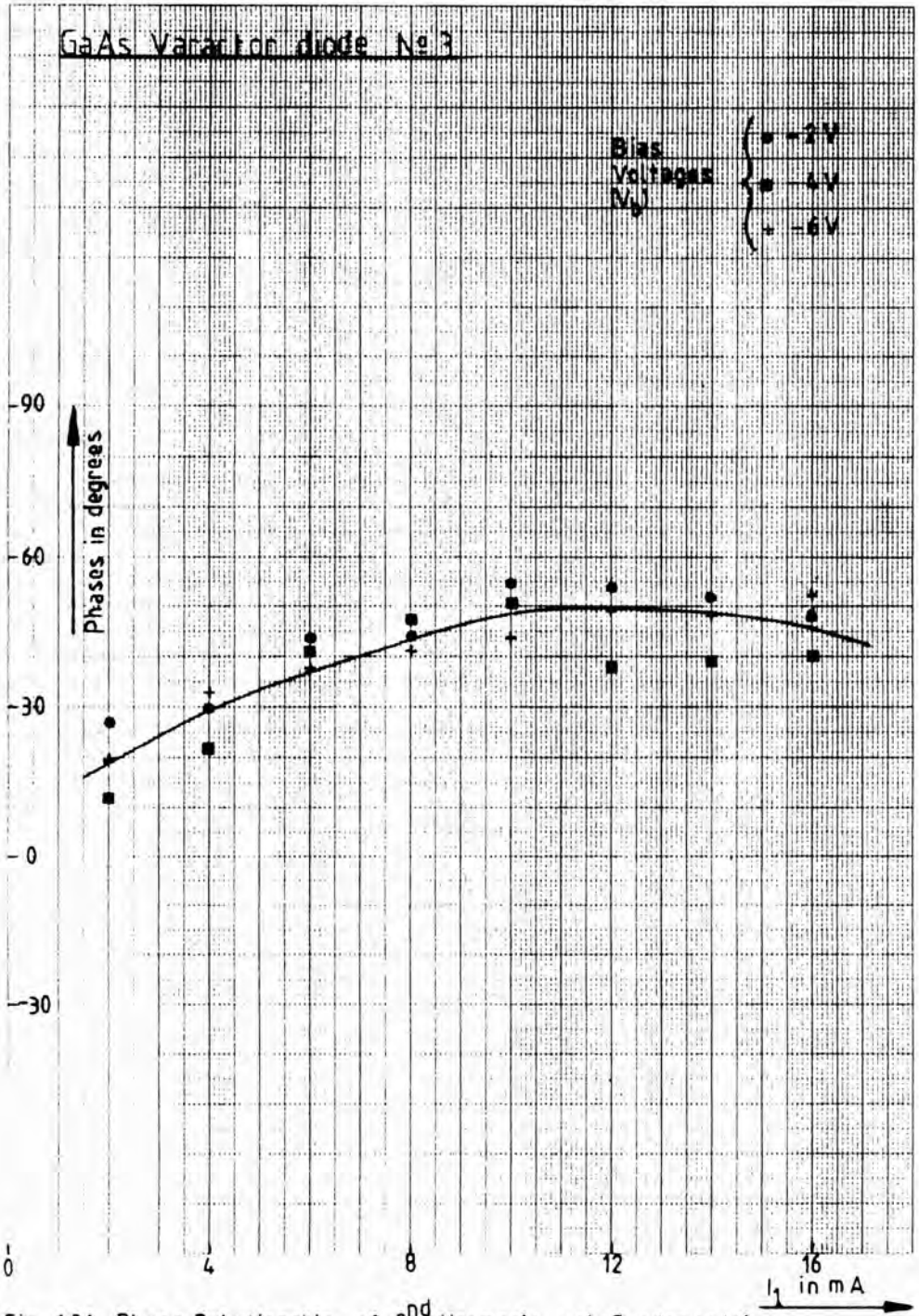

Fig. 6.36 Phase Relationship of 2nd Harmonic w.r.t. Fundamental

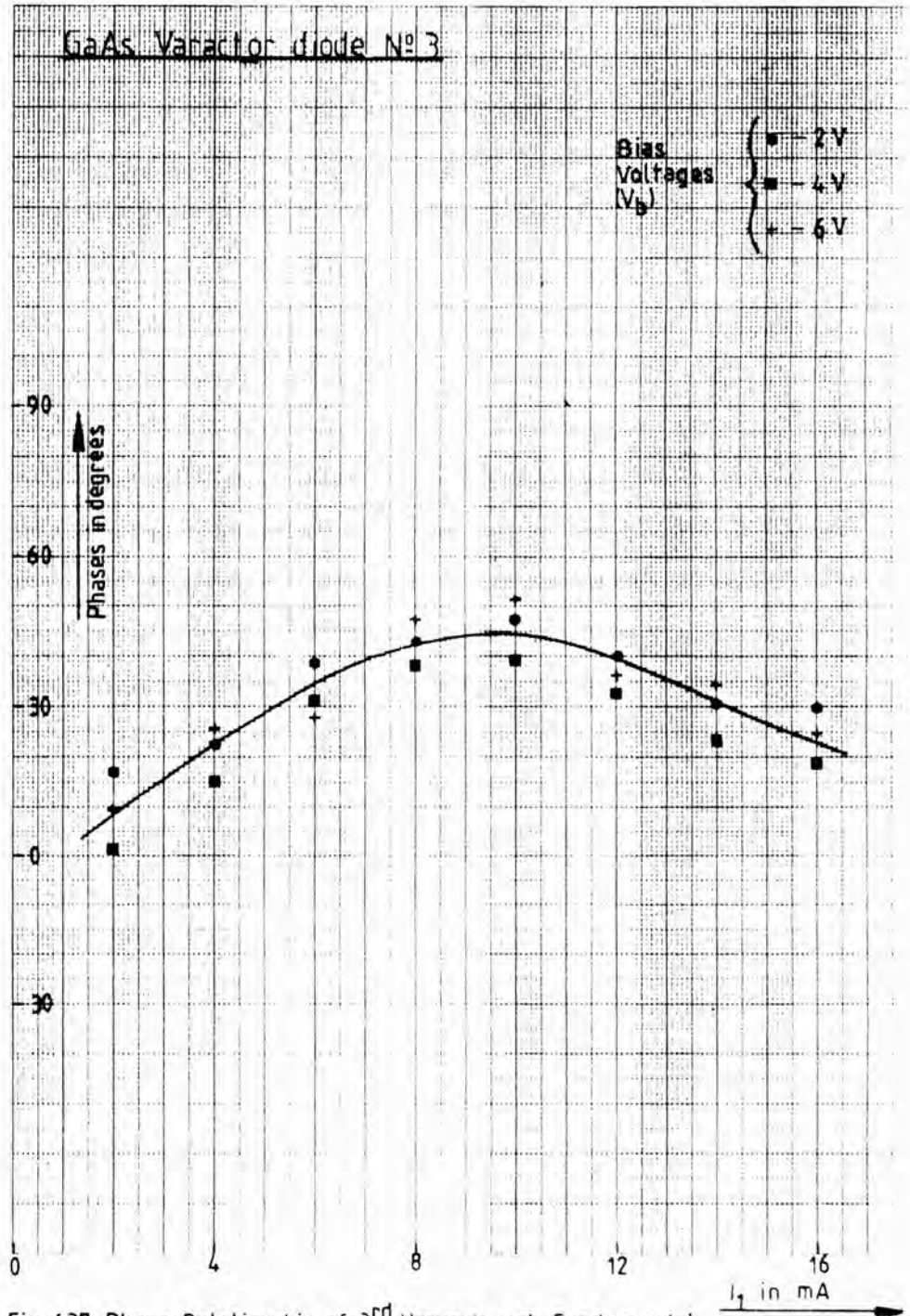

Fig. 6.37 Phase Relationship of 3rd Harmonic w.r.t. Fundamental

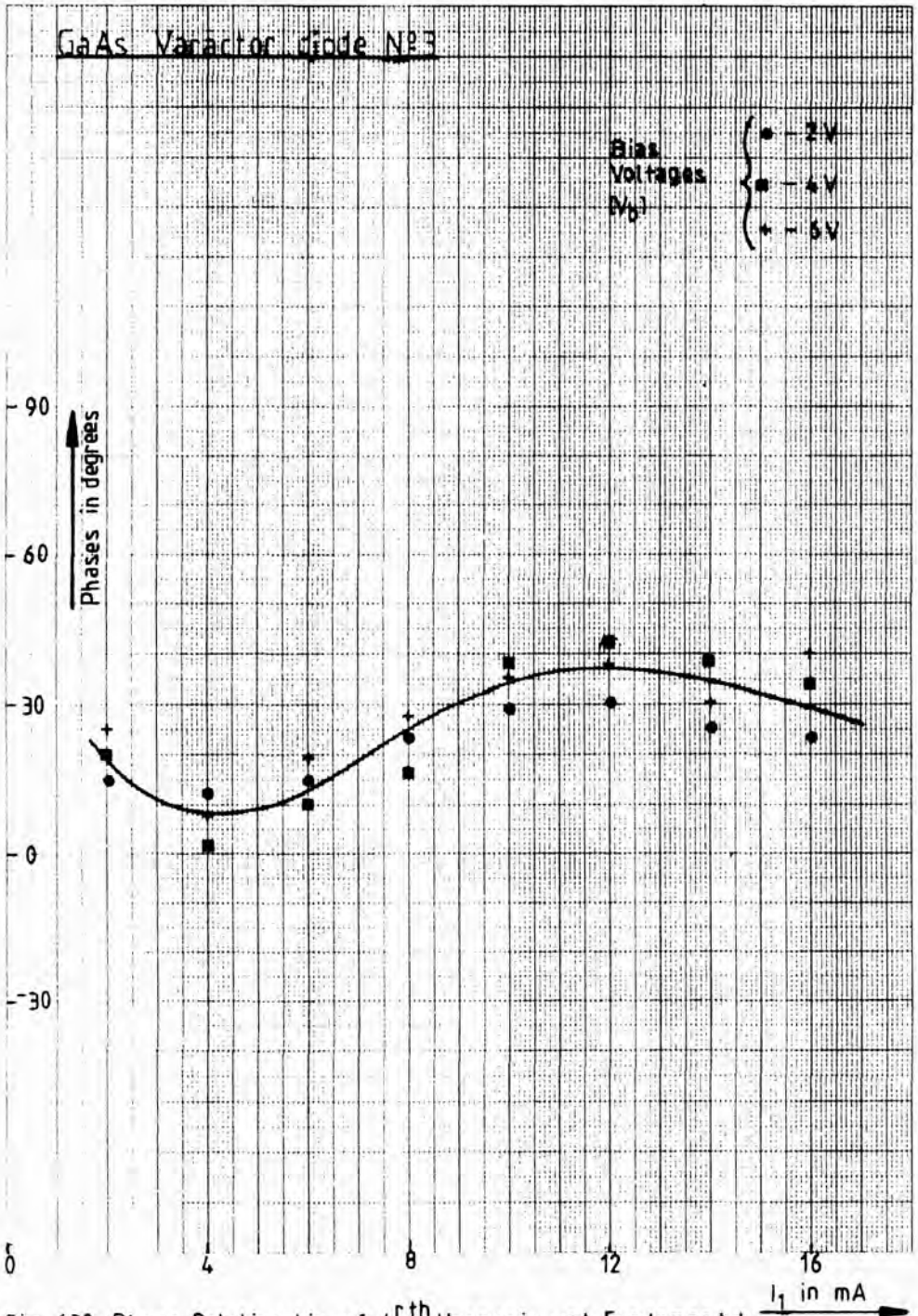

Fig. 6.38 Phase Relationship of 4^{rth} Harmonic w.r.t. Fundamental

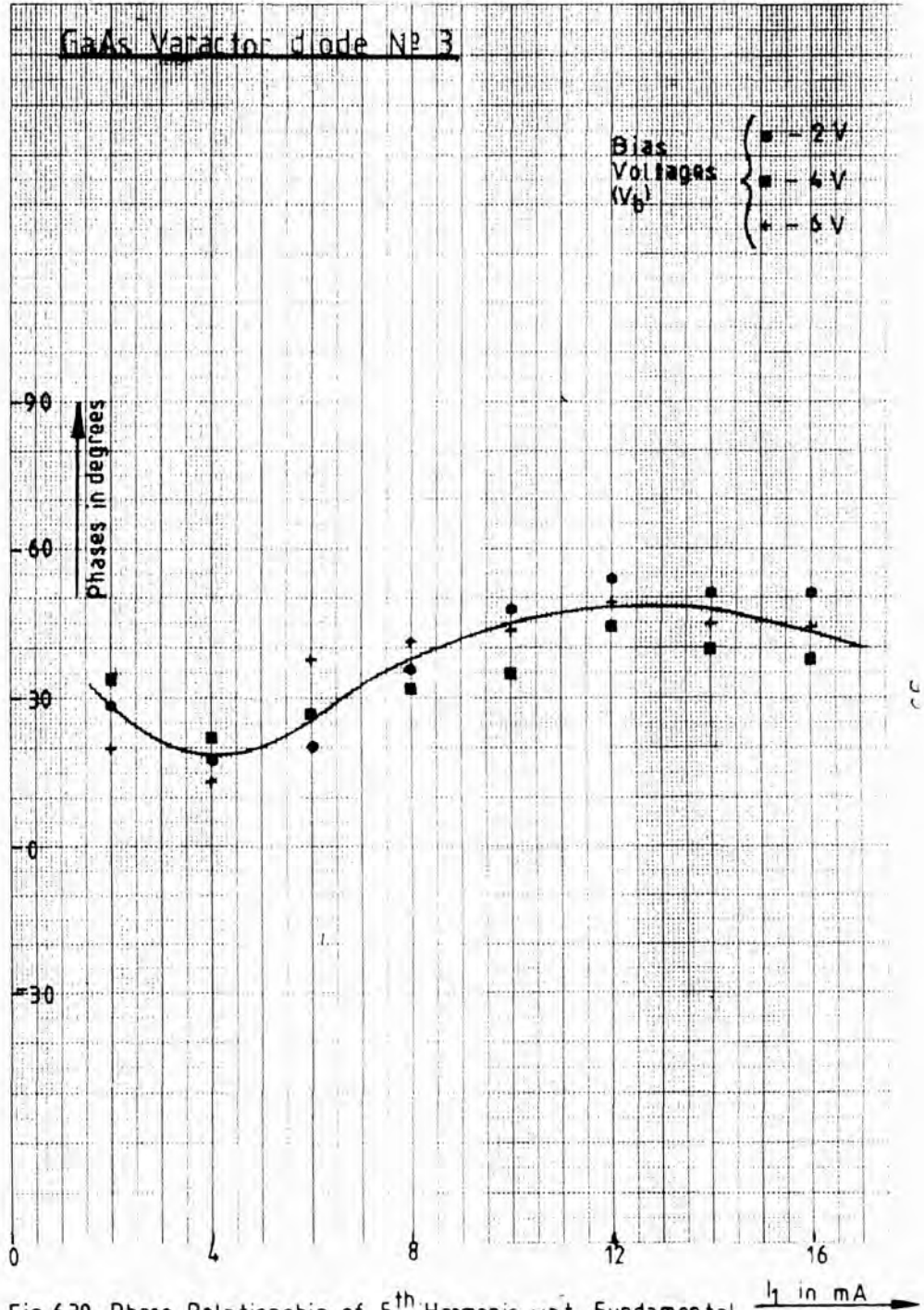

Fig. 6.39 Phase Relationship of 5th Harmonic w.r.t. Fundamental

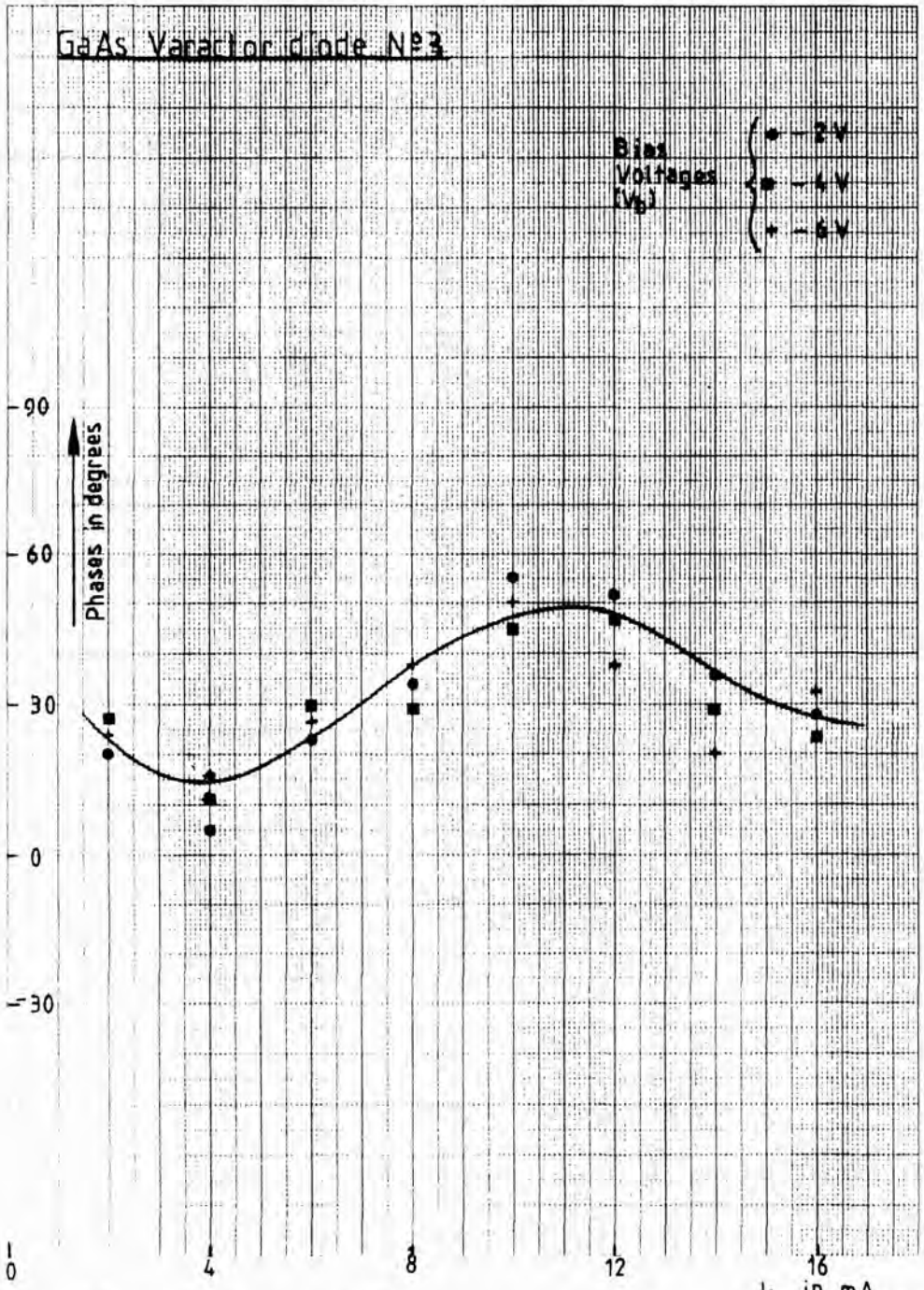

Fig. 6.40 Phase Relationship of 6th Harmonic w.r.t Fundamental

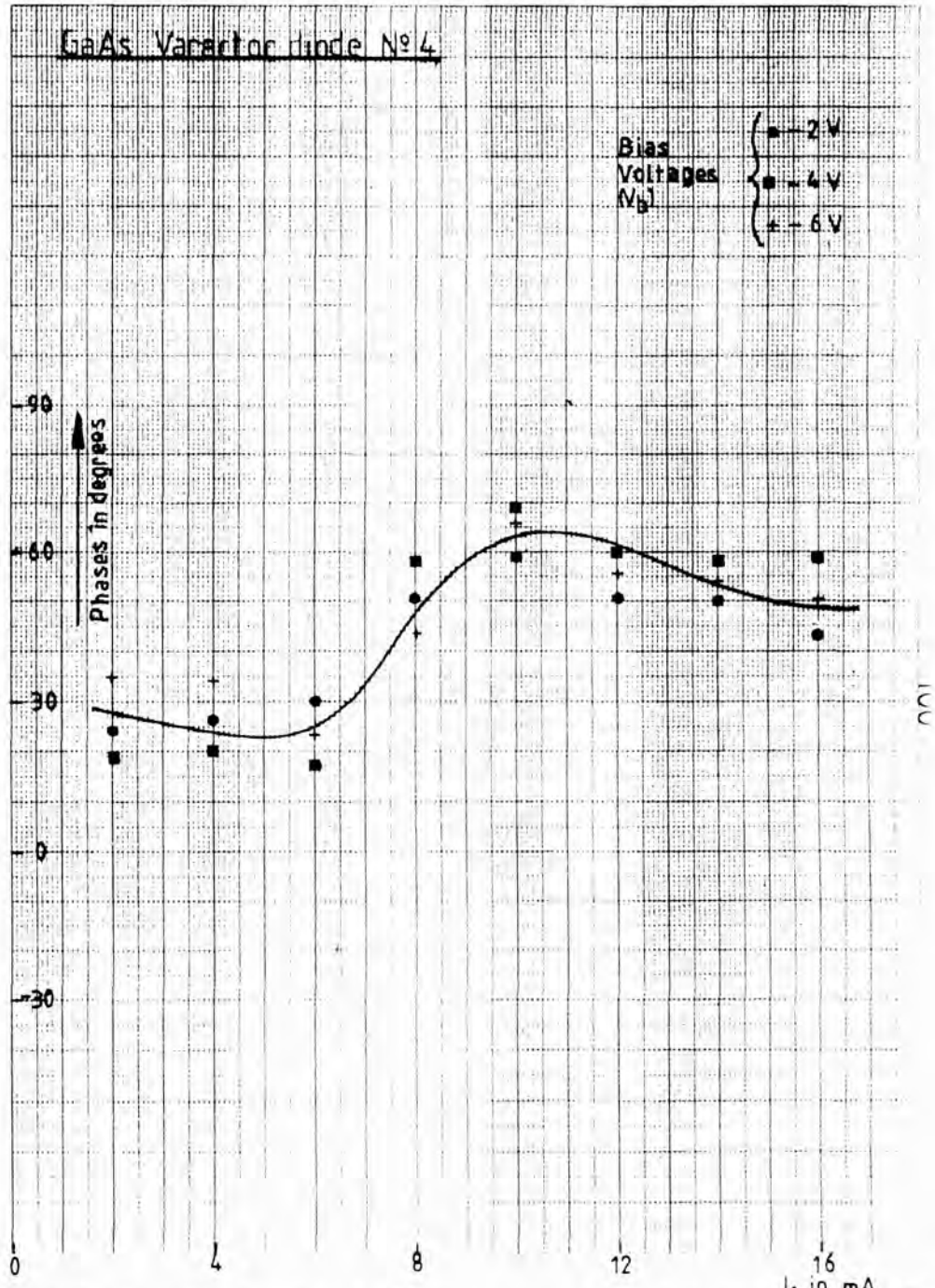

Fig. 6.41 Phase Relationship of 2nd Harmonic w.r.t. Fundamental

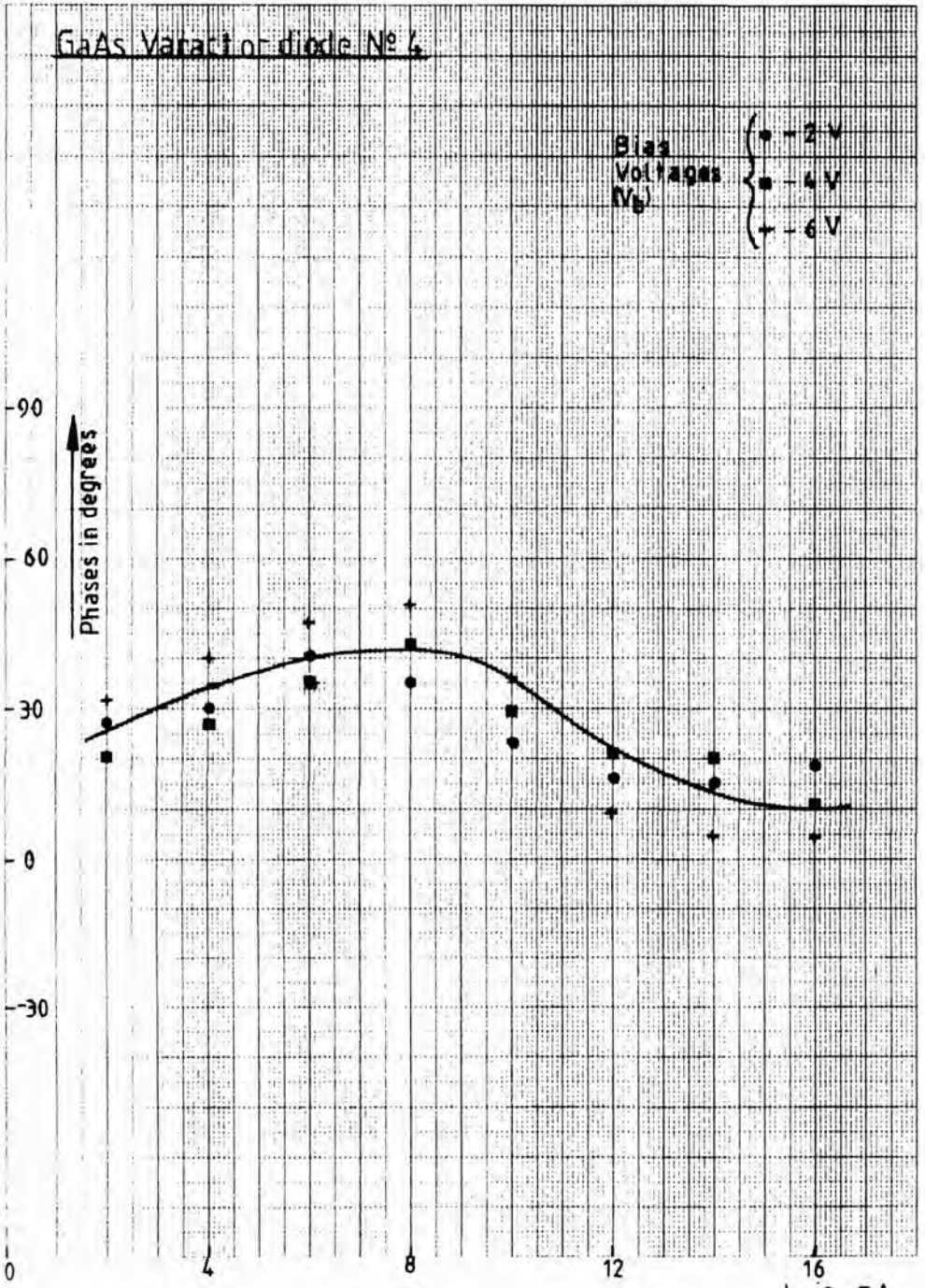

Fig. 6.42 Phase Relationship of 3rd Harmonic w.r.t. Fundamental

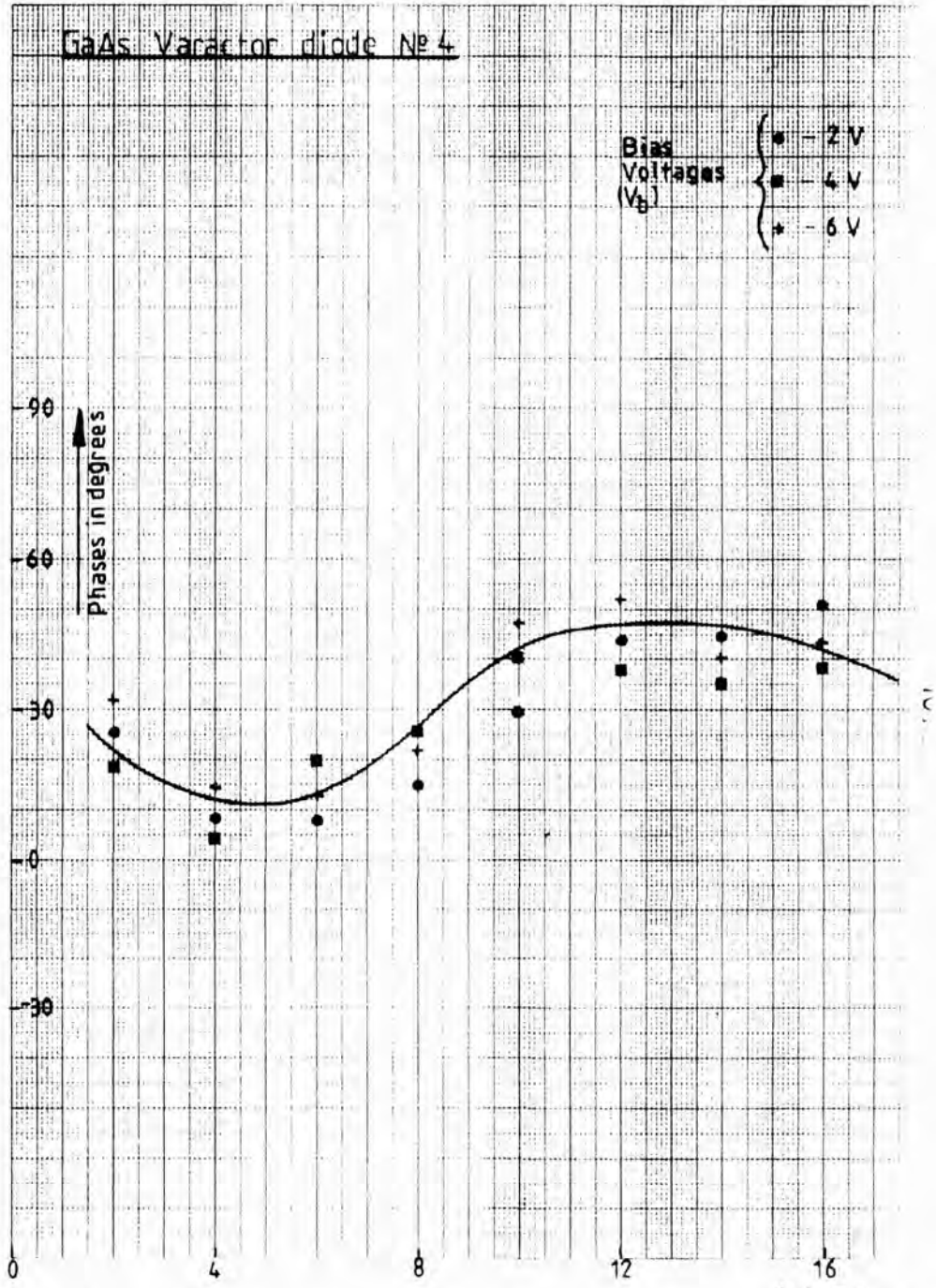

Fig. 6.43 Phase Relationship of 4rth Harmonic w.r.t. Fundamental

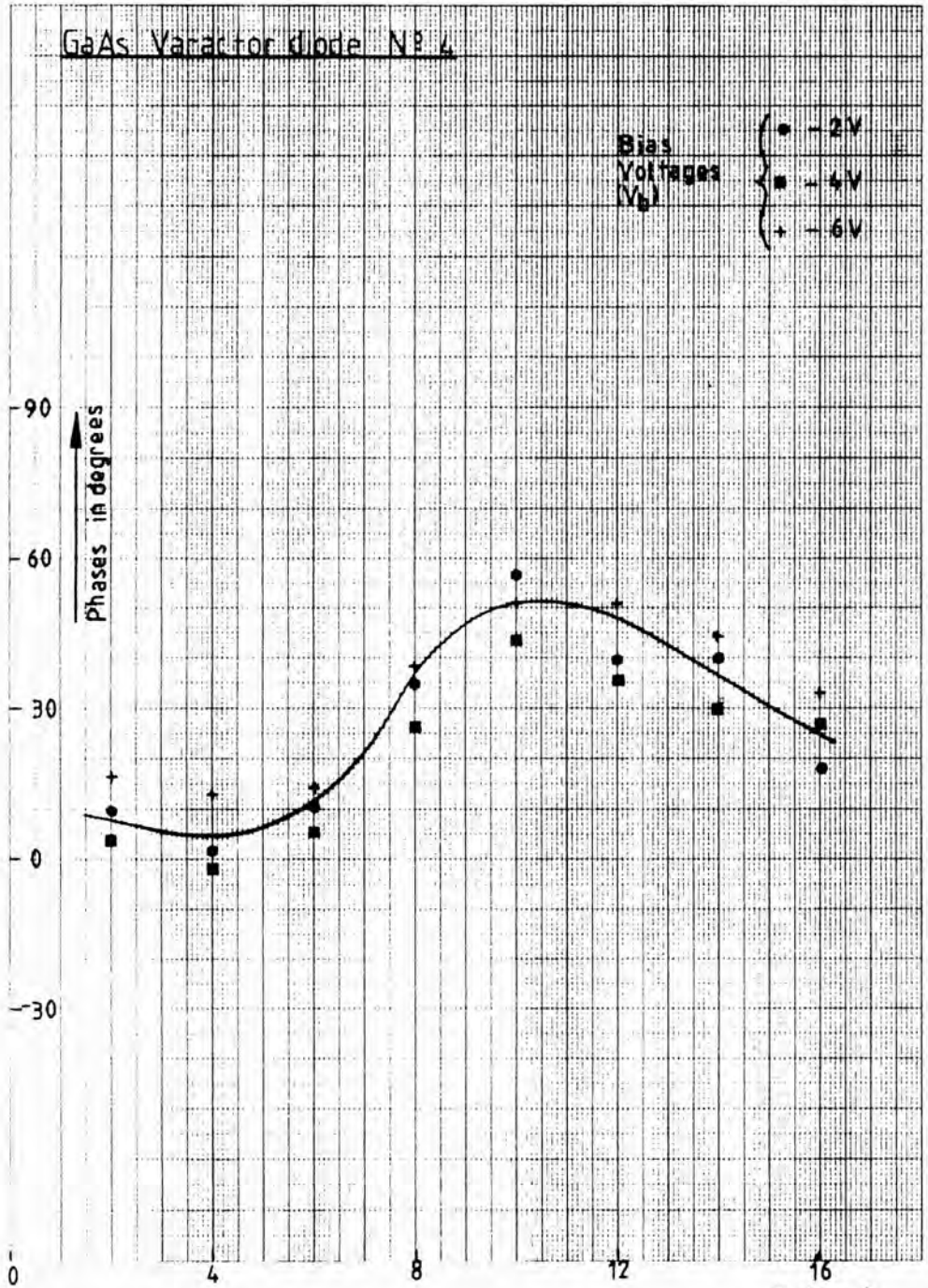

Fig. 6.44 Phase Relationship of 5th Harmonic w.r.t. Fundamental

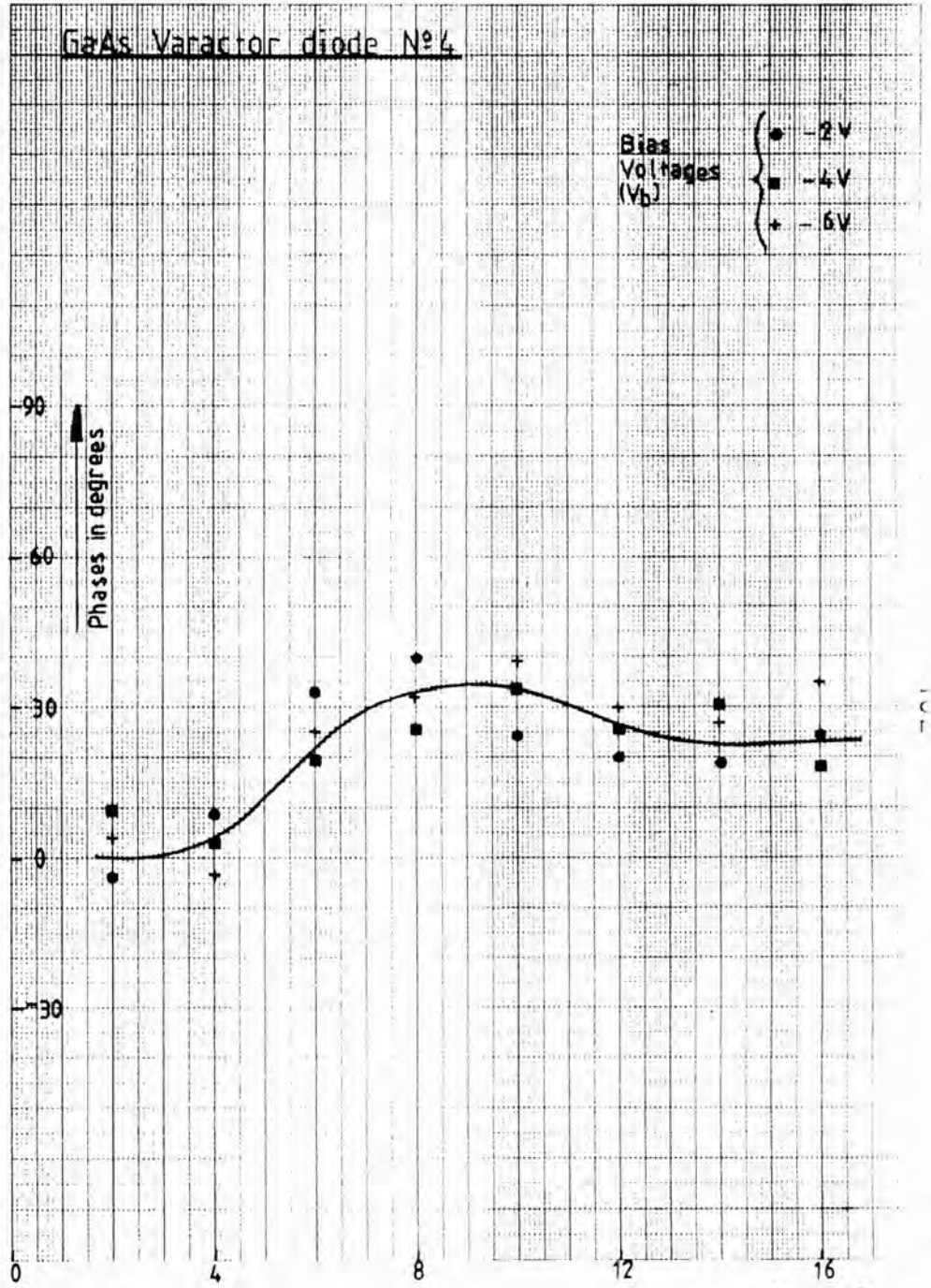

Fig. 6.45 Phase Relationship of 6th Harmonic w.r.t. Fundamental

most stayed in the area betweeen -10 and +45 degrees.

6.5 Spectrum Analyzer Method Results

It was mentioned in chapter 5 that there was a need to confirm the validity of the sampling method. To achieve this spectrum analyzer measurements were used. The results obtained using this method were carried out under the same circuit conditions and are presented in Figs. 6.46-6.65. However, the verification could not have been complete since spectrum analyzer can only measure harmonic amplitudes and can determine their relative phases. The resulting graphs show a reasonable agreement between the measurements obtained using sampling method and spectrum analyzer. This confirmation justifies the use and the application of the sampling method.

The shapes of the plots for different harmonics of the diodes were similar to the once obtained in the sampling method. Point by point comparisons has indicated in many instances a very close agreement between the two measurements as expected. The positions of the dips or the transition point for higher harmonics have also occurred at similar drive levels. All the harmonic amplitudes are presented in Figs. 6.46-6.65.

6.6 Discussion

An attempt has been made to give a simple and useful picture of the behaviour of varactor diodes which may

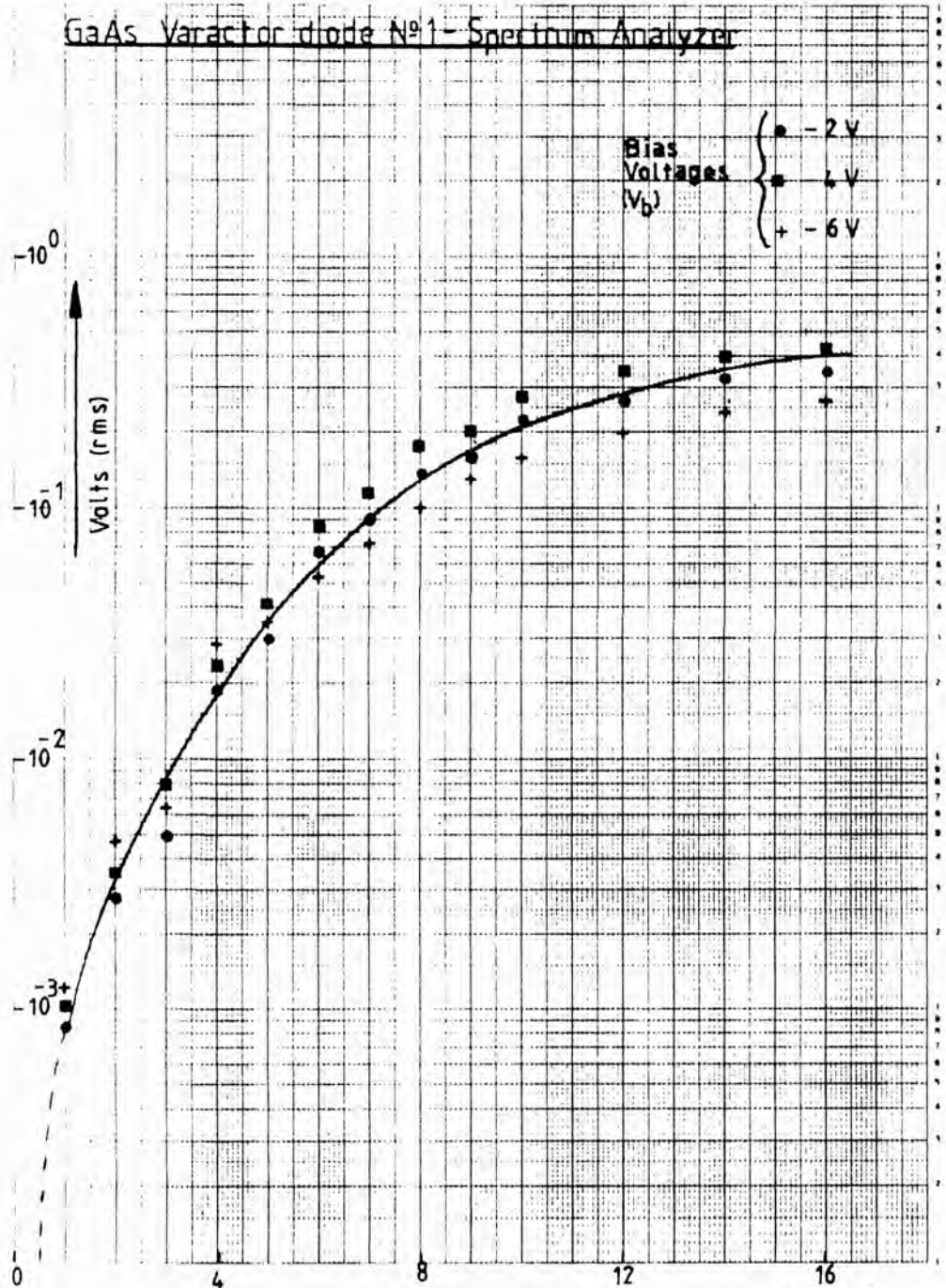

Fig. 6.46 2nd Harmonic Amplitudes v Drive Level

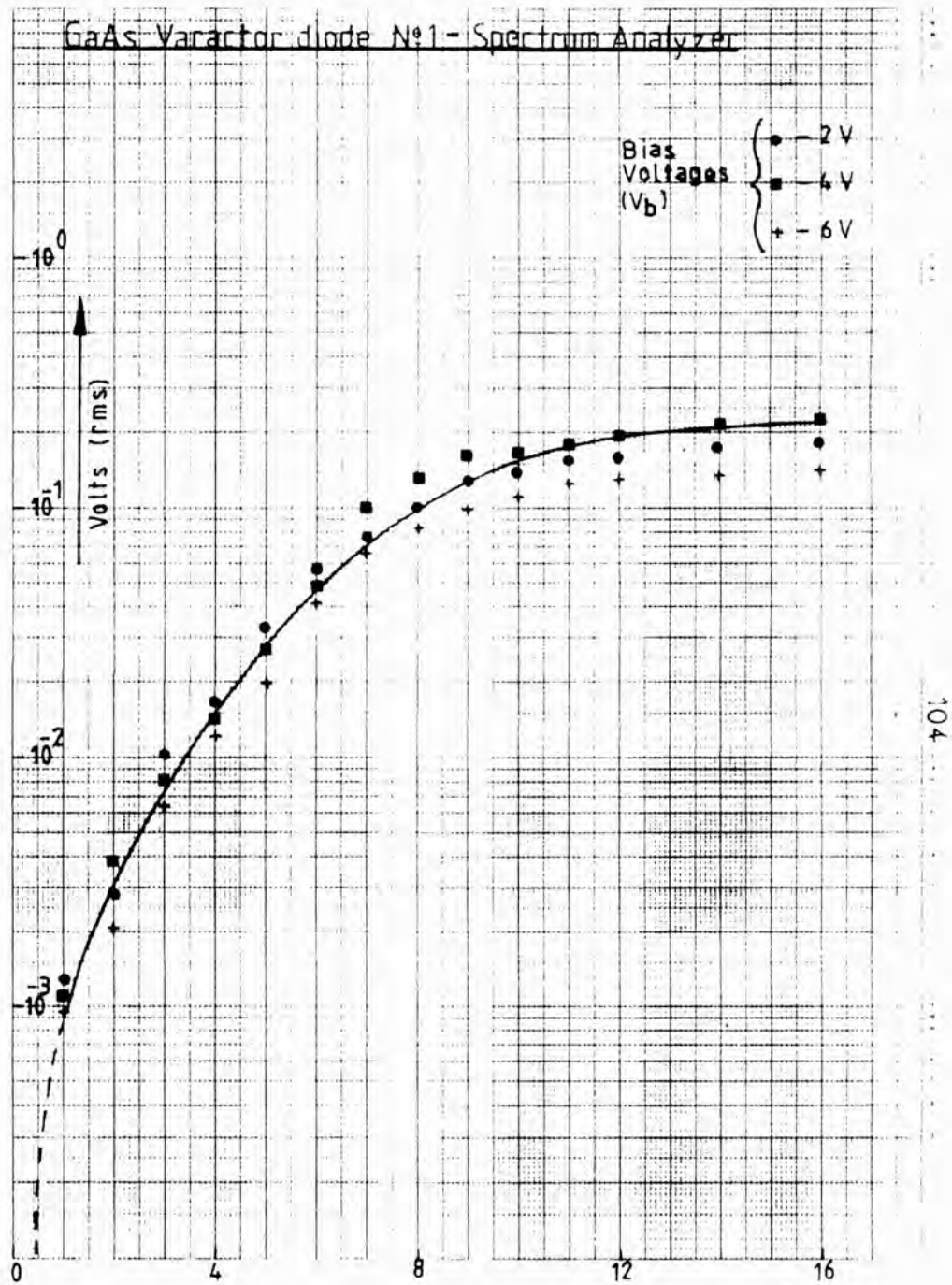

Fig. 6.47 3rd Harmonic Amplitudes v Drive Level

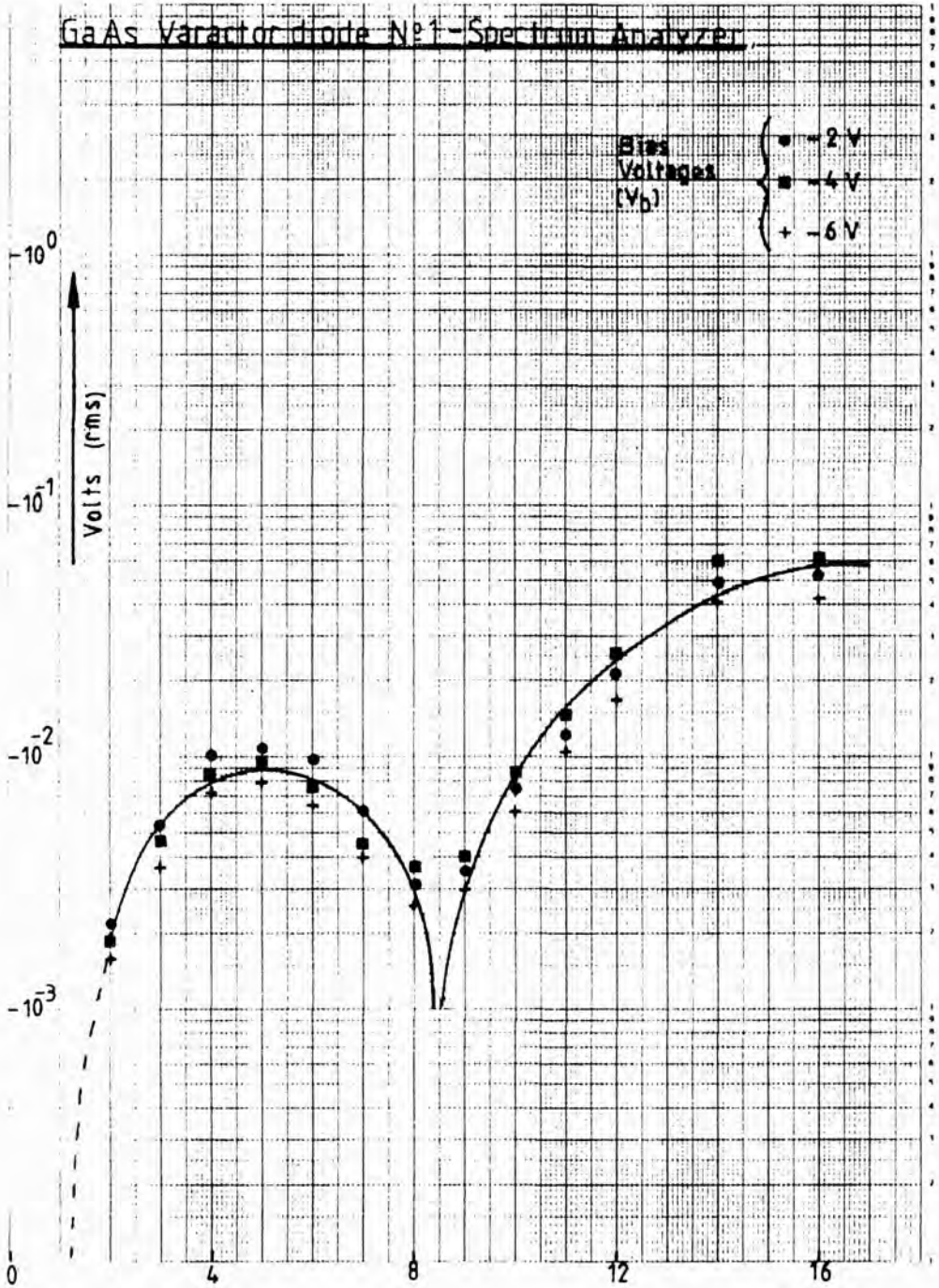

Fig.6.48 4th Harmonic Amplitudes v Drive Level

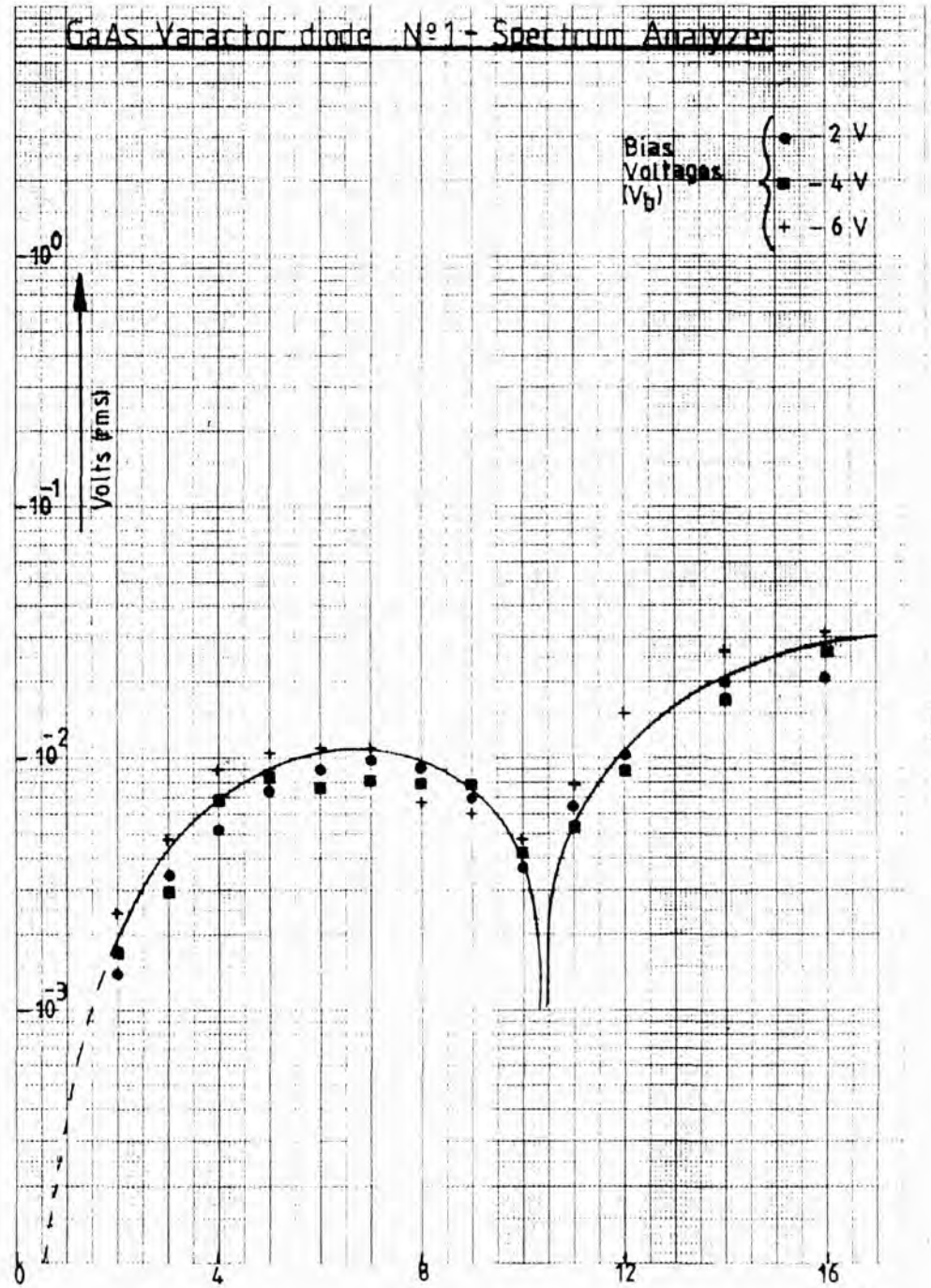

Fig. 6.49 5th Harmonic Amplitudes v Drive Level

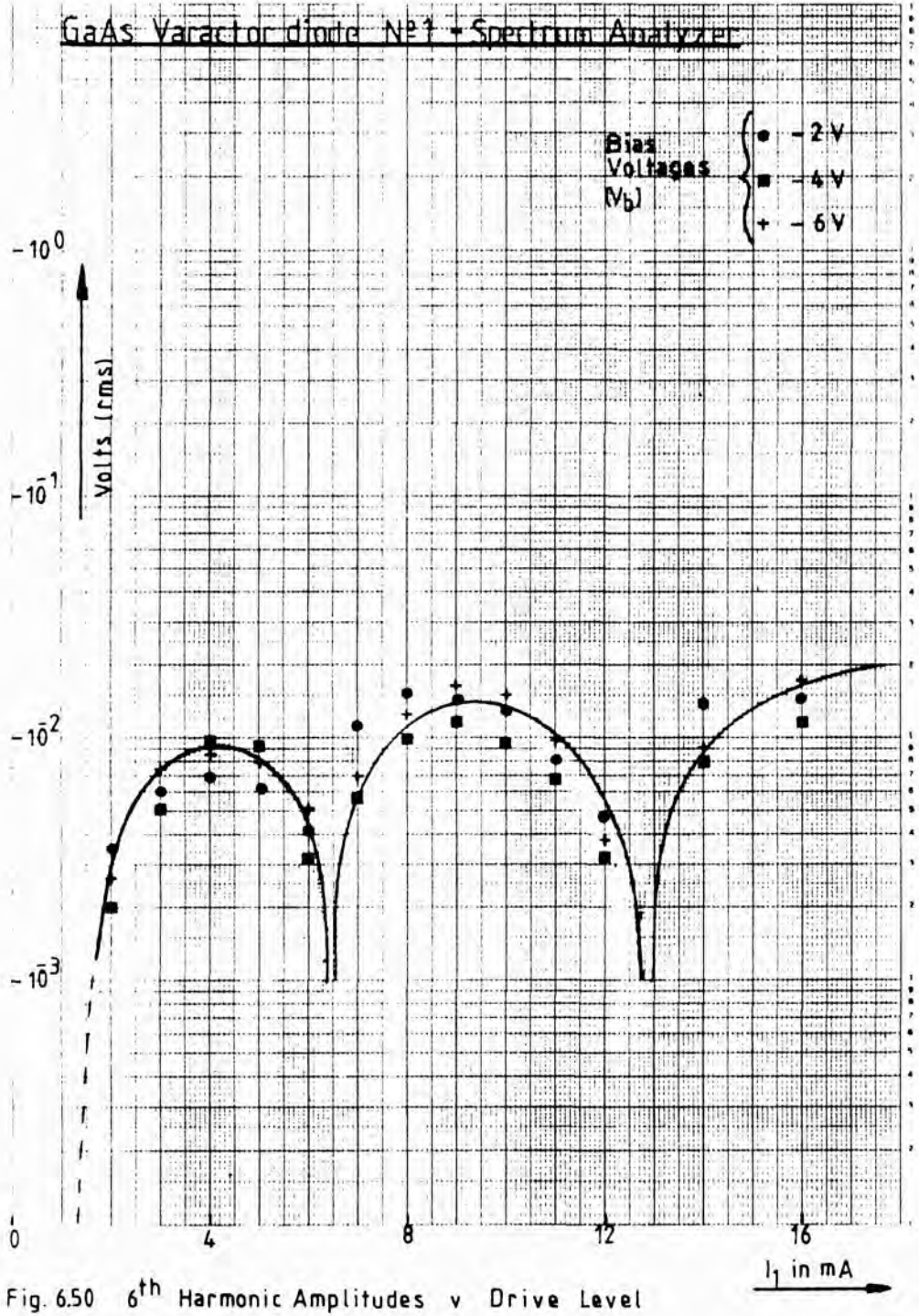

Fig. 6.50 6th Harmonic Amplitudes v Drive Level

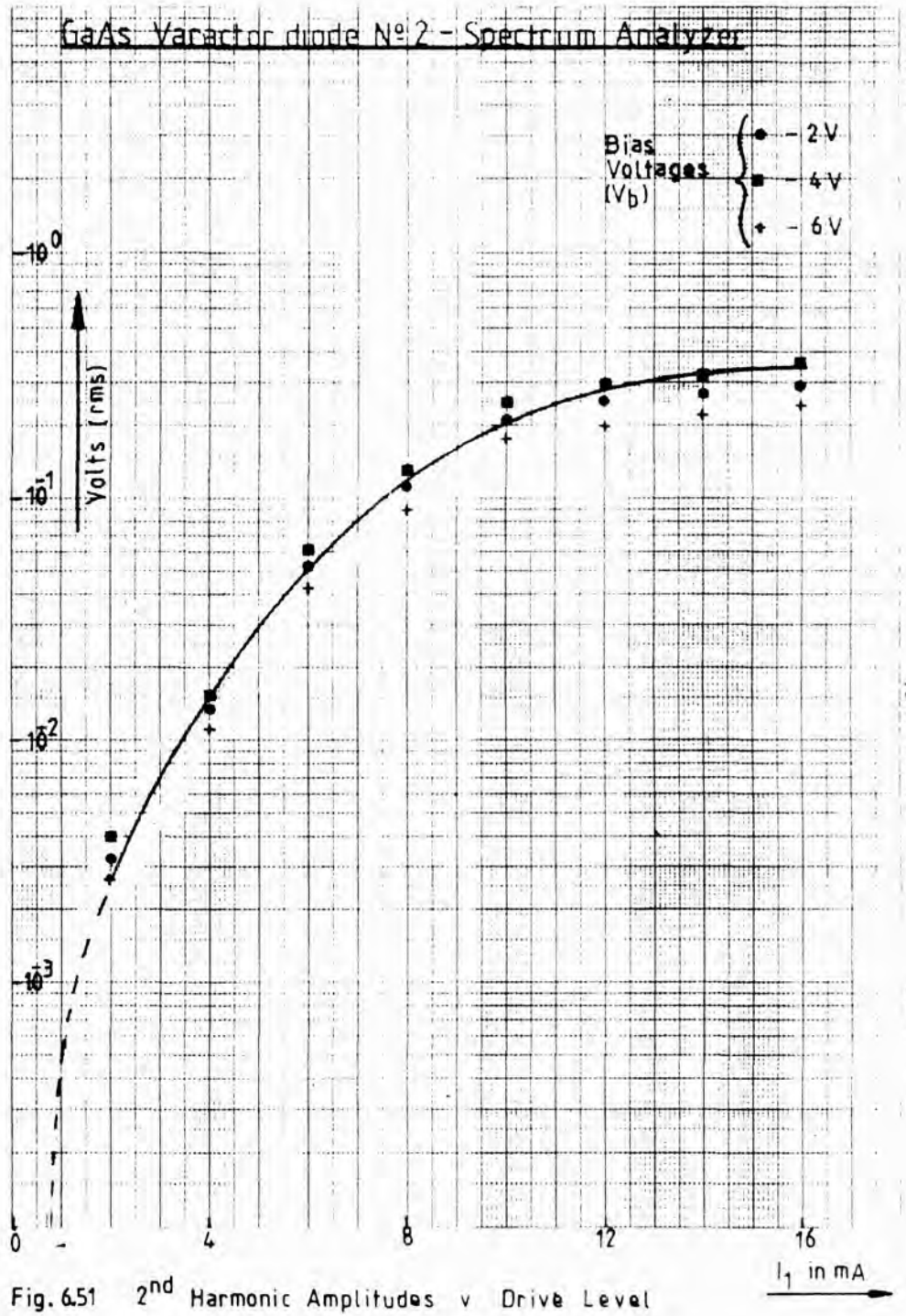

Fig. 6.51 2nd Harmonic Amplitudes v Drive Level

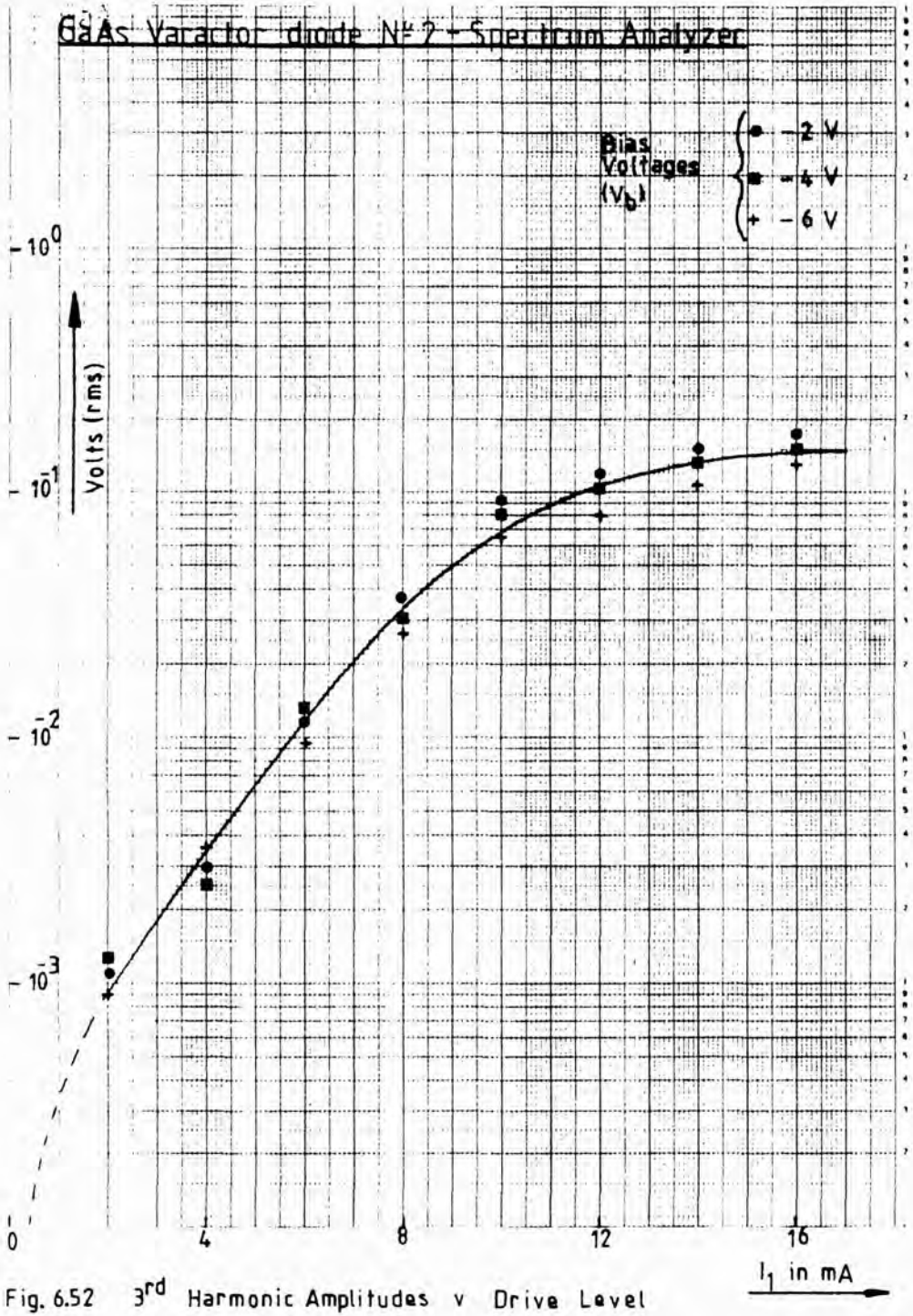

Fig. 6.52 3rd Harmonic Amplitudes v Drive Level

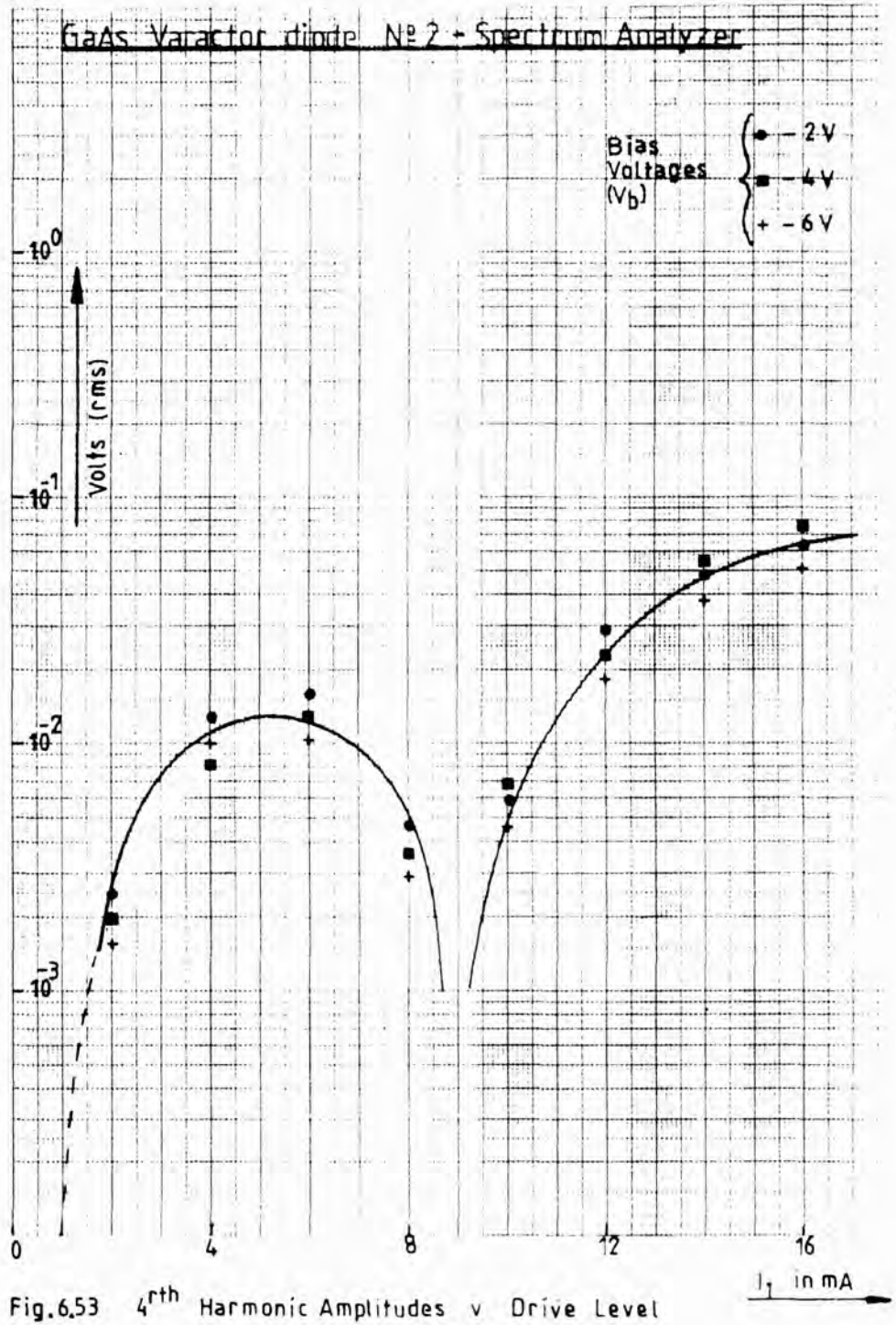

Fig. 6.53 4rth Harmonic Amplitudes v Drive Level

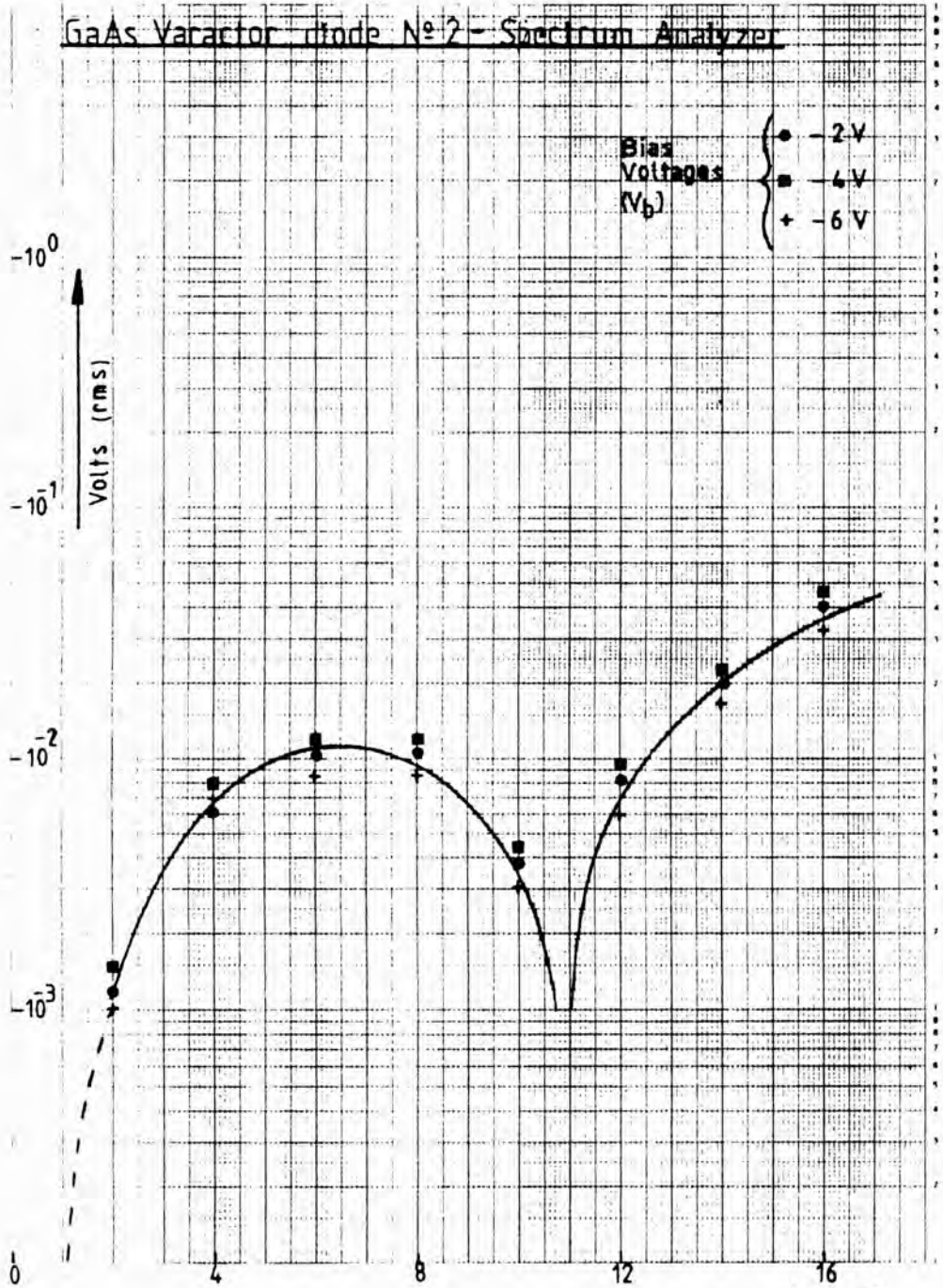

Fig.6.54 5th Harmonic Amplitudes v Drive Level

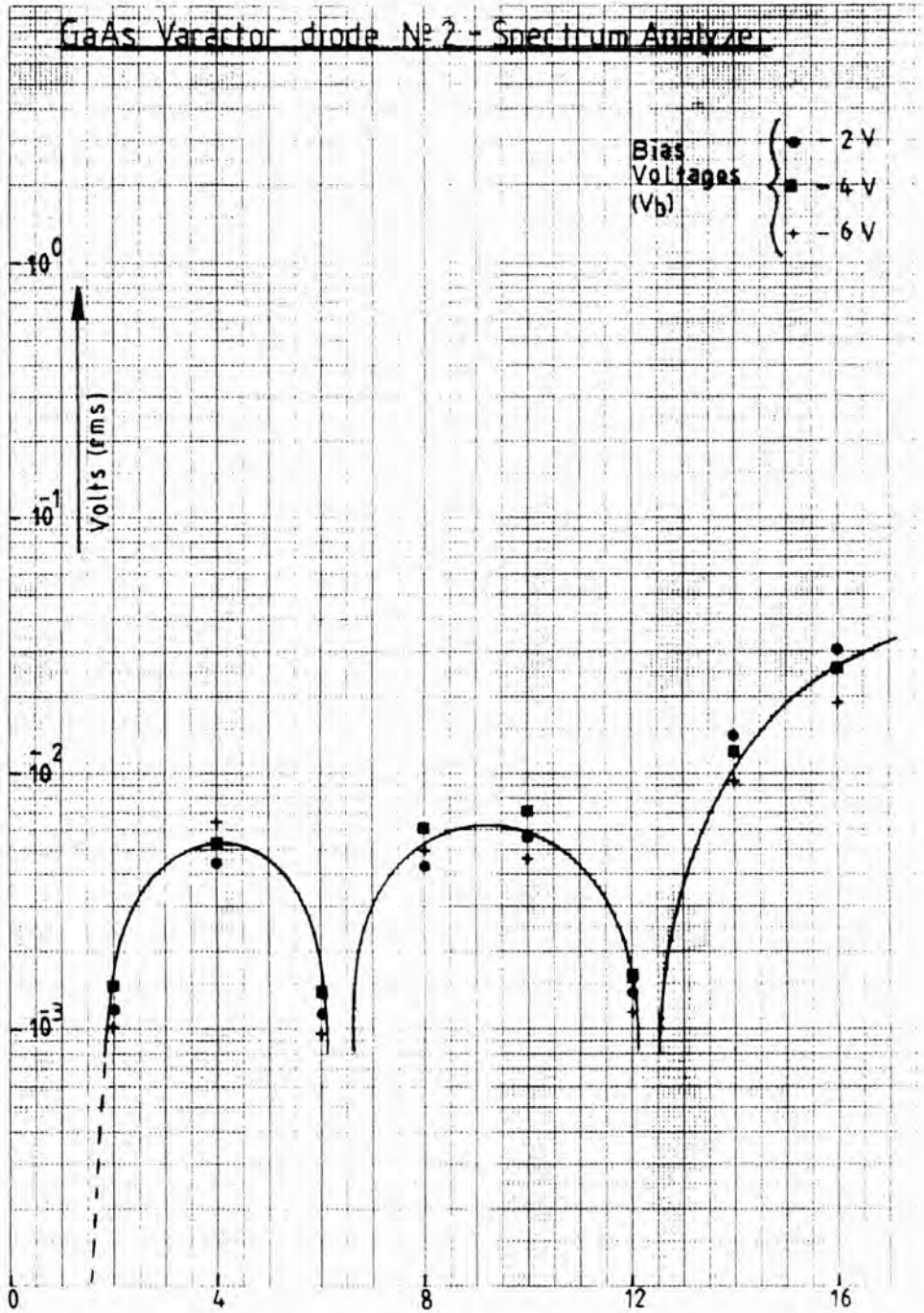

Fig.6.55 6th Harmonic Amplitudes v Drive Level

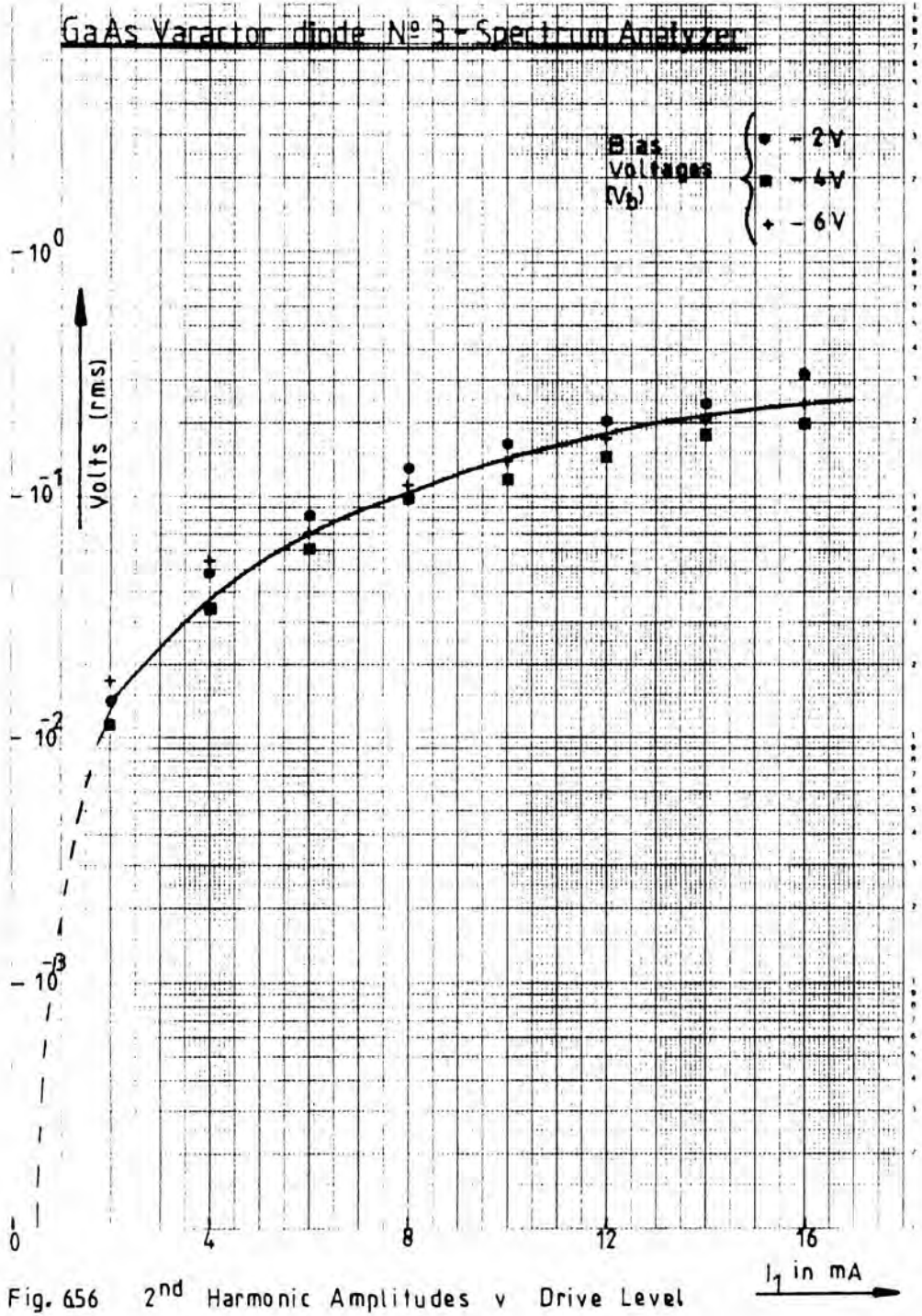

Fig. 656 2nd Harmonic Amplitudes v Drive Level

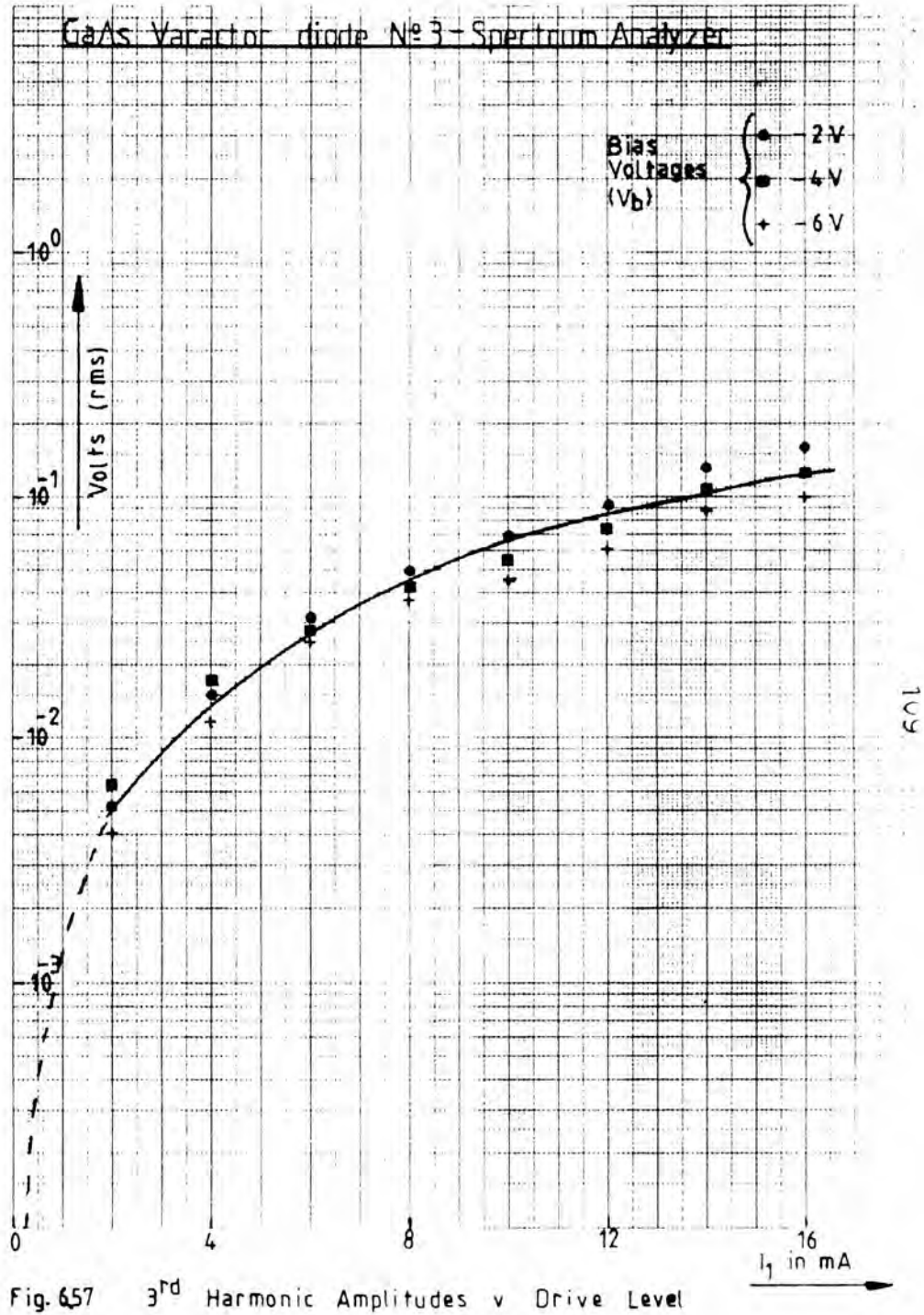

Fig. 657 3rd Harmonic Amplitudes v Drive Level

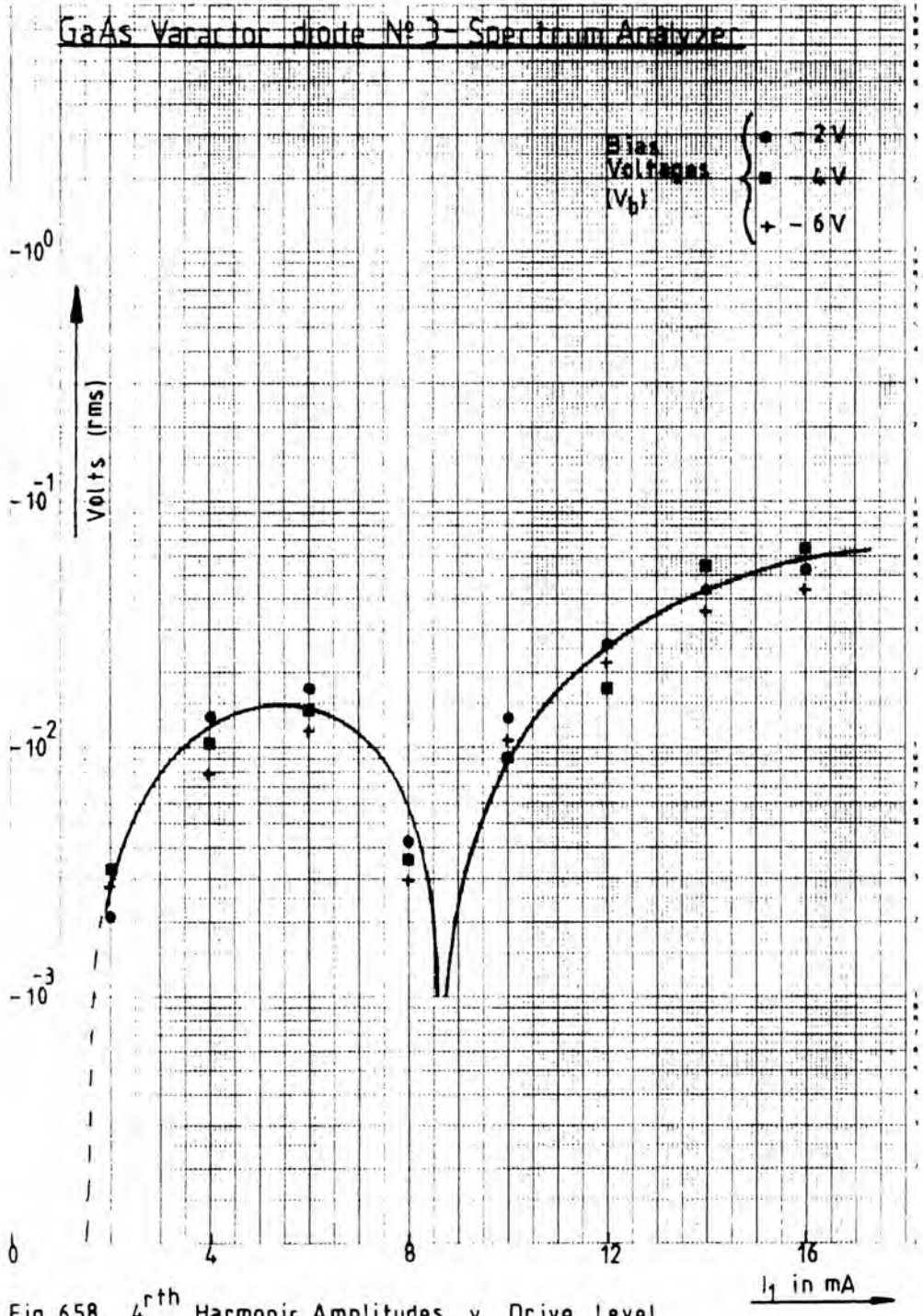

Fig. 658 4rth Harmonic Amplitudes v Drive Level

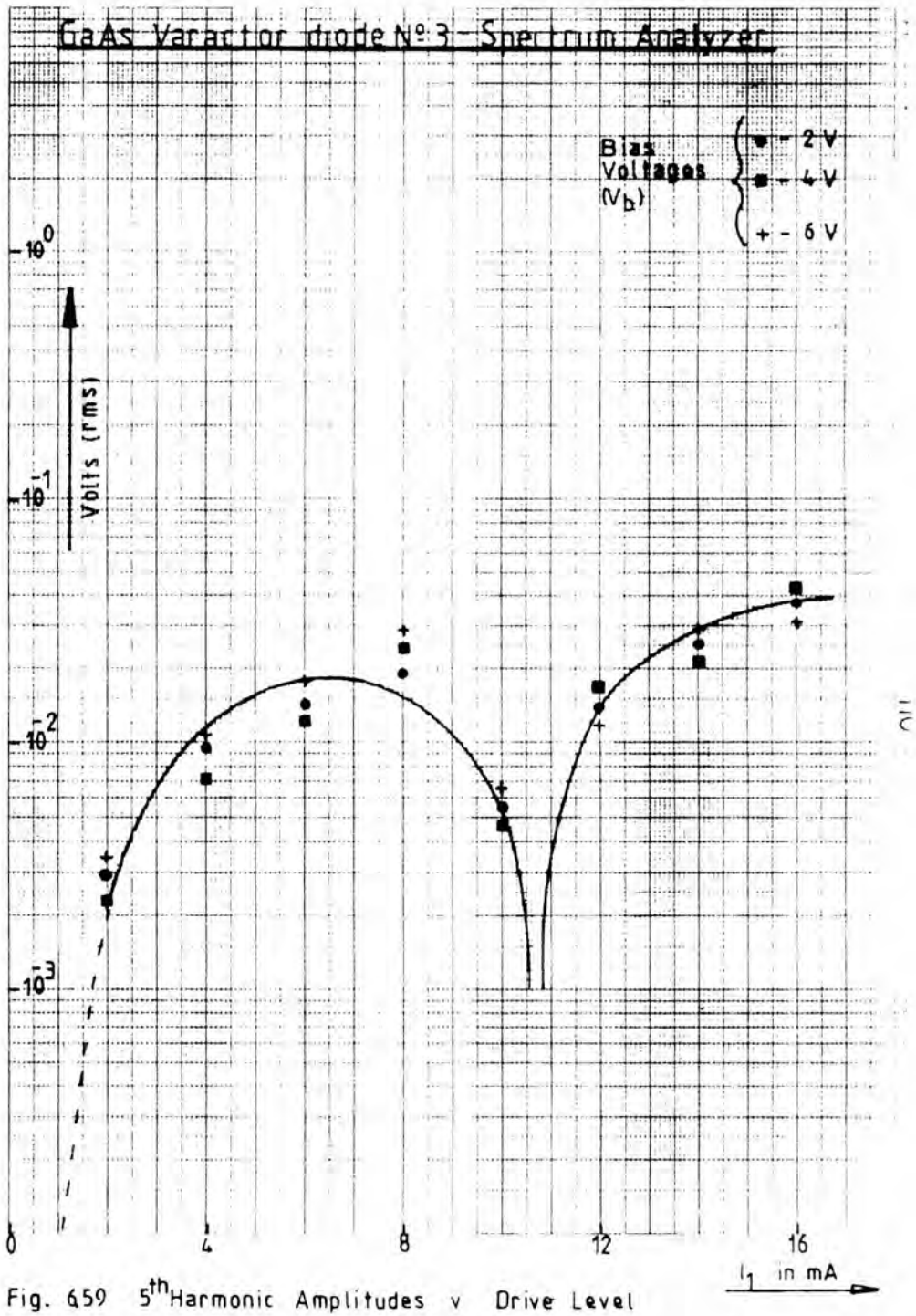

Fig. 659 5th Harmonic Amplitudes v Drive Level

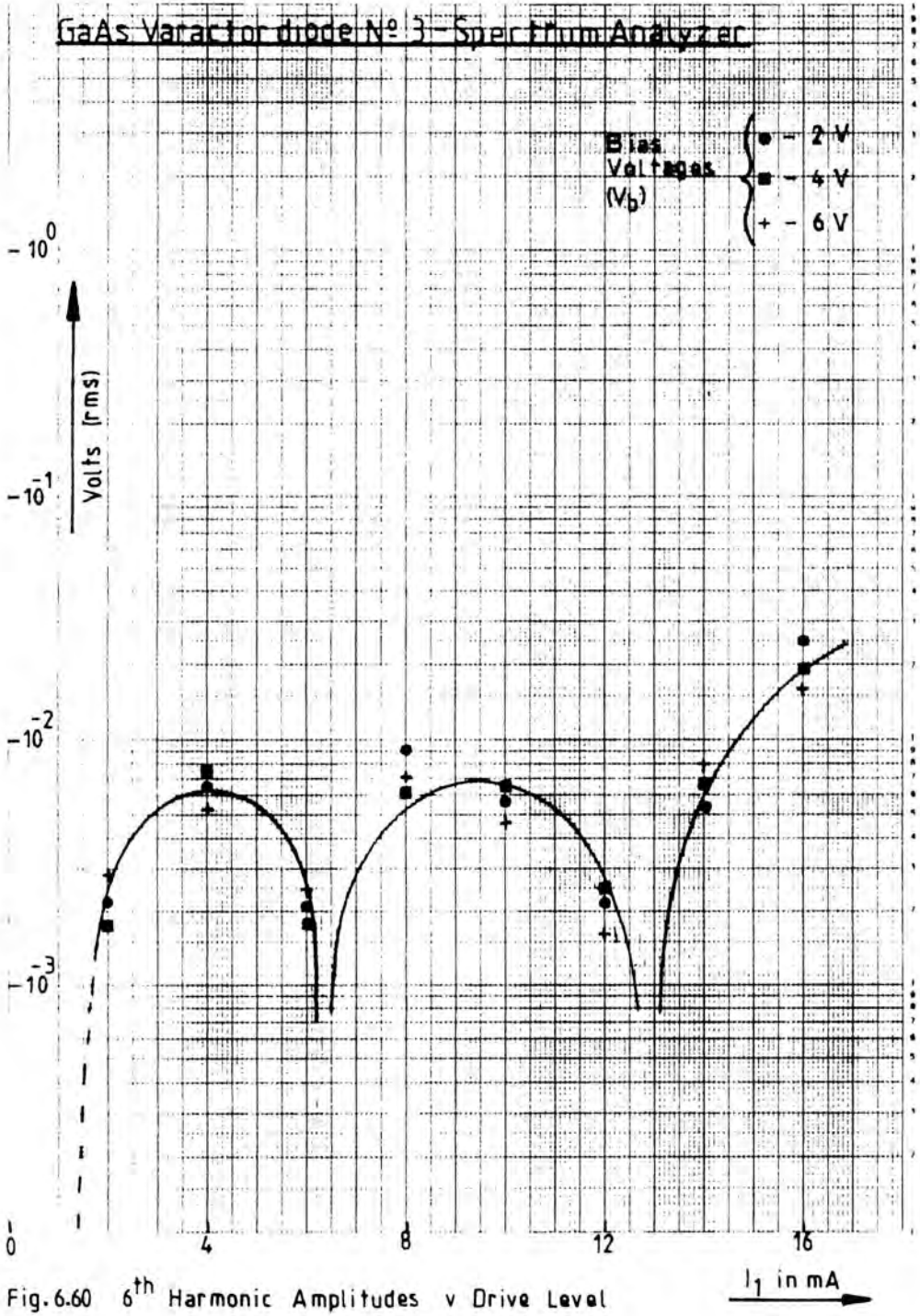

Fig. 6.60 6th Harmonic Amplitudes v Drive Level

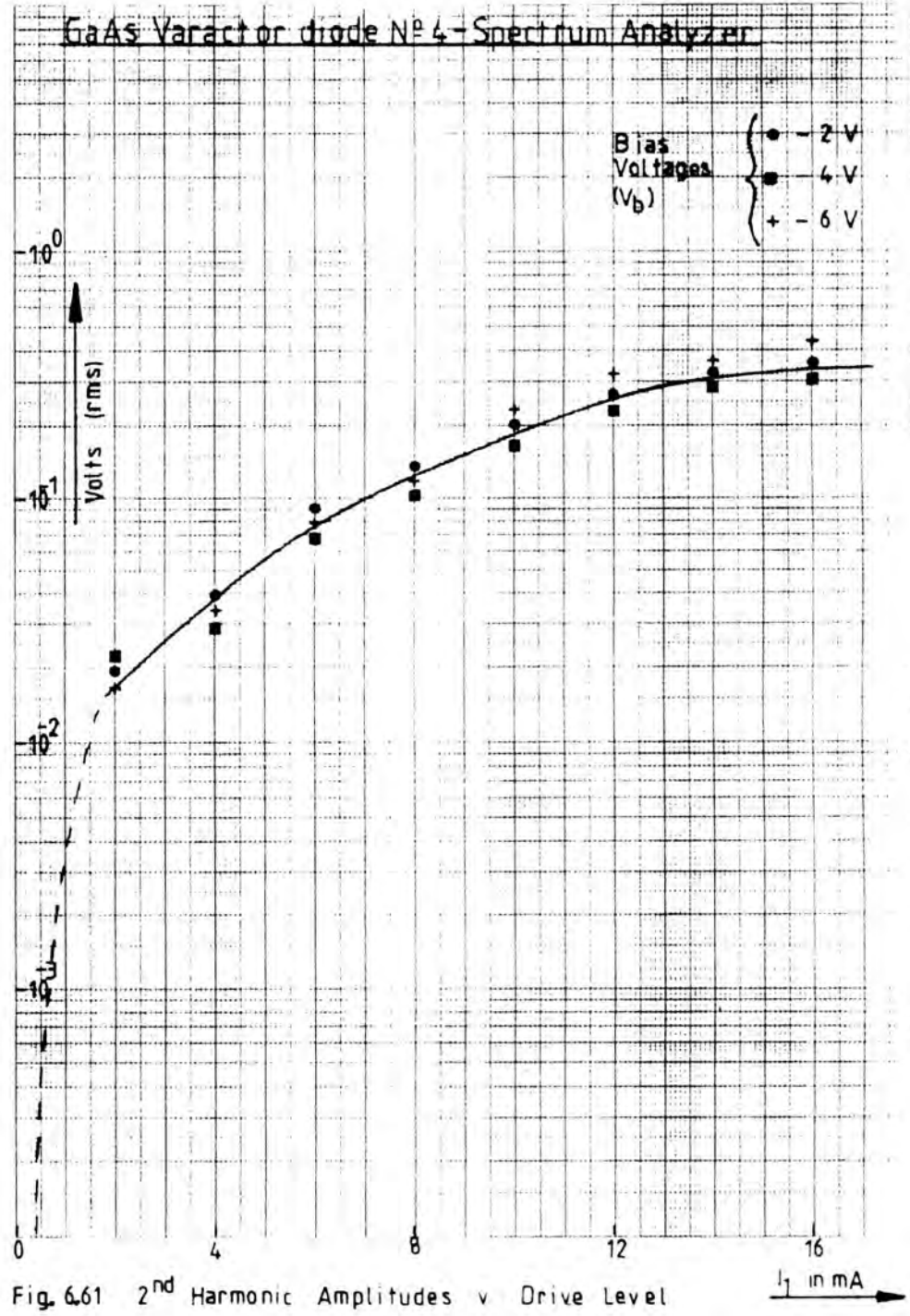

Fig. 6.61 2nd Harmonic Amplitudes v Drive Level

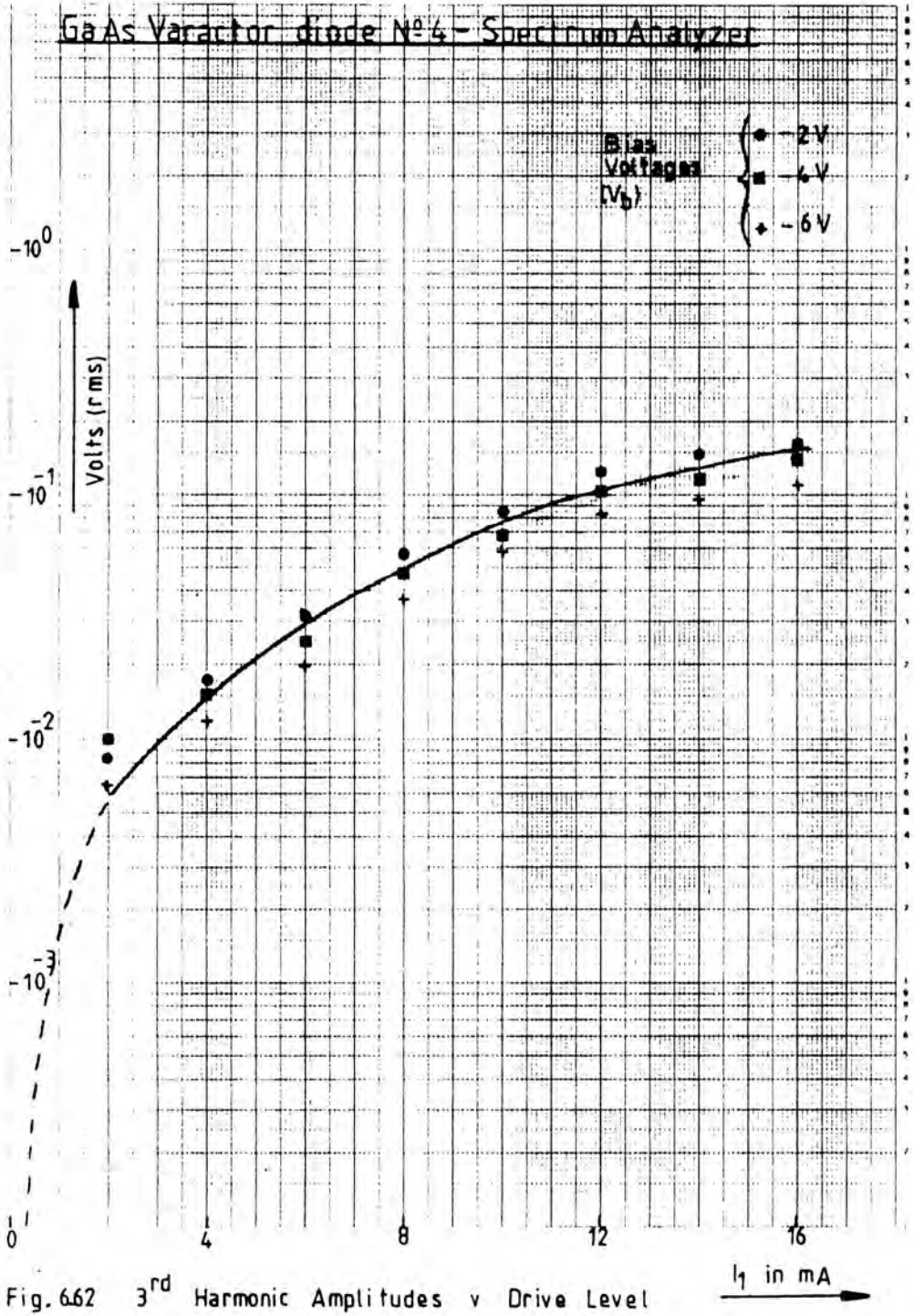

Fig. 6.62 3rd Harmonic Amplitudes v Drive Level

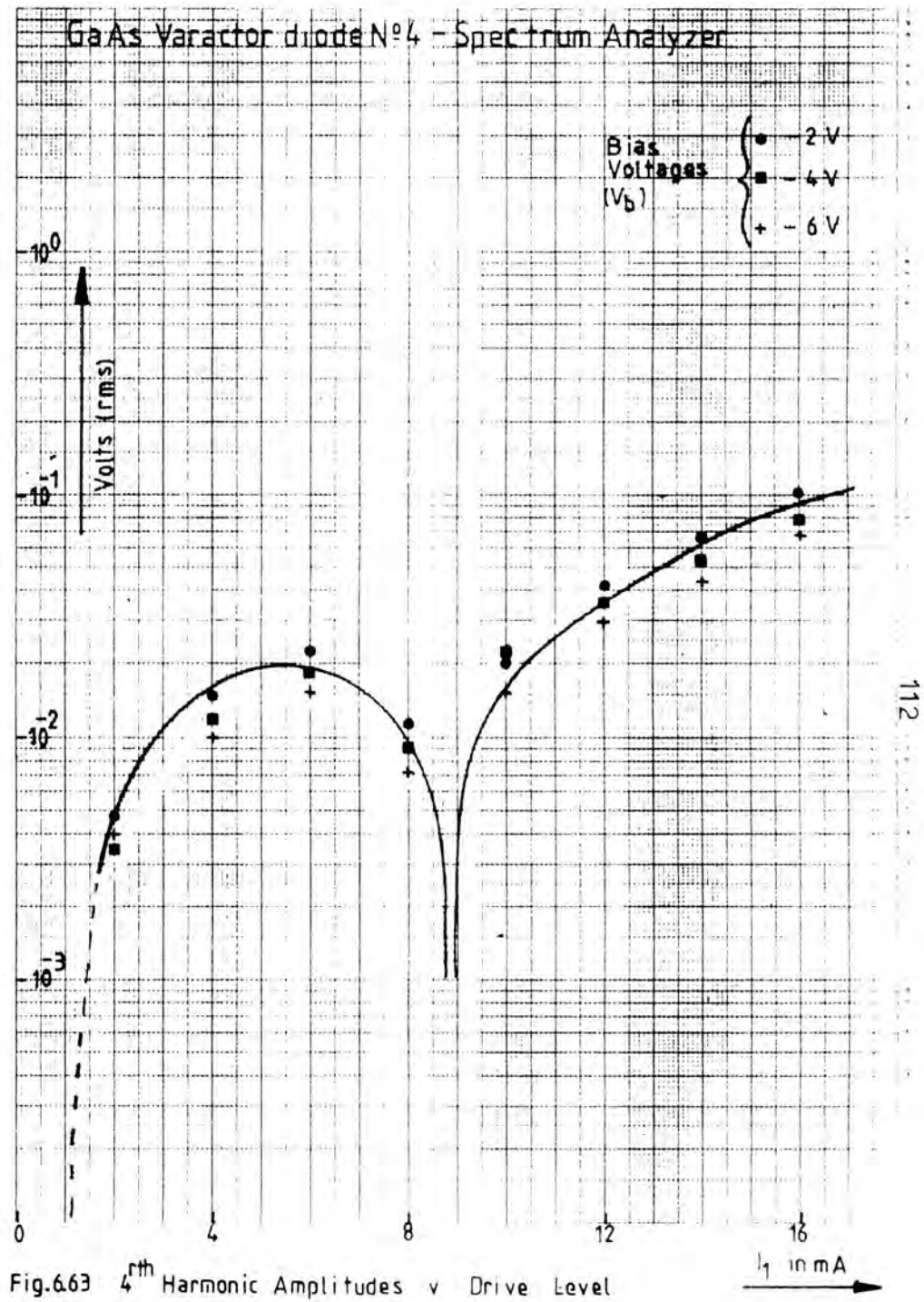

Fig. 6.63 4th Harmonic Amplitudes v Drive Level

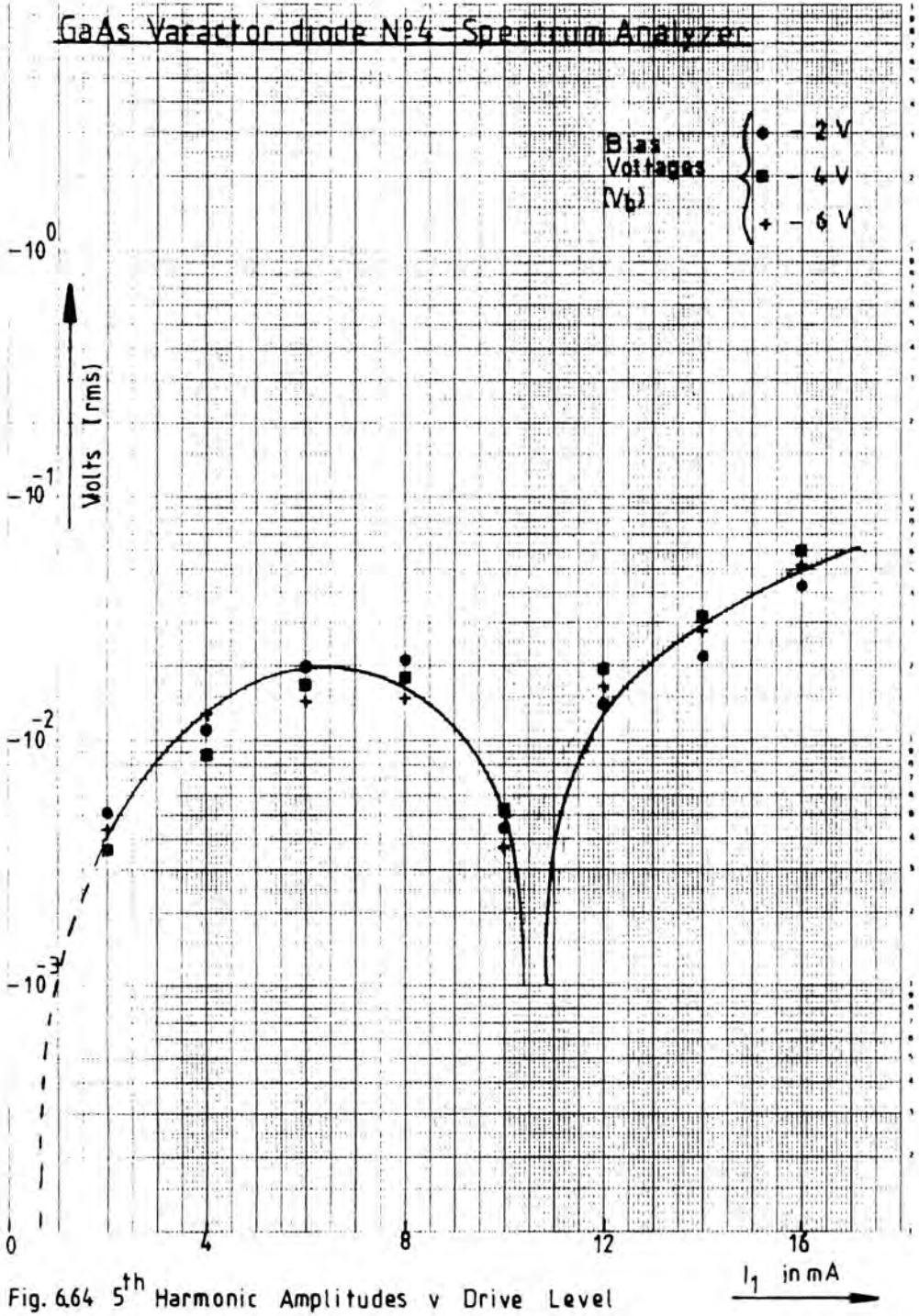

Fig. 6.64 5th Harmonic Amplitudes v Drive Level

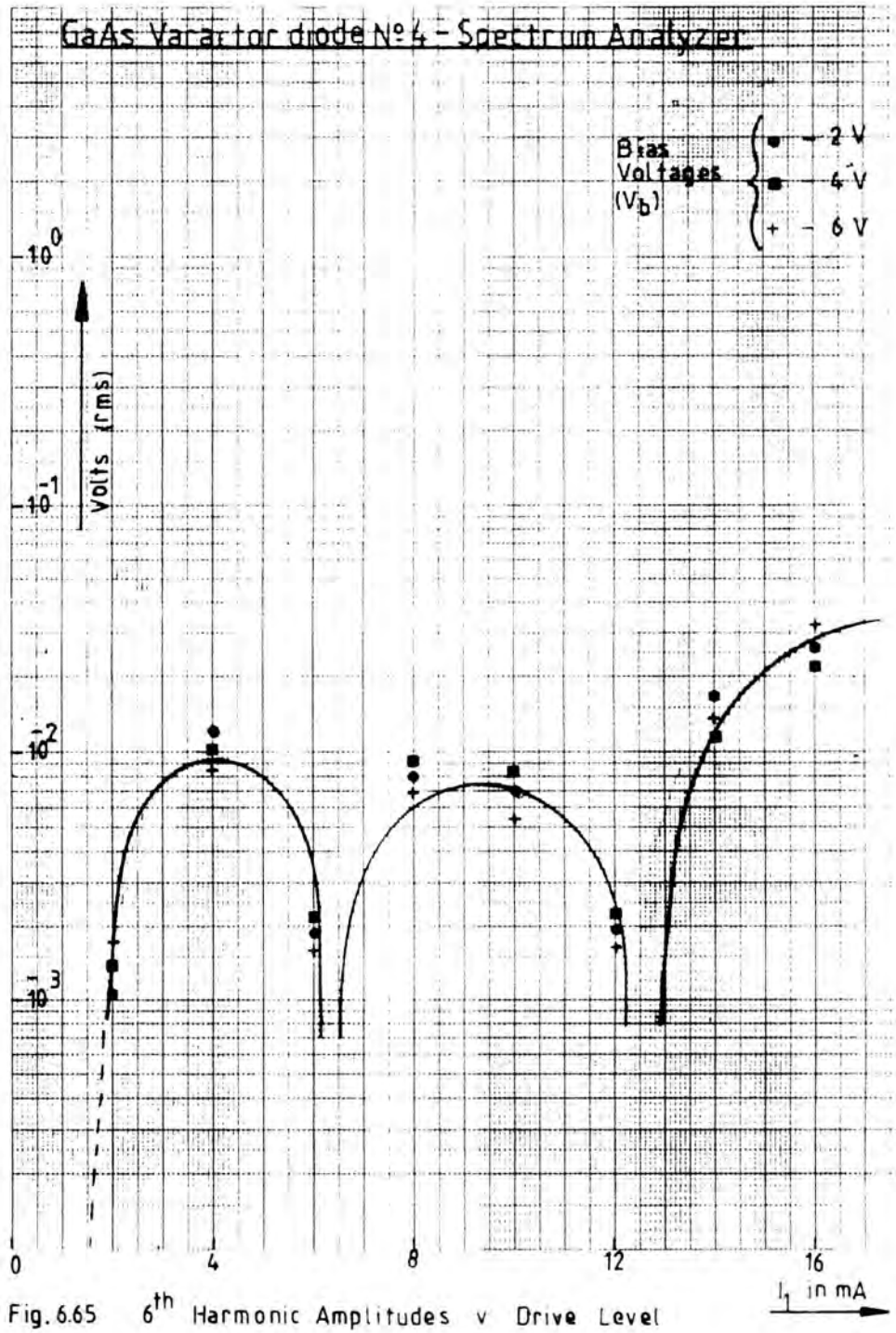

Fig. 6.65 6th Harmonic Amplitudes v Drive Level

reveal a wealth of information necessary for their applications. The results of the sampling and spectrum analyzer methods have illustrated the general effects of the diodes.

The curves of the harmonic voltages have been explored over a wide range of applied drive levels which served as a guide to experimental optimization to harmonic amplitudes and relative phases and a satisfactory agreement between the two methods was obtained.

An outstanding feature of the sampling method is that the computation of the Fourier Coefficients may produce information for many parameters of the diodes.

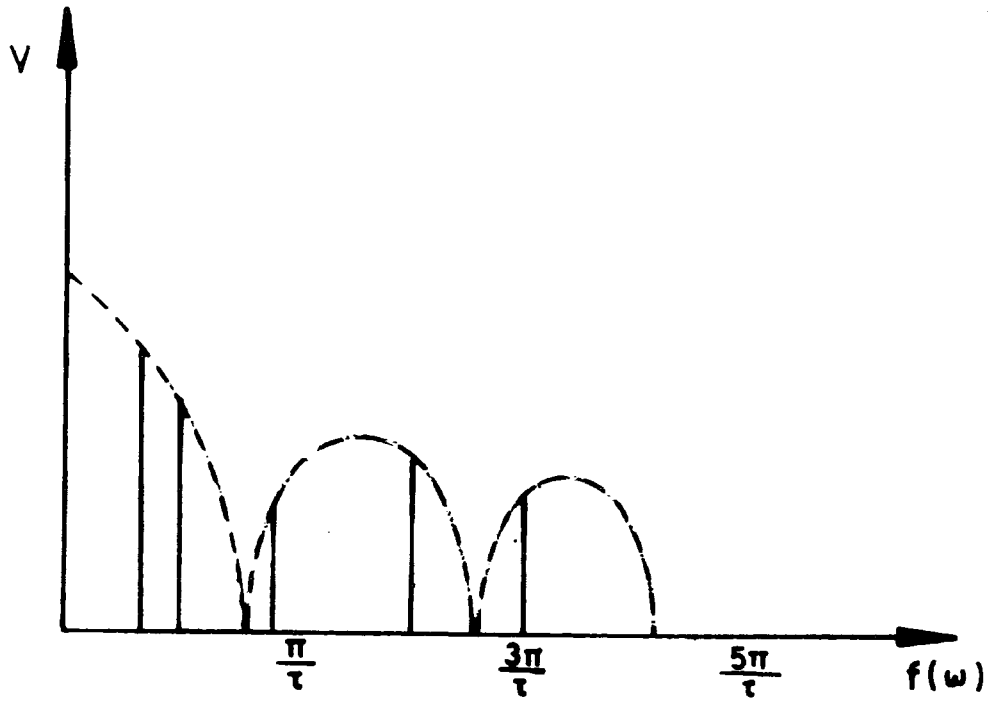

Fig. 6.66 Typical Spectrum of a Varactor Diode

CHAPTER 7

CONCLUSIONS

7.1 Introduction

The techniques and the experimental procedures of the sampling method and the direct measurements using spectrum analyzer were described in chapters 4 and 5, respectively. The amplitudes and phases of the generated spectra for each varactor diode were presented in chapter 6, then followed by a discussion of the harmonics' behaviour. As the measurements were made for four different diodes but of the same type, the comparison of the results was appropriate. The validity of the developed sampling method was confirmed by the direct measurements for the same diode circuit conditions using the spectrum analyzer. Typical estimated errors for the amplitudes between the two sets of results were about 3 to 4% for most of the measured harmonic amplitudes with a maximum deviation of about 10%.

The harmonic spectra of amplitudes and relative phases were presented as functions of the drive level. The spectrum of generated frequencies at any excitation level of the varactor and bias can be obtained by extraction from the plots. The changes in the amplitudes of the harmonics and their relative phases for different energising levels represented the changes in the generating properties of the nonlinear capacitance of the varactor diodes. The points of

transition between the lobes of the harmonic spectra are clearly seen to occur at particular drive levels. Such knowledge of the diode behaviour and actual amplitude values of the harmonics generated within it can be very useful in the design of numerous frequency-converting circuits which play an essential role in many applications.

7.2 Device Characterisation

It is evident that in any planned design undertaking one requires as much measured data on the devices to be used before a satisfactory performance can be achieved. It is also necessary to establish relationships between the device parameters and its dynamic behaviour. The information supplied by the manufacturers has always been limited and usually carried out only at certain test frequencies and at one or two points of the device characteristic.

In order to overcome these serious deficiencies there was a need to introduce a suitable method of classifying the nonlinear properties of devices for frequency converting applications. Spectral characterisation dealt with in this project is such a method that can satisfy these requirements. It is based on the fact that the nonlinearity of the device must be reflected in the spectrum of harmonics it generates. Such "fingerprinting" of the nonlinearity of the device is only valid for a particular drive levels which does not, however, diminish

its apparent advantages.

There are many benefits in being able to identify the nonlinear devices by means of its generated spectrum, i.e. its "fingerprint". The main ones can be in

(i) the comparison of the devices of the same type, e.g. quality test in manufacture,

(ii) the assessment of the device capabilities and hence possible early prediction of its performance in a circuit by the customer,

(iii) for matching purposes in the design of multi-device circuits,

and (iv) for the replacement of devices in complex systems without the need of circuit redesign.

A practical device will normally be encapsulated in a type of package which will inherently have parasitic components. As a consequence of this the device nonlinear characteristic under dynamic operating conditions at high frequencies will depart widely from the static d.c. characteristic. To represent such a device by an equivalent circuit will be difficult and therefore the equivalent "fingerprinting" can be considered as an alternative and appropriate representation.

At high and microwave frequencies it is the harmonic spectrum generated by the device that will give indication of the degree of nonlinearity and device capability for use

in frequency-converting circuits. For experimental verification and theoretical analysis it was decided to consider current driven varactors. It was assumed that the energising level of the device may be accurately represented by the current at the fundamental frequency measured in the output load. As a reference, V-I d.c. measurements have also been carried out on each one of the diodes under test.

The theoretical analysis carried out in chapter 3 had shown the difficulties involved and the need for many approximations to be introduced before the values of individual harmonics can be found. This conclusion supported even more the necessity for an experimental method which will overcome these problems. None of the results of the analysis produced closed analytical solutions that could be used in the prediction of harmonics generated in the varactor. The reasons for this were because the resulting expressions were of the series type and sometimes did not converge rapidly. However, on comparison it was found that the calculated values using limited number of terms agreed within reasonable tolerances with the results obtained experimentally.

Such verification was a proof of the method validity and accuracy. The processes used in the sampling method can be easily computerised and can provide a basic technique for a wideband high frequency testing.

The availability of the sampling method or even a

limited (because of lack of phase data) direct-measurement method using spectrum analyzer for the purposes of spectral characterisation of nonlinear devices could be very useful when circuit designs are planned. This could be on the grounds of economy as in many cases the prices of the devices are high. Selecting nonlinear devices for a particular frequency converting circuit is important if the predicted performance is to be achieved. Use of unsuitable devices can increase the cost of the design and development. It is probably up to the manufacturers to provide more data of the right kind to the customer so that a correct choice can be made.

This new measurement method also offers a means of determining a complete spectrum (amplitudes and phases) generated within a nonlinear element over a wide frequency range. The resultant spectra which are the "fingerprints", represent new forms of device characterisations. The pattern may show a regular trend consistent with the normal behaviour of the device. It may also display an anomalous trend which signifies the peculiarity of the device under certain defined conditions. Regarding the accuracy, there are no mathematical approximations involved except for the experimental errors. It is hoped that this project will stimulate industrial interest because of its additional facility of phase determination, not available in any spectral analyzer.

7.3 Future Work

This sampling method of characterising nonlinear devices, i.e. varactors in this project, produced reasonably good results. There is, however, a need for more work to be done basically, first, to eliminate test circuit and system imperfections and second speed up the procedures. The areas needing improvements are as follows:

(1) it would be very useful to have a computer with a good graphics display facility which would allow more precise determination of the points on the waveform to be analysed. As a result a comparison can also be made between the sampler output and input waveforms in the system and hence check on any distortions in the sampler circuits.

(2) a modern and higher precision sampler unit could be of great benefit. The existing sampler we have used was the weakest link in the system. It was very difficult to stabilise the signal output because of sensitive trigger controls.

(3) there is a need for another numerical method and appropriate computer algorithm for calculating the Fourier Coefficients and which can also account for the presence of noise. Alternatively this may be achieved by inputing the data a number of times and then averaging the values before calculating the coefficients and hence reduce any random

noise in the sampler-interface connection. The result of this, would be a more accurate determination of the low level harmonics.

(4) a thorough examination of the input connections would also be required. High frequency problems were occasionally encountered when certain cable and generator power level combinations were used. There is also a need to have a higher power source to increase the drive levels and hence measured harmonic spectra of fully driven devices.

An improved system could probably have a very wide industrial application in microwave testing. This will have advantages over a single frequency measurements which would normally be carried out using a slotted line assembly. The method is much quicker and can produce the direct information over a band of frequencies.

REFERENCES

1. VAN DER ZIEL,A., "On the Mixing Properties of Nonlinear Condensers", J.A.P., Vol.19, No. 11, 999-1006, November 1948.
2. BAKANOWSKI,A.E. et al., "Diffused Ge and Si Nonlinear Capacitor Diodes", Presented at the IRE-AIEE Semicon. Dev. Res. Conference, Boulder, Colc., July 1957.
3. SHIMIZU,A. & NISHIZAWA, J., "Alloy-Diffused Variable Capacitance Diode with Large Figure of Merit", IRE Trans. Electron Devices (USA), Vol.ED., No 5, 370-7, Sept. 1961.
4. SUKEGAWA,T. et al., "Si Alloy-Diffused Variable Capacitance Diode", Solid State Electronics (GB), Vol.6, 1-24, Jan. 1963.
5. WATSON,H.A., "Microwave Semiconductor Devices and their Circuit Applications", McGraw-Hill, N.Y., 1969.
6. HOWES,M.S. & MORGAN,D.V., "Variable Impedance Devices", John Wiley and Sons 1978.
7. LIAO,S.Y., "Microwave Solid State Devices", Prentice Hall Inc.,New Jersey, 1985.
8. PENFIELD,Jr.P. & RAFUSE R.P., "Varactor Applications", MIT Press, Cambridge, 1962.
9. SHURMER,H.V., "Microwave Semiconductor Devices", Pitman Publishing, 1971.
10. LEVINE,S.N. & KURZOK,R.R., "Selected Papers on Semiconductor Microwave Electronics", Dover Publications 1964.

11. HASSAN, Y.M., "Spectral Characterisation of Devices at High Frequencies and Measurement Methods", Ph.D. thesis, Durham Univ., England, 1984.

12. PAPOULIS,A., "The Fourier Integral and its Applications", McGraw-Hill, N.Y., 1962.

13. AHMED, N. & NATARAJAN,T., "Discrete time Signals and Systems", Reston Publishing Company, 1983.

14. JOLLEY,L.B.W., "Summation of Series", Dover Publication London, 1961.

15. PUTEH,R.P., "Studies and Computing Techniques in the Spectral Characterisation of Solids", Ph.D. thesis, Durham Univ. England, 1984.

16. "Instruction Manual of the Sampling Adaptor Type 158" G. & E. Bradley Ltd., London.

17. PIPES,L.A. & HARVILL L.R., "Applied Mathematics for Engineers and Physicists", McGraw-Hill, London, 1970.

18. HEFFER,D.E., KING,G.A. & KEITH D., "Basic Principles and Practiceof Microprocessors", Edward Arnold Ltd., 1981.

19. DOWNEY,J.M. & ROGERS,S.M., "Pet Interfacing", Howard W.Sams and Co, Inc., USA, 1981.

20. BARNA, A. & PORAT, D.I., "Integrated Citcuits in Digital Electronics", John Wiley and Sons 1973.

21. GARRETT, R.H., "Analog I/O Design", Reston Publishing Company 1981.

22. SEITZER,D., PRETZL,G., & HAMDY N.A., "Electronic Analog-to-Digital Converters", John Wiley and Sons 1983.

23. CHIPMAN,R.A., "Transmission Lines", Schaum Outline Series

in Engineering, McGraw-Hill, London, 1956.

24. HARVEY,A.E., "Microwave Engineering", Academic Press, London, 1963.
25. TERMAN, F.E., "Radio Engineers' Handbook", McGraw-Hill Company Ltd., London, 1950.
26. DAVIDSON,C.W., "Transmission Lines for Communication", The MacMilland Press Ltd., 1978.
27. DUNLOP,J. & SMITH,D.G., "Telecomunications Engineering", Van Nostrad Reinhold, London, 1984.
28. SCOTT,R.E., "Linear Circuits", Addison-Wesley, London, 1960.
29. KATIB , M.K., "Evaluation of Harmonic Generating Properties of Schottky Barrier Diodes", Ph.D. thesis, Durham Univ. England, 1976.
30. FOX, L. & MAYERS, D.F., "Computing Methods for Scientists and Engineers", Clarendon Press, Oxford, 1968.
31. HUNTER,L.P., "Handbook of Semiconductor Electronics", McGraw-Hill Inc. London 1970.
32. LIAO,S.Y., "Microwave Devices and Circuits", Prentice-Hall, USA, 1980.
33. SHARMA,B.L., "Metal Semiconductor Schottky Barrier Junction and their Applications",Plenum Press, N.Y., 1984
34. STREMLER,F.G., "Introduction to Communication System", Addison-Wesley, 1977.
35. LATHI,B.P., "Communication Systems", John Wiley & Sons, London, 1968.
36. CHAMPENEY,D.C., "Fourier Transforms and their Physical Applications", Academic Press, 1973.

37. CUNNINGHAM,W.J., "Introduction to Nonlinear Analysis", McGraw-Hill Book Company, 1955.

38. BARLOW,H.M. & CULLEN,A.L., "Microwave Measurements", Constable and Company Ltd., 1950.

39. EVERITT,W.L. & ANNER,G.E., " Communication Engineering", Third Edition., McGraw-Hill Book Co.Inc., 1956.

40. KULESZA, B.L.J., "Efficient Harmonic Generation and Frequency Changing using Semiconductor Devices", Ph.D. Thesis, Birmingham Univ., UK., 1967.

41. ARMSTRONG, R., "Spectral Identification of Nonlinear Devices", Ph.D. Thesis, Durham Univ., UK., 1983.

42. SAUL, P.H., "Evaluation of a Step-Recovery Diode in a Broad-Band Frequency Multiplier", Ph.D. Thesis, Durham Univ., UK., 1974.

43. SCHEID, F., "Numerical Analysis", Schaum's Outline Series, McGraw-Hill Book Company, 1968.

44. ABRAMOWITZ, M. and STEGUN, I.A., "Handbook of Mathematical Function", Dover, 1964, New York, 1965.

APPENDIX A

Let $i = I \sin\omega t$

$$q = \int_{i_\phi}^{i} i\,dt = \int_{i_\phi}^{i} \left(I \sin\omega t \right) dt = \left(\frac{-I}{\omega} \cos\omega t \right)_{i_\phi}^{i}$$

$$C(t) = C_o \frac{1}{\left(1 - \frac{V}{\phi}\right)^{\gamma}} = \frac{1}{S(t)} = \frac{C_o \phi^{\gamma}}{(\phi - V)^{\gamma}} = \frac{K}{(\phi - V)^{\gamma}}$$

$$i = C(t) \frac{dV}{dt} = \frac{K}{(\phi - V)^{\gamma}} \frac{dV}{dt}$$

$$\therefore \int i\,dt = \int \frac{K}{(\phi - V)^{\gamma}}\, dV = \frac{K}{1-\gamma} (\phi - V)^{1-\gamma}$$

$$\int_{i_\phi}^{i} i\,dt = \left(-\frac{I}{\omega} \cos\omega t \right)_{i_\phi}^{i} = \left(-\frac{I}{\omega} \cos\omega t - \left(-\frac{I_\phi}{\omega} \cos\omega t \right) \right)$$

$$= \frac{\cos\omega t}{\omega} (I_\phi - I) = q_\phi - q$$

$$\therefore q_\phi - q = \frac{K}{1-\gamma} (\phi - V)^{1-\gamma}$$

where

$q = Q_b$ and $v = V_b$

i.e.

$$q_{\phi} - Q_{m} = \frac{K}{1 - \gamma} (\phi - V_{m})^{1-\gamma}$$

or

$$\frac{K}{1 - \gamma} = \frac{q_{\phi} - Q_{m}}{(\phi - V_{m})^{1-\gamma}}$$

$$\frac{q_{\phi} - q}{q_{\phi} - Q_{m}} = \frac{\phi - V}{\phi - V_{m}}^{1-\gamma}$$

or

$$\frac{q_{\phi} - q}{q_{\phi} - Q_{m}}^{(1/1-\gamma)} = \frac{\phi - V}{\phi - V_{m}}$$

APPENDIX B

"FAST FOURIER TRANSFORM PROGRAM"

```
READY.

 10 REM*******************************************************
 20 REM************ FOURIER TRANSFORM PROGRAM *************
 40 REM*******************************************************
 100 DIM A(30),B(30),P(30),PS(30),SQ(30),TH(30),E(30)
 110 DIM F(71),NF(71)
 120 DIM L(256),C(256),D(256),J(256)
 500 REM************ INTRODUCTION ************
 510 PRINT"■■■■■■■■■■"
 520 PRINT"      FOURIER TRANSFORM PROGRAM"
 530 PRINT"      ═══════════════════════"
 540 PRINT:PRINT:PRINT:PRINT
 550 PRINT"(PRESS ANY KEY TO CONTINUE)"
 560 GET A$:IF A$="" THEN 560
 570 PRINT"■■"
 580 PRINT"         PROGRAM NOW RUNNING"
 600 GOSUB 6000
 610 GOTO 1400
 1000 REM************ READ IN DATA PTS. ************
 1010 POKE 59426,0
 1020 FORI=0TO255:POKE59426,I:NEXT:FORK=1TO1000:NEXT
 1030 POKE59426,0:POKE59468,192:POKE59468,224
 1040 Z=PEEK(59457)-130
 1050 PRINT Z
 1060 IF Z=0 GOTO 1080
 1070 IF Z<>0 THEN 1030
 1080 FOR I=0 TO 255
 1090 POKE59468,192:POKE59468,224:POKE59426,I
 1100 K=PEEK(59457)
 1110 L(I)=(K-130)*5.251/127*25
 1120 PRINT I;L(I)
 1130 NEXT I
 1200 REM************ PRINT# DATA READ IN ? ************
 1210 MF=1000:REM MULTIPLYING FACTOR USED BELOW
 1220 PRINT:PRINT"DO YOU WISH TO PRINT# DATA HELD IN ARRAY L(I) ?"
 1230 INPUT"  1=YES   0=NO ";Z
 1240 IF Z=0 THEN 1400
 1250 IF Z=1 THEN 1280
 1260 PRINT:PRINT" INPUT ERROR PLEASE TRY AGAIN"
 1270 GOTO 1230
 1280 OPEN2,4,0:CMD2
 1290 FOR Y=0 TO 255 STEP 4
 1300 J(Y)=INT(MF*L(Y))/MF
 1310 J(Y+1)=INT(MF*L(Y+1))/MF
```

```
1320 J(Y+2)=INT(MF*L(Y+2))/MF
1330 J(Y+3)=INT(MF*L(Y+3))/MF
1340 PRINT Y;;J(Y),Y+1;;J(Y+1),
1350 PRINT Y+2;;J(Y+2),Y+3;;J(Y+3)
1360 NEXT Y
1370 PRINT#2
1380 CLOSE 2
1400 REM********** CALCULATE COEFFICIENTS **********
1410 PRINT
1420 INPUT"NUMBER OF HARMONICS";H
1430 INPUT"STARTING POINT";S
1440 INPUT"END POINT";E
1450 PRINT:PRINT"DO YOU WISH TO CHANGE THESE VALUES ?"
1460 INPUT"  1=YES    0=NO ";B
1470 IF B=1 THEN 1410
1480 IF B=0 THEN 1500
1490 PRINT"INPUT ERROR PLEASE TRY AGAIN":GOTO 1460
1500 IF S<1 THEN 1560
1510 IF S>=(E-1) THEN 1560
1520 IF E>255 THEN 1560
1530 IF H<1 THEN 1580
1540 IF H>30 THEN 1580
1550 GOTO 1600
1560 PRINT:PRINT"ERROR    START>1   END<256   END>START+1"
1570 GOTO 1410
1580 PRINT:PRINT"ERROR   1< NUMBER OF HARMONICS >30"
1590 GOTO 1410
1600 REM***** CALCULATE A0 *****
1610 R=E-S:DT=2*π/(R+1):A=0
1620 FOR I=S TO E
1630 A=A+L(I)
1640 NEXT I
1650 A0=A/R/(2↑0.5)
1660 REM***** CALCULATE AN AND BN *****
1670 FOR N=1 TO H
1680 M=1
1690 C(S-1)=0:D(S-1)=0
1700 FOR I=S TO E
1710 C(I)=C(I-1)+L(I)*COS(N*M*DT)
1720 D(I)=D(I-1)+L(I)*SIN(N*M*DT)
1730 M=M+1
1740 NEXT I
1750 A(N)=C(E)/R/(2↑0.5)/2
1760 B(N)=D(E)/R/(2↑0.5)/2
1770 NEXT N
1800 REM********** SCALE COEFFICIENTS **********
1810 Y=1/2
1812 T=10
1814 AA=ABS(A0)
1816 Q=1
1820 FOR N=1 TO H
1830 E(N)=ABS(A(N))
1840 NEXT N
1850 GOSUB 5200
1860 FOR N=1 TO H
1870 E(N)=ABS(B(N))
1880 NEXT N
1890 GOSUB 5200
1900 IF AA<10 THEN T=100
1910 IF AA<1 THEN T=1000
1920 FOR N=1 TO H
1930 P=1
1935 R=1
1940 IF A(N)<0 THEN P=-1
1945 IF B(N)<0 THEN R=-1
1950 YY=ABS(T*B(N))
```

```
1955 ZZ=ABS(T*A(N))
1960 IF ZZ>Y THEN 1970
1962 A(N)=0
1965 GOTO 2000
1970 X=ZZ-INT(ZZ)
1980 IF X>=Y THEN 1990
1982 A(N)=P*INT(ZZ)/T
1985 GOTO 2000
1990 A(N)=P*INT(ZZ+1)/T
2000 IF YY>Y THEN 2030
2010 B(N)=0
2020 GOTO 2080
2030 Q=YY-INT(YY)
2040 IF Q>=Y THEN 2070
2050 B(N)=R*INT(YY)/T
2060 GOTO 2080
2070 B(N)=R*INT(YY+1)/T
2080 SQ(N)=INT(T*SQR(A(N)*A(N)+B(N)*B(N)))/T
2090 IF A(N)=0 THEN 2120
2100 TH(N)=INT(T*180/π*ATN(B(N)/A(N)))/T
2110 GOTO 2130
2120 TH(N)=90
2130 NEXT N
2140 IF AO<0 THEN O=-1
2150 XX=ABS(T*AO)
2160 IF XX>Y THEN  2190
2170 AO=0
2180 GOTO 2300
2190 W=XX-INT(XX)
2200 IF W>=Y THEN 2230
2210 AO=O*INT(XX)/T
2220 GOTO 2300
2230 AO=O*INT(XX+1)/T
2300 REM********** PRINT COEFFICIENTS **********
2310 PRINT
2320 PRINT"   FOURIER COEFFICIENTS"
2330 PRINT
2350 PRINT"AO=";AO
2360 PRINT
2370 FOR N=1 TO H
2380 PRINT"N=";N
2390 PRINT"AN=";A(N);"   BN=";B(N);"   CN=";SQ(N)
2400 PRINT
2410 NEXT N
2500 REM********** PRINT# COEFFICIENTS ? **********
2510 PRINT
2520 PRINT"DO YOU WANT TO PRINT# ABOVE RESULTS?"
2530 INPUT"  1=YES    0=NO";PO
2540 IF PO=1 THEN 2600
2550 IF PO=0 THEN 3000
2560 PRINT:PRINT"INPUT ERROR PLEASE TRY AGAIN"
2570 GOTO 2530
2600 REM***** PRINT# COEFFICIENTS *****
2610 OPEN3,4,0:CMD3
2620 PRINT:PRINT:PRINT
2630 PRINT" FOURIER COEFFICIENTS"
2640 PRINT" ━━━━━━━━━━━━━━━━━━━━━━";:PRINT
2650 PRINT"          ","AO=";AO
2660 PRINT
2670 FOR N=1 TO H
2680 IF N=10 GOTO 2750
2690 PRINT"   N=";N,
2700 PRINT" AN=";A(N);"          BN="B(N)
2710 PRINT"         "," CN=";SQ(N);"      PHASE=";TH(N)
2720 PRINT
2730 NEXT N
```

```
2740 IF H<10 THEN 2810
2750 FOR N=10 TO H
2760 PRINT"   N=";N,
2770 PRINT"AN=";A(N);"       BN="B(N)
2780 PRINT"          "," CN=";S0(N);"     PHASE=";TH(N)
2790 PRINT
2800 NEXT N
2810 PRINT#3
2820 CLOSE 3
3000 REM********** PRINT# GRAPH ? **********
3010 PRINT
3020 PRINT"DO YOU WANT TO PRINT# GRAPH ?"
3030 INPUT"  1=YES    0=NO";WO
3040 IF WO=1 THEN 3500
3050 IF WO=0 THEN 4900
3060 PRINT:PRINT"INPUT ERROR PLEASE TRY AGAIN":PRINT
3070 GOTO 3030
3500 REM***** PRINT# GRAPH *****
3510 PRINT
3520 INPUT"HOW MANY VERTICAL POINTS DO YOU WANT ON THE GRAPH";SF
3530 IF SF<5 THEN 3570
3540 IF SF>50 THEN 3570
3550 SF=2*INT(SF/2)
3560 GOTO 3650
3570 PRINT
3580 PRINT"ERROR   5< VERTICAL RANGE <50"
3590 GOTO 3510
3650 REM***** CALCULATE F(T)S *****
3660 X=π*2/70
3670 FOR T=0 TO 70
3680 PS(0)=0
3690 FOR N=1 TO H
3700 IF A(N)<>0 THEN 3720
3710 IF B(N)=0 THEN 3740
3720 PS(N)=PS(N-1)+A(N)*COS(N*T*X)+B(N)*SIN(N*T*X)
3730 GOTO 3760
3740 PS(N)=0
3760 NEXT N
3770 F(T)=PS(H)+A0
3780 NEXT T
3800 REM***** NORMALISE F(T)S *****
3810 A=ABS(F(0))
3820 G=-3
3830 FOR T=1 TO 70
3840 IF A>=ABS(F(T)) THEN 3860
3850 A=ABS(F(T))
3860 NEXT T
3870 FOR T=0 TO 70
3880 NF(T)=INT(SF*F(T)/A)
3890 IF G<=NF(T) THEN 3910
3900 G=NF(T)
3910 IF NF(T)>0 THEN U=1
3920 IF NF(T)<0 THEN D=1
3930 NEXT T
4000 REM***** PLOT# GRAPH *****
4010 OPEN1,4,0:CMD1
4020 PRINT:PRINT:PRINT
4030 PRINT" GRAPH CONSTRUCTED FROM FOURIER COEFFICIENTS"
4040 PRINT" ═══════════════════════════════════════"
4050 PRINT" STARTING POINT=";S;"  END POINT="E
4060 PRINT
4070 IF U=0 THEN 4250
4080 FOR L=SF TO 1 STEP-1
4090 IF L<>SF THEN 4110
4100 PRINT"    1 |";:GOTO 4170
4110 IF L<>(SF-3) THEN 4130
```

```
4120 PRINT" F(T) |";:GOTO 4170
4130 IF L<>SF/2 THEN 4160
4140 PRINT"  1/2|":
4150 GOTO 4170
4160 PRINT"      |";
4170 FOR T=0 TO 70
4180 IF NF(T)=L THEN 4210
4190 PRINT" ";
4200 GOTO 4220
4210 PRINT".";
4220 NEXT T
4230 PRINT
4240 NEXT L
4250 PRINT"    0 |";
4260 FOR T=0 TO 70
4270 IF NF(T)=0 THEN 4300
4280 PRINT"_";
4290 GOTO 4310
4300 PRINT".";
4310 NEXT T
4320 PRINT
4330 PRINT"      |";
4340 FOR T=0 TO 70
4350 IF NF(T)<>-1 THEN 4380
4360 PRINT".";
4370 GOTO 4510
4380 IF T=17 THEN 4440
4390 IF T=34 THEN 4460
4400 IF T=49 THEN 4480
4410 IF T=69 THEN 4500
4420 PRINT" ";
4430 GOTO 4510
4440 PRINT"π/2";:T=19
4450 GOTO 4510
4460 PRINT"π";
4470 GOTO 4510
4480 PRINT"3π/2";:T=52
4490 GOTO 4510
4500 PRINT"2π";:T=70
4510 NEXT T
4520 IF D=0 THEN 4740
4530 PRINT"        |";
4540 FOR T=0 TO 70
4550 IF NF(T)=-2 THEN 4570
4560 PRINT" ";:GOTO 4580
4570 PRINT".";
4580 NEXT T
4590 PRINT
4600 FOR L=3 TO ABS(G)
4610 IF L<>SF/2 THEN 4630
4620 PRINT" -1/2|";:GOTO 4660
4630 IF L<>SF THEN 4650
4640 PRINT"   -1 |";:GOTO 4660
4650 PRINT"      |";
4660 FOR T=0 TO 70
4670 IF NF(T)=(-1*L) THEN 4700
4680 PRINT" ";
4690 GOTO 4710
4700 PRINT".";
4710 NEXT T
4720 PRINT
4730 NEXT L
4740 PRINT#1
4750 CLOSE 1
4900 REM********** END PROG? **********
4910 PRINT
```

```
4920 PRINT"DO YOU WISH TO INPUT MORE DATA OR TO RE-USE ABOVE DATA"
4930 PRINT"    OR TO END PROGRAM ?"
4940 INPUT" 1=MORE    2=RE-USE    3=END":EP
4950 IF EP=1 THEN 500
4960 IF EP=2 THEN 1200
4970 IF EP=3 THEN 9999
4980 PRINT"INPUT ERROR PLEASE TRY AGAIN":PRINT
4990 GOTO 4940
5200 REM********** SCALING SUBROUTINE **********
5210 FOR N=1 TO H
5220 IF E(N)<=AA THEN 5240
5230 AA=E(N)
5240 NEXT N
5250 RETURN
6000 REM PLOT SQUARE WAVE
6010 FOR H=1 TO 63
6020 L(H)=10:L(H+190)=10
6030 NEXT H
6050 FOR J =64 TO 189
6060 L(J)=0
6070 NEXT J
6080 OPEN4,4,0:CMD 4
6090 PRINT:PRINT
6100 PRINT" DATA IN ARRAY L(I)=10 FOR 1<=I<=63"
6110 PRINT"                    =0 FOR 64<=I<=189"
6115 PRINT"                    =10 FOR 190<=I<=253"
6120 PRINT#4
6130 CLOSE4
6140 RETURN
6200 REM SINEWAVE
6201 REM S=1 E=255
6205 DX=π/127:Z=10
6210 FOR H=1 TO 256
6220 L(H)=Z*SIN((H-1)*DX)
6230 NEXT H
6240 OPEN 5,4,0:CMD5
6250 PRINT:PRINT:PRINT
6260 PRINT"   DATA IN ARRAY L(I)=10*SIN(I)   WHERE 1<=I<=255"
6270 PRINT#5
6280 CLOSE5
6290 RETURN
6300 REM COS WAVE
6301 REM S=1 E=128
6310 DX=π/64
6320 FOR K=1 TO 129
6330 L(K)=COS((K-1)*DX)+1
6340 NEXT K
6350 RETURN
9999 END
```

READY.